



Cross-section measurements for the production of a Z boson in association with high-transverse-momentum jets in pp collisions at $\sqrt{s} = 13$ TeV with the ATLAS detector

The ATLAS Collaboration

Cross-section measurements for a Z boson produced in association with high-transverse-momentum jets ($p_T \geq 100$ GeV) and decaying into a charged-lepton pair (e^+e^- , $\mu^+\mu^-$) are presented. The measurements are performed using proton–proton collisions at $\sqrt{s} = 13$ TeV corresponding to an integrated luminosity of 139 fb^{-1} collected by the ATLAS experiment at the LHC. Measurements of angular correlations between the Z boson and the closest jet are performed in events with at least one jet with $p_T \geq 500$ GeV. Event topologies of particular interest are the collinear emission of a Z boson in dijet events and a boosted Z boson recoiling against a jet. Fiducial cross sections are compared with state-of-the-art theoretical predictions. The data are found to agree with next-to-next-to-leading-order predictions by NNLOJET and with the next-to-leading-order multi-leg generators MADGRAPH5_AMC@NLO and SHERPA.

1 Introduction

The measurement of Z -boson production¹ in association with jets, Z + jets, constitutes a powerful test of perturbative quantum chromodynamics (QCD) [1, 2] and, in the case of high-energy jets, it provides a way to probe the interplay between QCD and higher-order electroweak (EW) processes [3–6]. The large Z + jets production cross section and the easily identifiable decays of the Z boson to charged-lepton final states offer a clean experimental signature which can be measured precisely. Such processes also constitute non-negligible backgrounds in measurements of the Higgs boson [7, 8] and in searches for new phenomena [9–11], which often exploit the presence of high- p_T jets to enrich a data sample with potential signal. In those studies, predictions are used to extrapolate Z + jets backgrounds from control regions to the signal regions and to model the distributions of the final discriminants.

In the calculations of Z + 1-jet production at leading order (LO), the Z boson recoils against a quark or a gluon. At next-to-leading order (NLO), real and virtual QCD and EW effects play a role in Z + jets production, such as in topologies corresponding to dijet events where a real Z boson is emitted from an incoming or outgoing quark leg [3–6]. Example Feynman diagrams for LO and NLO Z + jets production processes are shown in Figure 1. The latter case can lead to production rate enhancements proportional to $\alpha_s \ln^2(p_{T,j1}/m_Z)$, where α_s is the strong coupling constant, $p_{T,j1}$ the transverse momentum of the leading jet, and m_Z the mass of the Z boson, and thus the effect can become very large for events with high- p_T jets. These events exhibit a collinear enhancement in the distribution of the angular distance between the Z boson and the closest jet. Although the enhancement can be probed in the region of small angular separation, this region also contains contributions where the Z boson is produced in association with larger numbers of jets, which must be included in the predictions. The measurements presented in this paper target QCD-only Z + jets production, treating EW Z + 2-jets (EW Zjj) production [12] as a background. Measurements where the EW Zjj contribution is treated as signal and not subtracted as background are also performed and published in the HEPData entry [13] of this measurement.

The ATLAS Collaboration [14] at the Large Hadron Collider (LHC) [15] first measured angular distributions in high- p_T W boson production with jets (W + jets) in the 8 TeV pp -collision data set [16]. The first similar measurement in Z + jets events was published by the CMS Collaboration and used a partial 13 TeV data set corresponding to 35.9 fb^{-1} [17]. Both measurements highlight the fact that the collinear region, where the angular separation between the W/Z boson and the closest jet is small, represents a major challenge for contemporary Monte Carlo (MC) generators. The measurements presented in this paper include a wide range of new observables sensitive to the presence of high- p_T jets and to the collinear emission of a Z boson in dijet events. The statistical power of the full LHC Run-2 data set makes it possible to tighten the collinear selection, and to measure key observables separately for collinear and non-collinear topologies.

This publication focuses on events that contain a Z -boson candidate reconstructed from either an e^+e^- or $\mu^+\mu^-$ pair in association with hadronic jets defined as jets having transverse momentum greater than or equal to 100 GeV. The phase-space region with at least one associated jet is labelled as the *inclusive* region. In this region, the measured quantities are the transverse momentum of the leading jet ($p_{T,j1}$), the transverse momentum of the Z boson ($p_{T,\ell\ell}$), the scalar sum of the transverse momentum of all selected jets and leptons (H_T), and the jet multiplicity. A *high- p_T* region is selected by requiring the presence of a jet with $p_T \geq 500$ GeV. To test the prediction that this region is composed of two characteristic topologies, the soft radiation of a Z boson from a jet (*collinear* topology) and the hard scatter of a Z boson against a jet (*back-to-back* topology), the *high- p_T* region is split to cover different ranges of the angle between

¹ Throughout this paper, Z/γ^* -boson production is simply referred to as Z -boson production.

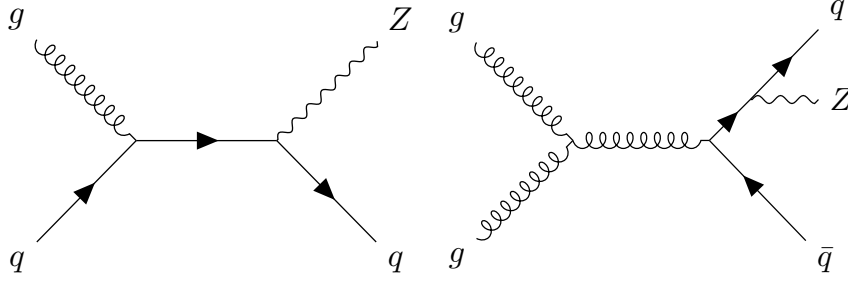


Figure 1: Representative Feynman diagrams for the production of a Z boson in association with high- p_T jets. The $Z + 1$ -jet events (left) are expected to populate the *back-to-back* region where the Z boson is balanced against a single high- p_T jet. In dijet events (right), the Z boson is expected to be radiated from the quark leg, with kinematics leading to small values of the angular distance between the Z boson and the closest jet, $\Delta R_{Z,j}^{\min}$, and therefore populating the *collinear* region.

the Z boson and the closest jet, and selected key observables are measured separately for each region. In the *high- p_T* region, the following observables sensitive to the presence of collinear Z-boson emission are studied:

- $\Delta R_{Z,j}^{\min}$, the angular distance² between the Z boson and the closest jet. Real Z-boson radiation is expected to be enhanced at low values of $\Delta R_{Z,j}^{\min}$. At large values of $\Delta R_{Z,j}^{\min}$, the Z boson is balanced by a recoiling jet and large virtual EW corrections are expected. To enrich these two topologies, *collinear* and *back-to-back* regions are constructed by requiring $\Delta R_{Z,j}^{\min} \leq 1.4$ and $\Delta R_{Z,j}^{\min} \geq 2.0$, respectively.
- $r_{Z,j}$, the ratio of the Z-boson p_T to the closest-jet p_T , defined as

$$r_{Z,j} \equiv \frac{p_{T,\ell\ell}}{p_T(\text{closest jet})}.$$

Collinear Z-boson radiation is expected to be dominated by soft Z bosons, resulting in very small values for this ratio.

- N_{jets} , the jet multiplicity. The *back-to-back* region is expected to be dominated by $Z + 1$ -jet events, whereas the *collinear* region would be dominated by $Z + 2$ -jets events.

The measurements of jet multiplicity and $r_{Z,j}$ are performed both in the full *high- p_T* region and separately in the *collinear* and *back-to-back* regions.

Measurements of jet multiplicity and $\Delta R_{Z,j}^{\min}$ are also performed in an alternative high-energy region, constructed by requiring the scalar sum of the transverse momentum of all selected jets, S_T , to be at least 600 GeV. This alternative region probes high-energy events but does not depend on the presence of a single very energetic object. In this region, called the *high- S_T* region, a large fraction of the events have higher jet multiplicity.

² ATLAS uses a right-handed coordinate system with its origin at the nominal interaction point (IP) in the centre of the detector and the z-axis along the beam pipe. The x-axis points from the IP to the centre of the LHC ring, and the y-axis points upwards. Cylindrical coordinates (r, ϕ) are used in the transverse plane, ϕ being the azimuthal angle around the z-axis. The pseudorapidity is defined in terms of the polar angle θ as $\eta = -\ln(\theta/2)$. The angular distance is defined as $\Delta R \equiv \sqrt{(\Delta y)^2 + (\Delta\phi)^2}$. When dealing with massive jets and particles, the rapidity $y = (1/2) \ln[(E + p_z)/(E - p_z)]$ is used, where E is the jet/particle energy and p_z is the z-component of the jet/particle momentum.

Predictions from the most recent generators combine NLO multi-leg matrix elements (ME) with a parton shower (PS) and hadronisation model [18–21]. Fixed-order parton-level theoretical predictions for Z + jets production at next-to-next-to-leading order (NNLO) are available for up to one associated jet [22–25]. In this paper, the cross-section measurements are compared with state-of-the-art multi-leg ME+PS generators and NNLO fixed-order Z + jets predictions from NNLOJET [24, 25]. Virtual EW corrections were made available recently [26, 27] and are included in one of the SHERPA [19] predictions studied in this paper.

The paper is organised as follows. Section 2 contains a brief overview of the ATLAS detector. The data and simulated samples, as well as additional predictions used in the analysis, are described in Section 3. The object definition and the event reconstruction at detector level are presented in Section 4, while Section 5 describes the background modelling and presents a comparison of measured and predicted yields at detector level. After background subtraction, the data are unfolded to particle level in a fiducial phase space with a procedure described in Section 6. The experimental and theoretical systematic uncertainties are estimated in Section 7. Section 8 presents the unfolded cross-section results and the comparisons with predictions. Conclusions are provided in Section 9.

2 ATLAS detector

The ATLAS experiment at the LHC is a multipurpose particle detector with a forward–backward symmetric cylindrical geometry and a near 4π coverage in solid angle. It consists of an inner tracking detector surrounded by a thin superconducting solenoid providing a 2 T axial magnetic field, electromagnetic and hadron calorimeters, and a muon spectrometer. The inner tracking detector covers the pseudorapidity range $|\eta| < 2.5$. It consists of silicon pixel, silicon microstrip, and transition radiation tracking detectors. Lead/liquid-argon (LAr) sampling calorimeters provide electromagnetic (EM) energy measurements with high granularity. A steel/scintillator-tile hadron calorimeter covers the central pseudorapidity range ($|\eta| < 1.7$). The endcap and forward regions are instrumented with LAr calorimeters for both the EM and hadronic energy measurements up to $|\eta| = 4.9$. The muon spectrometer surrounds the calorimeters and is based on three large superconducting air-core toroidal magnets with eight coils each. The field integral of the toroids ranges between 2.0 and 6.0 T m across most of the detector. The muon spectrometer includes a system of precision tracking chambers and fast detectors for triggering. A two-level trigger system is used to select events. The first-level trigger is implemented in hardware and uses a subset of the detector information to accept events at a rate below 100 kHz. This is followed by a software-based trigger that reduces the accepted event rate to 1 kHz on average depending on the data-taking conditions. An extensive software suite [28] is used in the reconstruction and analysis of real and simulated data, in detector operations, and in the trigger and data acquisition systems of the experiment.

3 Data set and simulated event samples

The data used in this analysis were recorded with the ATLAS detector from 2015 to 2018 in pp collisions at $\sqrt{s} = 13$ TeV (full Run-2 data set) and correspond to a total integrated luminosity of 139 fb^{-1} [29]. The mean number of pp interactions per bunch crossing, including the hard scattering and other interactions in the same and neighbouring bunch crossings (pile-up), was $\langle\mu\rangle = 34$.

MC simulation samples are used to estimate most of the contributions from background events, to unfold the data to particle level, and in comparisons with the unfolded data distributions. The generated samples were

Table 1: Summary of the programs used to produce the signal and the various background samples. For every process the name of the program used is indicated in the second column. The third column reports the order of the QCD calculation in the matrix elements, where np denotes the number of real parton emissions. The SHERPA 2.2.11 Z + jets processes include virtual electroweak corrections.

Process	Generator	Order pQCD	References
Signal			
$Z \rightarrow \ell\ell$ ($\ell = e, \mu$)	SHERPA 2.2.11	0–2p NLO, 3–5p LO	[19, 32–42]
$Z \rightarrow \ell\ell$ ($\ell = e, \mu$)	MG5_AMC+PY8 FxFx	0–3p NLO	[19–21, 42–45]
$Z \rightarrow \ell\ell$ ($\ell = e, \mu$)	SHERPA 2.2.1	0–2p NLO, 3–4p LO	[18, 32–40]
$Z \rightarrow \ell\ell$ ($\ell = e, \mu$)	MG5_AMC+PY8 CKKWL	0–4p LO	[43, 46–48]
$Z \rightarrow \ell\ell$ ($\ell = e, \mu$)	NNLOJET@NNLO	1p NNLO	[24, 25]
$Z \rightarrow \ell\ell$ ($\ell = e, \mu$)	NNLOJET@NLO	1p NLO	[24, 25]
Backgrounds			
EW $Zjj(\rightarrow \ell\ell$ ($\ell = e, \mu$))	HERWIG 7.1.5, VBFNLO 3.0.0	NLO	[49–51]
$Z \rightarrow \tau\tau$	SHERPA 2.2.1	0–2p NLO, 3–4p LO	[18, 32–40]
W + jets	SHERPA 2.2.1	0–2p NLO, 3–4p LO	[18, 32–40]
$t\bar{t}$	POWHEG BOX v2 + PYTHIA 8.230	NLO	[52–55]
Single top (t -, Wt -, s -channel)	POWHEG BOX v2 + PYTHIA 8.230	NLO	[52–55]
$Z/W(\rightarrow qq)Z(\rightarrow \ell\ell)$	SHERPA 2.2.1	0–1p NLO, 2–3p LO	[18, 32–40]
$W(\rightarrow \ell\nu)Z(\rightarrow qq)$	SHERPA 2.2.1	0–1p NLO, 2–3p LO	[18, 32–40]
$W^\pm(\rightarrow qq)W^\mp(\rightarrow \ell\nu)$	SHERPA 2.2.1	0–1p NLO, 2–3p LO	[18, 32–40]
$\ell\ell\nu\nu, \ell\ell\nu, \ell\ell\ell\ell$	SHERPA 2.2.2	0–1p NLO, 2–3p LO	[18, 32–40]
$V(\rightarrow \ell\ell) + \gamma$	SHERPA 2.2.8	0–1p NLO, 2–3p LO	[18, 32–40]

processed using the GEANT4-based ATLAS detector simulation [30, 31] and the same event-reconstruction algorithms are used for both the MC samples and the data. A summary of the MC generators and calculations used for the simulation of signal and background processes is provided in Table 1.

The production of Z bosons in association with jets was simulated with the ATLAS configuration of SHERPA 2.2.11 [19], which includes matrix elements for up to five partons at LO and up to two partons at NLO. They are calculated with the Comix [32] and OPENLOOPS [33–35] libraries and matched with the SHERPA parton shower [36] using the MEPS@NLO prescription [37–40] with a set of tuned parameters (‘tune’) developed by the SHERPA authors. In contrast to SHERPA 2.2.1 [18], used previously in ATLAS publications, it includes a modified Catani–Seymour subtraction scheme [41], the Hessian NNPDF3.0_{NNLO} PDF set [42] is used, and an analytic enhancement technique has been introduced [19]. The cross section in the $high-p_T$ region has been considerably reduced relative to the prediction from the previous SHERPA version by switching to an improved matching scheme with a different treatment of unordered histories [40]. SHERPA 2.2.11 is also the only sample used in this paper which includes NLO virtual EW corrections [34, 35]. The samples were produced using three options for the combination of NLO EW and QCD corrections: an additive, a multiplicative, and an exponential scheme. The nominal prediction is derived via the additive scheme; a systematic uncertainty band is derived from the envelope of all schemes. In contrast to virtual EW corrections, EW parton showers are not included in any of the generators used in this paper. The

SHERPA 2.2.11 Z + jets samples are used for the nominal unfolding of the data distributions, to estimate the systematic uncertainties and in comparisons with the cross-section measurements.

A second Z + jets sample, referred to as MG5_AMC+Py8 FxFx [19], was produced by using the MADGRAPH5_AMC@NLO 2.6.5 [43] program to generate matrix elements at NLO accuracy in QCD for up to three additional partons in the final state. The NNPDF3.1_{NNLO} set [42] was used in the generation. The parton showering and subsequent hadronisation was performed using PYTHIA 8.240 [21] with the A14 tune [44] and the NNPDF2.3_{LO} PDF set [45]. The jet multiplicities were merged using the FxFx prescription [20]. This prediction is compared with the unfolded cross-section measurements.

A third sample of Z + jets events and an event sample from W + jets processes were produced with the SHERPA 2.2.1 [18] generator using NLO matrix elements for up to two partons, and LO matrix elements for up to four partons, calculated with the Comix and OPENLOOPS libraries. They were matched with the SHERPA parton shower using the MEPS@NLO prescription with a set of tuned parameters developed by the SHERPA authors. The MC replica version of the NNPDF3.0_{NNLO} set of PDFs was used. The SHERPA 2.2.1 Z + jets sample is used in comparisons with the unfolded cross-section measurements, as it was used as a standard in previous ATLAS Run-2 publications.

A fourth Z + jets sample, referred to as MG5_AMC+Py8 CKKW_L, was generated using LO-accurate matrix elements with up to four final-state partons calculated by MADGRAPH5_AMC@NLO 2.2.2 [43]. The ME calculation employed the NNPDF3.0_{NLO} PDF set and was interfaced to PYTHIA 8.186 [46] for the modelling of the parton shower, hadronisation, and underlying event. The overlap between matrix element and parton shower emissions was removed using the CKKW-L merging procedure [47, 48]. The A14 tune of PYTHIA was used with the NNPDF2.3_{LO} PDF set. This sample is used to validate the unfolding method and in comparisons with the unfolded cross-section measurements.

Two additional Z + jets samples were generated with the NNLOJET program [24, 25], which computes fixed-order parton-level predictions for inclusive jet processes at higher orders in QCD. The NLO and NNLO predictions, referred to as NNLOJET@NLO and NNLOJET@NNLO, respectively, were calculated as higher-order corrections to the parton-level LO process of Z + 1-jet production. The NNPDF3.1_{NNLO} set was used with a central scale choice of $\mu_0 = \frac{1}{2}(E_{T,Z} + \sum_{i \in \text{partons}} p_{T,i})$ with $E_{T,Z} = \sqrt{m_{\ell\ell}^2 + p_{T,Z}^2}$. These samples are pure QCD predictions at parton level. To match the fiducial selection of the measurement (see Section 6), scale factors to correct from the Born level to the dressed-lepton level are computed and applied to these predictions. The slightly different overlap-removal procedure for jets and leptons used in these samples, due to the NNLOJET program design, is addressed by overlap-removal correction scale factors. Both sets of scale factors, deviating from unity at the percent level and computed separately for each bin of the measured observables, are published in the HEPData entry [13] of this measurement. Non-perturbative corrections are found to be consistent with zero when $p_{T,j1}$ exceeds 100 GeV and are not needed to match the fiducial selection of these measurements. These samples are used in comparisons with the unfolded cross-section measurements.

The EW Zjj process is defined by the t -channel exchange of a weak boson and at tree level is calculated at $\mathcal{O}(\alpha_{\text{EW}}^4)$ when including the decay of the Z boson [12]. In contrast, the strong Zjj process, which is covered by the Z + jets samples, has no weak boson exchanged in the t -channel and at tree level is calculated at $\mathcal{O}(\alpha_{\text{EW}}^2 \alpha_s^2)$ when including the decay of the Z boson. The EW Zjj samples were produced in the vector-boson fusion (VBF) approximation with HERWIG 7.1.5 [49, 50] at NLO accuracy in the strong coupling, using VBFNLO 3.0.0 [51] to provide the loop amplitude. The MMHT2014_{LO} PDF set [56] was used along with the default set of tuned parameters for parton showering, hadronisation and the underlying event. To account for the interference between strong Zjj and EW Zjj processes, a uniform modelling

uncertainty of 25% in the EW Zjj cross section (40% in the collinear region), determined from simulation with MADGRAPH5_AMC@NLO 2.9.5, is applied [12].

The $t\bar{t}$ background in this measurement is derived with a data-driven method as described in Section 5. The MC $t\bar{t}$ events used for intermediate steps of the method were modelled using the POWHEG BOX v2 [52–55] generator at NLO with the NNPDF3.0_{NLO} PDF set and the h_{damp} parameter³ set to $1.5 m_{\text{top}}$ [57]. The events were interfaced to PYTHIA 8.230 [21] to model the parton shower, hadronisation, and underlying event, with parameters set according to the A14 tune and using the NNPDF2.3_{LO} set of PDFs. The $t\bar{t}$ sample is normalised to the cross-section prediction at NNLO accuracy, including the resummation of next-to-next-to-leading logarithmic (NNLL) soft-gluon terms calculated with TOP++ 2.0 [58–64].

Single top quark production in the s -channel, in the t -channel, and in association with a W boson (tW) was modelled using the POWHEG BOX v2 generator at NLO in QCD with the five-flavour scheme and the NNPDF3.0_{NLO} set of PDFs. The diagram-removal scheme [65] was used to remove interference and overlap with $t\bar{t}$ production. The tW cross section is corrected to the theory prediction at approximate NNLO accuracy [66, 67], while the s - and t -channel cross sections are corrected to the prediction at NLO accuracy [68, 69].

Samples of diboson final states (VV) were produced with the SHERPA 2.2.1 or SHERPA 2.2.2 generator depending on the process, including off-shell effects and Higgs boson contributions where appropriate. Fully leptonic final states and semileptonic final states, where one boson decays leptonically and the other hadronically, were generated using matrix elements at NLO accuracy in QCD for up to one additional parton and at LO accuracy for up to three additional parton emissions. The matrix element calculations were matched and merged with the SHERPA parton shower as detailed above for SHERPA 2.2.1, and the NNPDF3.0_{NNLO} set of PDFs was used.

The production of $V + \gamma$ final states was simulated with the SHERPA 2.2.8 [18] generator. Matrix elements at NLO QCD accuracy for up to one additional parton and LO accuracy for up to three additional parton emissions were matched and merged with the SHERPA parton shower as detailed above for SHERPA 2.2.1, and the NNPDF3.0_{NNLO} set of PDFs was used.

Background events involving semileptonic decays of heavy quarks, hadrons misidentified as leptons, and, in the case of the electron channel, electrons from photon conversions are referred to collectively as ‘multijet events’. The multijet background is estimated using data-driven techniques, as described in Section 5.

For bottom and charm hadron decays, the EVTGEN 1.7.0 program [70] was used for MG5_AMC+PY8 FxFx samples, and EVTGEN 1.2.0 was used for all other MADGRAPH and POWHEG samples. The effect of multiple interactions in the same and neighbouring bunch crossings (pile-up) was modelled by overlaying the simulated hard-scattering event with inelastic pp events generated with PYTHIA 8.186 [46] using the NNPDF2.3_{LO} PDF and the A3 tune [71]. The small differences in lepton reconstruction, isolation, and trigger efficiencies between simulation and data are corrected in the simulation on an event-by-event basis by applying efficiency scale factors for each lepton [72–74].

³ The h_{damp} parameter is a resummation damping factor and one of the parameters that control the matching of POWHEG matrix elements to the parton shower and thus effectively regulates the high- p_T radiation against which the $t\bar{t}$ system recoils.

4 Event reconstruction

Events are used if they were recorded during stable beam conditions and if they satisfy detector and data-quality requirements [75]. They are required to have a primary vertex, defined as the vertex with the highest sum of track p_T^2 , with at least two associated tracks with $p_T > 500$ MeV [76]. Events are selected using triggers [77–79] that require at least two electrons or two muons, or the combination of at least one electron and one muon; the efficiencies for these triggers plateau in the region of $p_T > 25$ GeV.

Electron candidates are reconstructed from inner-detector tracks which come from the primary vertex and are matched to clusters of energy deposits in the EM calorimeter. To fulfil the primary-vertex condition, the electron track’s transverse impact parameter significance must satisfy $|d_0|/\sigma(d_0) < 5.0$, where d_0 is the transverse impact parameter and $\sigma(d_0)$ its uncertainty, and the longitudinal impact parameter z_0 must satisfy $|z_0 \sin(\theta)| < 0.5$ mm, where θ is the angle of the track to the beamline. Electron candidates must satisfy the ‘Medium’ likelihood-based identification requirements [72] based on EM shower shapes, track quality, and track–cluster matching. They must also satisfy the ‘PflowLoose’ [72] isolation requirement. Electron candidates are used in the analysis if they have $p_T \geq 25$ GeV and $|\eta| < 1.37$ or $1.52 < |\eta| < 2.47$.

Muon candidates are identified by matching inner-detector tracks from the primary vertex to either full tracks or track segments reconstructed in the muon spectrometer. The candidates must satisfy the following primary-vertex requirements: the transverse impact parameter significance must satisfy $|d_0|/\sigma(d_0) < 3.0$ and the longitudinal impact parameter must satisfy $|z_0 \sin(\theta)| < 0.5$ mm, where d_0 , $\sigma(d_0)$, z_0 and θ are as defined above for the electrons. Muons are required to pass ‘Medium’ identification requirements [73, 74] based on quality criteria applied to the inner-detector and muon-spectrometer tracks. Muon candidates with $p_T \geq 300$ GeV must satisfy tighter identification requirements in the muon spectrometer in order to improve the muon- p_T resolution. Muons must also satisfy the ‘PflowLoose’ isolation requirement, built from tracking and calorimeter information, with a muon- p_T -dependent variable cone size ΔR [74]. Muon candidates are used in the analysis if they have $p_T \geq 25$ GeV and $|\eta| < 2.4$.

Jets of hadrons are reconstructed using a particle-flow algorithm [80] based on noise-suppressed positive-energy topological clusters in the calorimeter. Energy deposited in the calorimeter by charged particles is subtracted and replaced by the momenta of tracks which are matched to those topological clusters. The jets are clustered using the anti- k_t [81] algorithm implemented in the FASTJET package [82] with a radius parameter $R = 0.4$. They are further calibrated according to in situ measurements of the jet energy scale [83]. Analysis jets are required to have a calibrated $p_T \geq 100$ GeV and $|y| < 2.5$.

Electrons, muons and jets are reconstructed and identified independently. An overlap-removal procedure is then applied to uniquely identify these objects in an event. For the lepton–jet overlap removal, softer jets with $p_T \geq 30$ GeV and $|y| < 2.5$ are considered. Preselected jets with a high probability to have been initiated by an electron or a radiated photon such that ΔR between the jet and a lepton is smaller than 0.2 are removed. In a second step, leptons closer than $\Delta R = 0.4$ to any remaining jet are removed.

Events are selected if they contain a Z -boson candidate reconstructed from two same-flavour, opposite-charge leptons ($\ell = e, \mu$) and with dilepton invariant mass $71 \text{ GeV} \leq m_{\ell\ell} \leq 111 \text{ GeV}$. The selected events are also required to contain at least one analysis jet. Events which satisfy the above selection requirements define the *inclusive* Z + jets region. A dedicated *high- p_T* region is created by requiring the leading jet to have $p_{T,j1} \geq 500$ GeV. This latter region is split into the *collinear* region, where the angular distance between the Z boson and the closest jet must be $\Delta R_{Z,j}^{\min} \leq 1.4$, and the *back-to-back* region that requires

$\Delta R_{Z,j}^{\min} \geq 2.0$. An alternative phase space is also defined by requiring $S_T \geq 600$ GeV, labelled as the *high- S_T* region, where S_T is defined as the scalar sum of the p_T of the analysis jets.

5 Background estimation

Backgrounds from single-boson, diboson and single-top-quark processes are estimated using the MC samples described in Section 3, while top-pair production and ‘multijet event’ contributions from semileptonic decays of heavy quarks, hadrons misidentified as leptons, and electrons from photon conversions are estimated from data. A summary of the composition and relative importance of the backgrounds in the various signal regions is given in Table 2. The overall purity of the Z +jets selections (defined as the expected fraction of signal events after the final selection) ranges from 94% in the *inclusive* region to 87%, 86%, 87% and 88% in the *high- p_T* , *collinear*, *back-to-back* and *high- S_T* regions, respectively. Backgrounds are dominated by $t\bar{t}$, diboson and EW Zjj processes, with fractions of 2%–5%, 2%–6% and 1%–5%, respectively. The fraction of events arising from $Z \rightarrow \tau^+\tau^-$, W +jets, $V+\gamma$, and multijet backgrounds is below the percent level in all signal regions.

Table 2: Event yields in the different Z +jets signal regions in the electron and muon channels. Uncertainties correspond to the statistical and experimental systematic uncertainties added in quadrature. The Z +jets prediction is computed with SHERPA 2.2.11. The number of multijet events is negligible and not included.

$Z \rightarrow e^+e^-$	<i>Inclusive</i>	<i>High-p_T</i>	<i>Collinear</i>	<i>Back-to-back</i>	<i>High-S_T</i>
Z +jets	1 171 000 \pm 49 000	6 150 \pm 310	2 520 \pm 120	2 520 \pm 150	18 300 \pm 800
$t\bar{t}$	43 400 \pm 1 300	209 \pm 16	136 \pm 13	47.2 \pm 7.5	917 \pm 41
Diboson	19 530 \pm 750	428 \pm 29	183 \pm 16	167 \pm 16	1 008 \pm 53
EW Zjj	13 270 \pm 500	312 \pm 23	102 \pm 11	135 \pm 14	789 \pm 43
Single-top	2 430 \pm 160	27.9 \pm 5.5	14.0 \pm 3.8	9.8 \pm 3.2	54.2 \pm 8.2
$Z \rightarrow \tau\tau$	515 \pm 37	4.6 \pm 4.2	1.6 \pm 2.1	2.2 \pm 1.7	10.6 \pm 6.2
W +jets	93 \pm 16	3.4 \pm 1.9	0.3 \pm 0.6	2.9 \pm 1.7	3.4 \pm 1.9
$V+\gamma$	1 413 \pm 83	14.2 \pm 4.3	6.5 \pm 2.6	5.1 \pm 2.3	34.1 \pm 7.3
Total predicted	1 252 000 \pm 51 000	7 150 \pm 350	2 970 \pm 130	2 890 \pm 170	21 100 \pm 880
Data	1 312 145	7 539	2 955	3 231	21 746
$Z \rightarrow \mu^+\mu^-$	<i>Inclusive</i>	<i>High-p_T</i>	<i>Collinear</i>	<i>Back-to-back</i>	<i>High-S_T</i>
Z +jets	1 537 000 \pm 63 000	6 700 \pm 300	2 950 \pm 130	2 420 \pm 120	23 110 \pm 920
$t\bar{t}$	55 400 \pm 1 300	209 \pm 16	142 \pm 12	39.1 \pm 6.6	1 058 \pm 41
Diboson	24 160 \pm 870	438 \pm 27	198 \pm 16	157 \pm 14	1 149 \pm 55
EW Zjj	17 020 \pm 580	328 \pm 22	113 \pm 12	134 \pm 13	915 \pm 45
Single-top	3 110 \pm 190	29.1 \pm 5.5	13.6 \pm 3.8	11.2 \pm 3.5	70.0 \pm 9.2
$Z \rightarrow \tau\tau$	460 \pm 33	3.5 \pm 4.0	1.1 \pm 2.3	1.8 \pm 1.5	8.8 \pm 5.4
W +jets	128 \pm 14	1.9 \pm 1.4	0.3 \pm 0.5	1.5 \pm 1.3	2.7 \pm 2.0
$V+\gamma$	1 273 \pm 90	2.5 \pm 2.4	0.0 \pm 0.7	2.2 \pm 1.5	22.4 \pm 5.5
Total predicted	1 638 000 \pm 64 000	7 710 \pm 330	3 420 \pm 140	2 770 \pm 140	26 300 \pm 1 000
Data	1 673 057	7 896	3 372	3 059	26 567

The $t\bar{t}$ background is evaluated with a data-driven methodology. A $t\bar{t}$ -enriched control region is constructed with the same event selection as the signal region, but with $e^\pm\mu^\mp$ final states instead of the same-flavour e^+e^- or $\mu^+\mu^-$ pairs. This control region contains only percent-level contributions from Z + jets, W + jets, diboson, single-top and $Z \rightarrow \tau^+\tau^-$ events. The prediction for the $t\bar{t}$ distributions in the signal region is obtained by multiplying the corresponding measured distributions in the control region (after subtracting the non- $t\bar{t}$ contributions) by $ee/e\mu$ and $\mu\mu/e\mu$ scale factors [84]. These factors are computed bin by bin in the signal region for each distribution using simulation.

Diboson backgrounds are dominated by two contributions: semileptonic WZ and ZZ final states, and fully leptonic diboson final states where the decay products of a gauge boson are reconstructed as jets. The measured kinematics of the boson decay products, as well as the production of one or two additional jets, agrees with predictions from SHERPA, as demonstrated in Refs. [85–89] within the modelling uncertainties described in Section 7. The simulation of the EW Zjj events done with HERWIG+VBFNLO agrees with measurements performed in $(Z \rightarrow \ell^+\ell^-)$ -enriched phase spaces [12]. Due to their good performance in previous measurements, simulations are used to describe the diboson and EW Zjj backgrounds in this analysis.

Multijet events are assessed with a data-driven approach using a template fit of the $m_{\ell\ell}$ distribution. The $m_{\ell\ell}$ template for this background is derived from data in a multijet-enriched control region, which is defined by either inverting or dropping the lepton selection requirements associated with isolation, identification and charge. The sub-percent contributions to the multijet template that do not originate from the multijet background are evaluated and subtracted using simulation. The fit is performed over the range $51 \text{ GeV} \leq m_{\ell\ell} \leq 151 \text{ GeV}$. The contribution from multijet events in the analysis is then estimated in the invariant-mass interval of the signal region ($71 \text{ GeV} \leq m_{\ell\ell} \leq 111 \text{ GeV}$). The resulting fraction of multijet events is at the sub-percent level and so is neglected in this analysis.

Figure 2 shows the data and predicted event yields as a function of $p_{T,j1}$ in the electron channel and as a function of $\Delta R_{Z,j}^{\min}$ in the *high- p_T* region in the muon channel. The SHERPA 2.2.11 predictions agree with the data in general, but do not describe it precisely in the full range of the measurements. The distributions are discussed in more detail in Section 8.

6 Unfolding of detector effects

The cross-section measurements presented in this paper (see Section 1) are performed within the fiducial acceptance region defined by the following requirements:

- Two same-flavour, opposite-charge leptons with $p_T \geq 25 \text{ GeV}$ and $|\eta| < 2.5$
- $71 \text{ GeV} \leq m_{\ell\ell} \leq 111 \text{ GeV}$
- At least one jet, where jets must have $p_T \geq 100 \text{ GeV}$ and $|y| < 2.5$.

The *high- p_T* , *collinear*, *back-to-back*, and *high- S_T* signal regions are defined in analogy to the detector-level definitions.

The cross sections are defined at particle level, corresponding to ‘dressed’ electrons and muons. A dressed lepton is defined as the four-vector combination of a prompt lepton (that does not originate from the decay of a hadron or a τ -lepton, or from a photon conversion) and all prompt photons within a surrounding cone of size $\Delta R = 0.1$. The particle level also includes jets found by applying the anti- k_r algorithm with radius

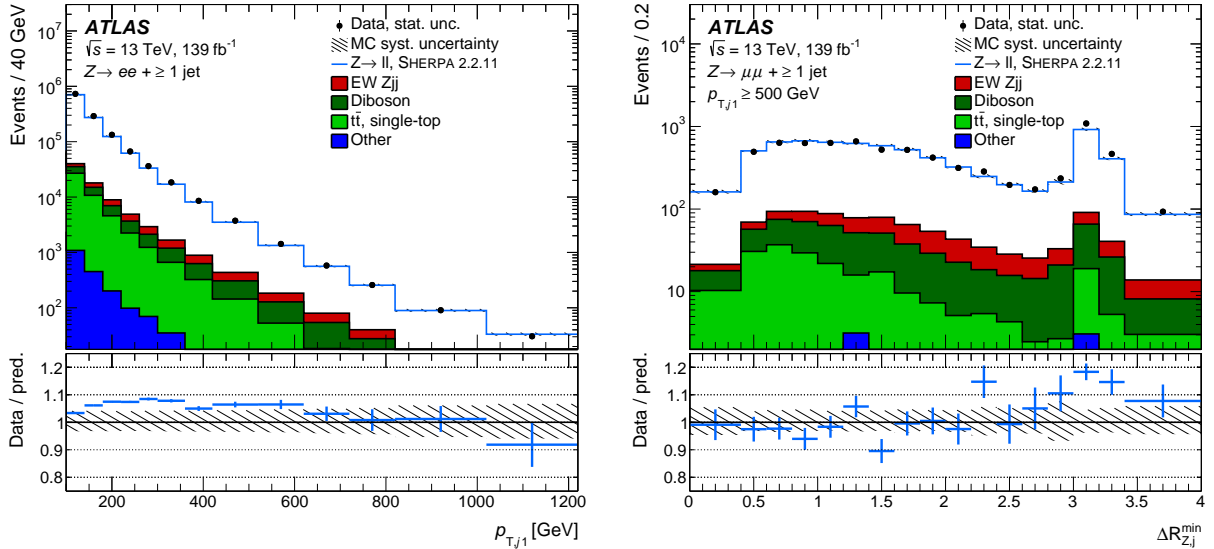


Figure 2: Distributions of the leading-jet p_T in the *inclusive* region in the electron channel (left) and the angular distance between the Z boson and the closest jet, $\Delta R_{Z,j}^{\min}$, in the *high- p_T* region in the muon channel (right). The signal and background samples are stacked to produce the figures. The W +jets, $Z \rightarrow \tau^- \tau^+$ and $V+\gamma$ processes are combined and labelled ‘Other’. The bottom panel shows the ratio of the data to the total prediction. Experimental uncertainties (described in Section 7) for the signal and background distributions are combined in the hatched band, and the data statistical uncertainty is shown as error bars.

parameter $R = 0.4$ to final-state particles with decay length $c\tau > 10$ mm, excluding dressed Z -boson decay products. Overlap removal is also applied at particle level: jets with $p_T \geq 30$ GeV within $\Delta R = 0.2$ of a dressed lepton are removed, followed by the removal of leptons within $\Delta R = 0.4$ of the remaining jets. This overlap removal is applied at particle level in order to best match the detector response, especially in the *collinear* region where the detector is not able to discriminate easily between nearby objects.

The fiducial cross sections are evaluated from the reconstructed kinematic observables for events that pass the selection described in Section 4. The expected background components, as described in Section 5, are subtracted from the distributions in data.

An iterative unfolding technique [90] with two iterations, as implemented in the RooUnfold package [91], is used to unfold the background-subtracted data to the particle level, thereby accounting for the impact of detector inefficiencies and resolution [72–74, 80, 83]. Before entering the iterative unfolding, the background-subtracted data are corrected for the expected fraction of events passing the detector-level selection but not the particle-level selection. The unfolding is carried out with the response matrices constructed from the SHERPA 2.2.11 Z +jets samples. The unfolded event yields are divided by the integrated luminosity of the data sample to provide the final fiducial cross sections [92]. The electron and muon channels are unfolded separately and then combined to measure the production cross section for a Z boson decaying into a single charged-lepton flavour ($Z \rightarrow \ell^+ \ell^-$).

The binning of all observables is optimised to keep the statistical uncertainty below 10% and to maximize the purity, or the fraction of reconstructed events where the reconstructed and truth values fall in the same bin. The latter is kept above 60%, with typical values of 70 – 90%. In order to mitigate the modelling uncertainty due to migration effects across the lower edge of the $p_{T,j1}$ distribution, this observable is

unfolded using two underflow bins within $60 \text{ GeV} \leq p_{T,j1} \leq 100 \text{ GeV}$. In a similar fashion, an underflow bin is added for the $p_{T,\ell\ell}$, H_T and jet multiplicity distributions for events where the leading jet does not pass the $p_T \geq 100 \text{ GeV}$ selection but instead has $60 \text{ GeV} \leq p_{T,j1} \leq 100 \text{ GeV}$. The unfolding of $r_{Z,j}$ is performed in two dimensions using three bins for the p_T of the closest jet for each bin of $r_{Z,j}$.

7 Systematic uncertainties

Theory modelling uncertainties

Theoretical modelling uncertainties from the MC predictions are considered when unfolding the data and in the comparisons with the cross-section measurements.

Modelling uncertainties are taken into account by varying the QCD scales, the PDFs and, in the case of SHERPA 2.2.11, the virtual EW corrections. The effect of QCD scale uncertainties is defined by the envelope of variations resulting from changing the renormalisation (μ_r) and factorisation (μ_f) scales by factors of two with an additional constraint of $0.5 \leq \mu_r/\mu_f \leq 2$. Uncertainties due to the PDF parameterisation are evaluated using sets of PDF variations [93]. The PDF uncertainties also include a comparison with the nominal MMHT2014_{NNLO} [56] PDF and the CT14_{NNLO} [94] PDFs. For SHERPA Z + jets and diboson processes, the PDF uncertainties also include a consistent variation of α_s in the PDF and in the hard scatter based on NNPDF3.0_{NLO} [42]. The prediction from SHERPA 2.2.11 also considers uncertainties related to the NLO virtual EW corrections, derived from the envelope of the additive, multiplicative and exponentiated EW correction schemes [19]. The uncertainties associated with the virtual EW corrections are maximal and amount to 5% where the EW corrections are largest: in the *back-to-back* region with large $p_{T,\ell\ell}$ and $\Delta R_{Z,j}^{\min} \approx \pi$. In comparison, the effect of QCD scale uncertainties on SHERPA 2.2.11 predictions ranges between 10% and 60%, with average values near 25%. The corresponding range in MG5_AMC+PY8 FxFx is between 5% and 20%. The differences between these two generators and their uncertainties are further explored in Ref. [19]. In the NNLO_{JET} predictions, the QCD scale uncertainties are typically in the range between 5% and 10% and constitute the dominant systematic component. Due to computational limitations in the NNLO_{JET} program, the predictions do not include PDF uncertainties.

The diboson predictions used in the background subtraction from data include PDF and scale uncertainties. The EW Zjj prediction includes the effects of scale, PDF and interference uncertainties, which amount to normalisation uncertainties of 9%, 2% and 25%–40% respectively (see Section 3). The effects of scale and PDF uncertainties on the single-top predictions amount to a total normalisation uncertainty of about 4%, primarily from the normalisation to theory predictions at NNLO and NLO accuracies.

Systematic uncertainties in cross-section measurements

Systematic uncertainties in the measured cross sections stem from experimental, MC-modelling and unfolding uncertainties. The uncertainties are propagated to the data cross sections by varying the subtracted background and the MC inputs to the unfolding procedure (response matrix, fraction of unmatched events, reconstruction efficiency). They are treated as being correlated over kinematic regions, over distributions of observables and, where applicable, over channels and between signal and background processes.

Experimental uncertainties specific to each leptonic final state ($Z \rightarrow e^+e^-$ and $Z \rightarrow \mu^+\mu^-$): Systematic uncertainties in the lepton-candidate selection are related to the reconstruction, identification, isolation,

and trigger [72, 73]. Uncertainties in the lepton calibrations can cause changes in the acceptance, owing to the migration of events across the p_T threshold and the $m_{\ell\ell}$ boundaries. The uncertainties in the electron energy scale and resolution are taken into account [95], as are those related to the muon momentum scale, inner-detector and muon-spectrometer resolution, and sagitta-bias correction [73].

Experimental uncertainties common to the electron and muon final states: Systematic uncertainties associated with jet reconstruction are addressed via jet-energy-scale (JES) variations in a 29- nuisance-parameter scheme and jet-energy-resolution (JER) variations in a 13- nuisance-parameter scheme [96, 97]. Imperfect modelling of the effects of pile-up leads to acceptance changes for different jet multiplicities. To assess this uncertainty, the average number of pile-up interactions is varied in simulation. The uncertainty in the combined 2015–2018 integrated luminosity is 1.7% [98], obtained using the LUCID-2 detector [99] for the primary luminosity measurements.

Modelling uncertainties: Distribution-shape variations from PDF, scale and EW uncertainties in the SHERPA 2.2.11 Z + jets simulation, computed as described above, are propagated to the unfolded cross sections via the response matrices and associated unmatched-events and efficiency corrections. Although the uncertainties in the simulation can be large, their effect on the cross-section measurement is minimised by the unfolding technique used. The systematic uncertainties in the modelling of background MC samples are propagated to the unfolded cross section via the background subtraction in the signal regions. The background-modelling uncertainty comes mainly from the diboson and EW Zjj backgrounds.

Systematic uncertainties associated with the unfolding procedure: Systematic uncertainties account for possible residual biases in the unfolding procedure, such as those due to the modelling of the signal events or the finite bin width used in each distribution. The limited size of a simulation sample can also create biases in the distribution used in the unfolding procedure. The following uncertainties from the unfolding procedure are considered:

- The statistical uncertainties of the MC inputs to the unfolding procedure are propagated to the unfolded cross sections with a ‘toy’ simulation method based on 1000 ensembles (pseudo-experiments) of unfolding inputs.
- The effects of the mismodelling of the data by the MC simulation on the results of unfolding procedure are derived by reweighting the SHERPA 2.2.11 Z + jets MC simulation at particle level for each unfolded observable, such that the MC simulation distribution matches the background-subtracted data at the reconstruction level. The reweighted MC simulation is unfolded with the non-reweighted response matrix and the uncertainty is obtained by comparing the unfolded result against the reweighted distribution at particle level (non-closure).
- An additional uncertainty is derived to account for more subtle differences between the SHERPA 2.2.11 and MG5_AMC+PY8 CKKWL generators (e.g. hadronisation models, additional soft objects, distributions in other kinematic dimensions) which are not accounted for by the previous method. A non-closure test is performed where the MG5_AMC+PY8 CKKWL samples are first reweighted to match SHERPA 2.2.11 particle-level distributions for each observable in turn and subsequently unfolded with SHERPA 2.2.11. The uncertainty is evaluated by comparing the unfolded result and the reweighted distribution at particle level.

The total fractional uncertainties of the unfolded differential cross sections in $p_{T,j1}$ and $\Delta R_{Z,j}^{\min}$ for the combined $Z \rightarrow \ell^+\ell^-$ measurement, performed as detailed in Section 8, are shown in Figure 3. Table 3 shows the breakdown of the total relative statistical and systematic uncertainties in the measured integrated cross sections for Z + jets production in the five kinematic search regions. In the *inclusive* and *high- S_T*

regions, jet uncertainties dominate with a relative contribution of 2.6% and 2.8%, respectively. In the *high-p_T* region and its *collinear* and *back-to-back* subregions the jet and data statistical uncertainties are largest, with relative contributions of 3.2% and 2.1% in the *high-p_T* region, respectively, 2.8% and 2.9% in the *collinear* region, and 3.6% and 2.7% in the *back-to-back* region.

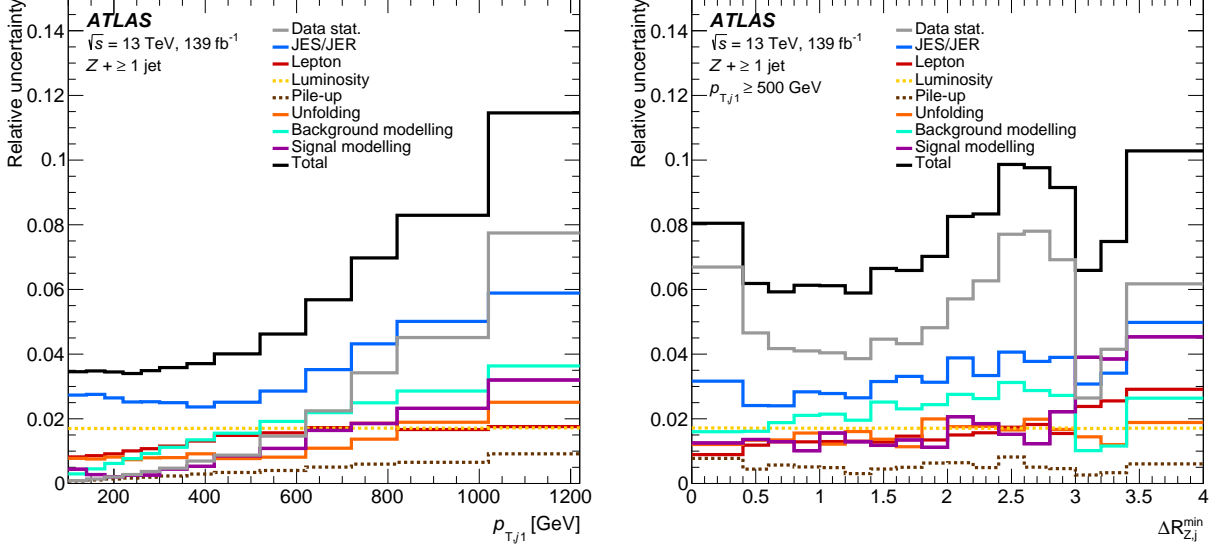


Figure 3: Fractional uncertainties in the measured differential cross-sections in $p_{T,j1}$ in the *inclusive* region (left) and in $\Delta R_{Z,j}^{\min}$ in the *high-p_T* region (right) from the combined $Z \rightarrow \ell^+\ell^-$ measurement.

Table 3: Relative statistical and systematic uncertainties (in %) in the measured integrated cross sections for $Z + \text{jets}$ production in the five search regions, computed by integrating over the respective jet-multiplicity distribution.

Uncertainty source [%]	<i>Inclusive</i>	<i>High-p_T</i>	<i>Collinear</i>	<i>Back-to-back</i>	<i>High-S_T</i>
JES/JER	2.6	3.2	2.8	3.6	2.8
Lepton	0.9	1.6	1.4	2.0	1.1
Luminosity	1.7	1.7	1.7	1.7	1.7
Pile-up	0.1	0.4	0.4	0.4	0.4
Unfolding	0.5	1.0	1.1	1.4	0.8
Background modelling	0.5	2.0	2.0	1.9	1.7
Signal modelling	0.5	1.2	1.1	1.1	1.1
Total syst. uncertainty	3.4	4.8	4.4	5.3	4.2
Data stat. uncertainty	0.1	2.1	2.9	2.7	1.2
Total uncertainty	3.4	5.3	5.3	5.9	4.4

8 Results

The integrated and differential fiducial cross sections are measured in the electron and muon channels separately, and the compatibility of the results from the two channels is tested. These results are then

combined using the Best Linear Unbiased Estimate (BLUE) method [100]. In the combination, all systematic uncertainties except the lepton-related experimental uncertainties are treated as correlated between the electron and muon channels. Data and MC statistical uncertainties are treated as uncorrelated between channels. The combined measurements are consistent with both individual decay channels for the full set of observables. In general, the uncertainties in the measured cross sections are dominated by the systematic uncertainties and are smaller than the uncertainties in the predictions, except for NNLO_{JET}@NNLO, which matches or exceeds the precision of the measurements in some kinematic regions.

Integrated fiducial cross sections for Z + jets production are evaluated in the *inclusive*, *high- p_T* , *collinear*, *back-to-back* and *high- S_T* signal regions (see Section 6) by summing over the respective unfolded jet-multiplicity distributions. The measured cross sections are compared with the predictions from SHERPA 2.2.11, MG5_AMC+PY8 FxFx, SHERPA 2.2.1 and with NNLO and NLO predictions from NNLO_{JET} in Table 4 and in Figure 4. The prediction from SHERPA 2.2.11 uniquely includes NLO virtual EW corrections (see Section 3). When these virtual corrections are removed from the SHERPA 2.2.11 prediction, its total cross sections for the *inclusive*, *high- p_T* , *collinear*, *back-to-back* and *high- S_T* regions increase by 0.065%, 6.9%, 3.8%, 11% and 3.0%, respectively. The cross sections predicted by the three generators and the NNLO_{JET} predictions agree with the measured values within the theory uncertainties.

Differential cross sections are measured and compared in Figures 5–11 with predictions from SHERPA 2.2.1, MG5_AMC+PY8 CKKWL, and the next-generation MC generators SHERPA 2.2.11 and MG5_AMC+PY8 FxFx, and with NLO and NNLO Z + jets calculations from NNLO_{JET}. In general, NNLO_{JET}@NNLO and MG5_AMC+PY8 FxFx provide the most precise predictions.

The Z -boson and jet transverse momenta (two correlated quantities) are fundamental observables of the Z + jets process and probe perturbative QCD over a wide range of scales. Moreover, understanding the kinematics of jets in events with vector bosons produced in association with several jets is essential for the modelling of backgrounds for other SM processes and searches beyond the SM. Figure 5 shows the differential cross section as a function of $p_{T,\ell\ell}$ and $p_{T,j1}$. The high- $p_{T,\ell\ell}$ region is dominated by the back-to-back topology and receives significant negative corrections due to EW effects. In contrast, events with a *high- p_T* jet typically result in both back-to-back and collinear topologies. The SHERPA 2.2.1 and MG5_AMC+PY8 CKKWL generators predict a harder $p_{T,j1}$ distribution than seen in the data, resulting in an overestimation of the cross section for high $p_{T,j1}$. In contrast, SHERPA 2.2.11 and MG5_AMC+PY8 FxFx show significantly better modelling of the $p_{T,j1}$ spectrum and are also in good agreement with the measured $p_{T,\ell\ell}$ spectrum. The smaller cross section from SHERPA 2.2.11 relative to SHERPA 2.2.1 in the *high- p_T* region is attributed to the improved matching scheme with a different treatment of unordered histories [19]. The prediction from MG5_AMC+PY8 FxFx models the data more precisely, due to the inclusion of NLO matrix elements with three partons. The NNLO_{JET}@NNLO predictions describe the data very precisely, except for very large values of $p_{T,\ell\ell}$ (and $p_{T,j1}$), where negative NLO virtual EW corrections of 10%–20% are expected and the QCD-only calculation overestimates the data.

Jet-multiplicity distributions provide an excellent probe of QCD. Whereas the Z + 1-jet bin is most sensitive to PDF effects, those with higher jet multiplicities are more sensitive to perturbative QCD effects [101]. Jet-multiplicity distributions also probe the validity of predictions in the presence of jet vetoes, which are frequently used in searches that require a specific number of jets in the selection. These vetoes create additional logarithmic terms, which are not explicitly included in the theoretical predictions presented in this paper. Figure 6 shows the differential cross section as a function of the jet multiplicity in the *inclusive* and *high- p_T* regions. As expected [101], the jet multiplicity in the *inclusive* phase space follows a downward staircase pattern, whereas in the *high- p_T* phase space, the cross section increases between 1-jet and 2-jet events followed by a downward pattern for higher jet multiplicities. While SHERPA 2.2.1 and

Table 4: Measured integrated fiducial cross sections for Z + jets production in the five signal regions and predictions from SHERPA 2.2.11, MG5_AMC+Py8 FxFx, SHERPA 2.2.1, NNLOJET@NNLO and NNLOJET@NLO. Systematic uncertainties in the measured and predicted cross sections are calculated as described in Section 7.

<i>Inclusive Z + jets</i>					
Data	13.90	± 0.01 (stat)	± 0.47 (syst)		pb
SHERPA 2.2.11	13.3	$^{+0.2}_{-0.2}$ (PDF)	$^{+3.1}_{-1.8}$ (Scale)	$\pm \leq 0.1$ (EW)	pb
MG5_AMC+Py8 FxFx	14.5	$^{+0.1}_{-0.1}$ (PDF)	$^{+0.8}_{-1.2}$ (Scale)		pb
SHERPA 2.2.1	13.8	$^{+0.5}_{-0.5}$ (PDF)	$^{+5.2}_{-3.4}$ (Scale)		pb
NNLOJET@NNLO	13.83		$^{+0.18}_{-0.27}$ (Scale)		pb
NNLOJET@NLO	13.5		$^{+1.1}_{-0.9}$ (Scale)		pb
<i>High-p_T: $p_{T,j1} \geq 500$ GeV</i>					
Data	72.3	± 1.5 (stat)	± 3.5 (syst)		fb
SHERPA 2.2.11	69	$^{+2}_{-1}$ (PDF)	$^{+28}_{-17}$ (Scale)	$^{+2}_{-2}$ (EW)	fb
MG5_AMC+Py8 FxFx	78	$^{+4}_{-1}$ (PDF)	$^{+9}_{-12}$ (Scale)		fb
SHERPA 2.2.1	95	$^{+4}_{-3}$ (PDF)	$^{+40}_{-26}$ (Scale)		fb
NNLOJET@NNLO	76		$^{+10}_{-12}$ (Scale)		fb
NNLOJET@NLO	71		$^{+14}_{-11}$ (Scale)		fb
<i>Collinear: High-p_T and $\Delta R_{Z,j}^{\min} \leq 1.4$</i>					
Data	27.9	± 0.8 (stat)	± 1.2 (syst)		fb
SHERPA 2.2.11	28	$^{+1}_{-1}$ (PDF)	$^{+14}_{-8}$ (Scale)	$\pm \leq 1$ (EW)	fb
MG5_AMC+Py8 FxFx	29.6	$^{+1.3}_{-0.3}$ (PDF)	$^{+3.1}_{-4.3}$ (Scale)		fb
SHERPA 2.2.1	39	$^{+2}_{-1}$ (PDF)	$^{+18}_{-11}$ (Scale)		fb
NNLOJET@NNLO	27.0		$^{+5.7}_{-7.2}$ (Scale)		fb
NNLOJET@NLO	24.1		$^{+7.0}_{-5.1}$ (Scale)		fb
<i>Back-to-back: High-p_T and $\Delta R_{Z,j}^{\min} \geq 2.0$</i>					
Data	31.6	± 0.8 (stat)	± 1.7 (syst)		fb
SHERPA 2.2.11	28.1	$^{+0.6}_{-0.3}$ (PDF)	$^{+7.9}_{-4.9}$ (Scale)	$^{+1.4}_{-1.4}$ (EW)	fb
MG5_AMC+Py8 FxFx	34.4	$^{+1.6}_{-0.3}$ (PDF)	$^{+4.6}_{-5.6}$ (Scale)		fb
SHERPA 2.2.1	38	$^{+2}_{-1}$ (PDF)	$^{+15}_{-10}$ (Scale)		fb
NNLOJET@NNLO	35.3		$^{+1.9}_{-2.4}$ (Scale)		fb
NNLOJET@NLO	36.0		$^{+3.5}_{-3.3}$ (Scale)		fb
<i>High-S_T: $S_T \geq 600$ GeV</i>					
Data	226.0	± 2.6 (stat)	± 9.5 (syst)		fb
SHERPA 2.2.11	220	$^{+10}_{-10}$ (PDF)	$^{+110}_{-60}$ (Scale)	$\pm \leq 10$ (EW)	fb
MG5_AMC+Py8 FxFx	247	$^{+10}_{-2}$ (PDF)	$^{+30}_{-37}$ (Scale)		fb
SHERPA 2.2.1	280	$^{+10}_{-10}$ (PDF)	$^{+130}_{-80}$ (Scale)		fb
NNLOJET@NNLO	223		$^{+43}_{-47}$ (Scale)		fb
NNLOJET@NLO	168		$^{+45}_{-33}$ (Scale)		fb

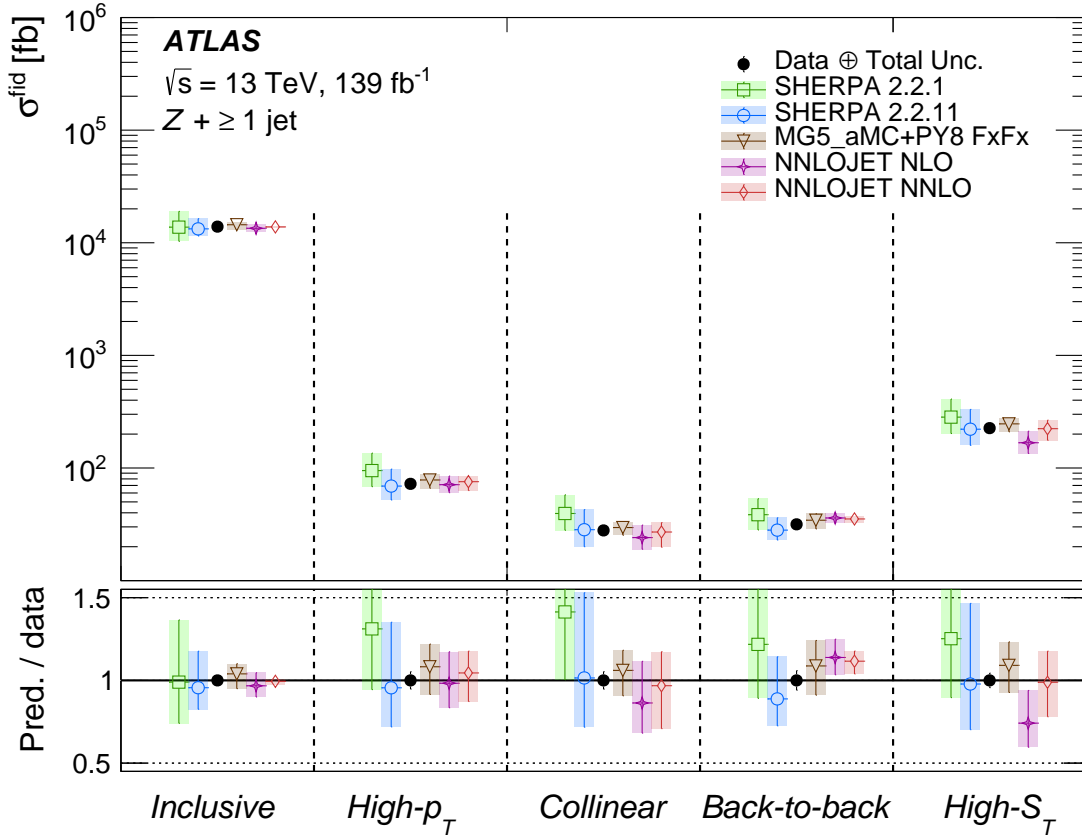


Figure 4: Summary of integrated fiducial cross-section results. The measured cross sections are shown with black points and the error bars represent the total uncertainty. Data are compared with predictions from MC generators and fixed-order calculations. The uncertainties in the predictions are found by adding in quadrature the uncertainties from the variations of the PDF (excluding NNLOJET predictions), QCD scales and, for SHERPA 2.2.11, virtual EW contributions, as explained in Section 7.

MG5_AMC+PY8 CKKWL tend to overestimate the cross section for higher jet multiplicities, SHERPA 2.2.11 and MG5_AMC+PY8 FxFx agree with the data for both the *inclusive* and *high- p_T* regions, the latter generator at a higher level of precision. The NNLOJET predictions agree with the data in the *inclusive* and *high- p_T* phase spaces at high precision when it is expected from the order of the calculation, and at lower precision when the order of the calculation is exceeded.

The angular distance between the Z boson and the closest jet, $\Delta R_{Z,j}^{\min}$, and the ratio of the Z-boson transverse momentum to the closest-jet transverse momentum, $r_{Z,j}$, provide a way to distinguish between the presence of collinear Z-boson emission and back-to-back topologies. In the *high- p_T* selection, the collinear region is sensitive to logarithmic enhancements in production proportional to $\alpha_s \ln^2(p_{T,j1}/m_Z)$, whereas the back-to-back region receives non-negligible virtual EW corrections. Figure 7 shows the differential cross sections as a function of $\Delta R_{Z,j}^{\min}$ and $r_{Z,j}$ in the *high- p_T* region. Both distributions show an accumulation of events at low and high values of these two quantities: *collinear* events populate the figures at values $\Delta R_{Z,j}^{\min} \leq 1.4$ and $r_{Z,j} \leq 0.4$, while the *back-to-back* events are observed with $\Delta R_{Z,j}^{\min} \approx \pi$ and $r_{Z,j} \approx 1.0$. The collinear events are expected to be dominated by diagrams corresponding to the EW radiation of a Z boson from one of the legs of a dijet event. Consequently, they are expected to correspond to the

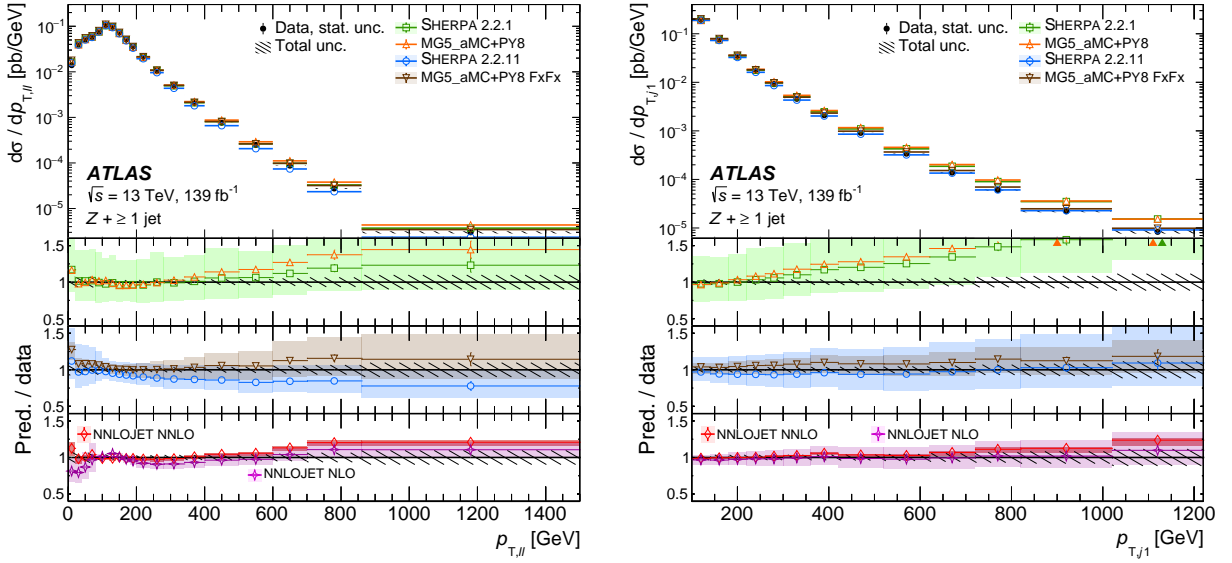


Figure 5: Differential cross section as a function of the transverse momentum of the Z boson (left) and of the transverse momentum of the leading jet (right) in the *inclusive* region. The unfolded data are shown with the black points where the statistical uncertainty is given as an error bar and the total uncertainty as a hatched region. The data are compared with predictions from MC generators and fixed-order calculations. In the ratio panels, the error bars correspond to the statistical uncertainty of the prediction and solid triangles indicate that the prediction is outside the vertical-axis range, while the total uncertainty of the unfolded data is represented as the hatched region. The uncertainties in the predictions, dominated by the scale uncertainties, are shown only in the ratio panels, except for MG5_AMC+PY8 CKKWL which is not included. They are found by adding in quadrature the uncertainties from the variations of the PDF (excluding NNLOJET predictions), QCD scales and, for SHERPA 2.2.11, virtual EW contributions, as explained in Section 7.

accumulation of events with low values of $r_{Z,j}$. This hypothesis is validated in Figure 8, which shows the measurement of the $r_{Z,j}$ distribution for the subset of *collinear* events defined by $\Delta R_{Z,j}^{\min} \leq 1.4$ where only the accumulation of low- $r_{Z,j}$ events is observed. In contrast, the measurement of the $r_{Z,j}$ distribution for the *back-to-back* selection defined by $\Delta R_{Z,j}^{\min} \geq 2.0$ is populated by events with $r_{Z,j} \approx 1$. The jet multiplicity is also measured separately for the *collinear* and *back-to-back* topologies as shown in Figure 9. It is found that the *collinear* region is dominated by dijet events whereas the *back-to-back* region is dominated by Z + 1-jet events.

Figures 7–9 show that while still marginally in agreement with data within modelling uncertainties of up to 50%, SHERPA 2.2.1 central values increasingly overestimate the cross section with decreasing values of $\Delta R_{Z,j}^{\min}$. A similar trend is observed for MG5_AMC+PY8 CKKWL. The modelling is improved by the state-of-the-art generators MG5_AMC+PY8 FxFx and SHERPA 2.2.11. Good agreement of MG5_AMC+PY8 FxFx and SHERPA 2.2.11 with data even for very collinear events indicates that resummation of the additional logarithmic terms, e.g. via EW showers, is not needed at the present level of theoretical and experimental precision in the experimentally accessible kinematic regime. The NNLOJET@NNLO prediction models the data distribution in both the *collinear* and the *back-to-back* regions with high precision. The good performance in the *collinear* phase space is remarkable, as this region contains a large fraction of events with at least three jets, which are simulated only at LO in NNLOJET@NNLO and not at all by NNLOJET@NLO. The QCD-only calculation overestimates the cross section for exact *back-to-back* events in the *high-p_T*

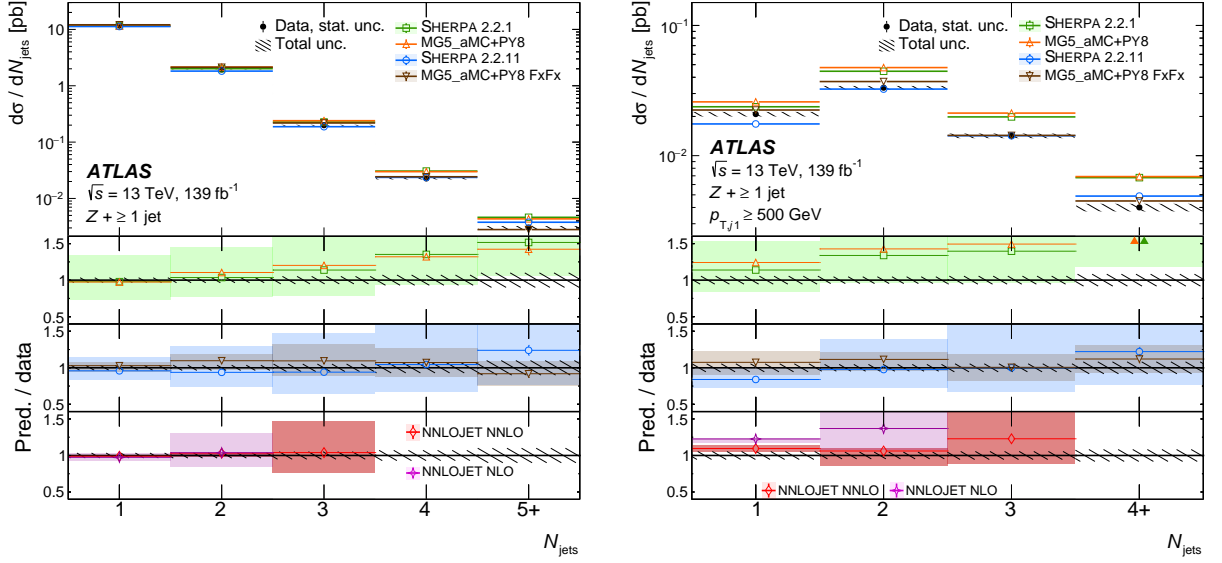


Figure 6: Differential cross section as a function of the jet multiplicity in the *inclusive* region (left) and *high- p_T* region (right). In each case, the last bin is inclusive in higher jet multiplicities. Further details are provided in the caption of Figure 5.

region, dominated by high- $p_{T,\ell\ell}$ events, consistent with the pattern observed in Figure 5.

An alternative way to select a high-energy phase space is by requiring a large value of H_T or S_T . The former is often used as a dynamical scale choice, whereas the latter is more suited to selecting a phase space similar to the *high- p_T* region. Figure 10 shows the differential cross section as a function of H_T . The central values from SHERPA 2.2.1 increasingly overestimate the cross section with increasing H_T , while still marginally agreeing with the data within modelling uncertainties of up to 50%. The prediction from MG5_AMC+PY8 CKKWL shows a similar trend. In contrast, the state-of-the-art predictions from SHERPA 2.2.11, MG5_AMC+PY8 FxFx and NNLOJET@NNLO model the data well, the last with higher precision. Figure 11 shows the differential cross section as a function of $\Delta R_{Z,j}^{\text{min}}$ and jet multiplicity in the *high- S_T* region. The *high- S_T* region probes high-energy events where the energy is typically shared by several jets. Compared to the *high- p_T* region, the jet multiplicity distribution is shifted towards higher values, and the *back-to-back* peak in the $\Delta R_{Z,j}^{\text{min}}$ distribution is suppressed relative to events where a jet is in closer proximity to the Z boson. As in the *high- p_T* region, SHERPA 2.2.1 is marginally consistent with the data within a large theoretical uncertainty, with the overestimation of the central values most pronounced in the *collinear* region and for higher jet multiplicities, with MG5_AMC+PY8 CKKWL showing a similar trend. Both SHERPA 2.2.11 and MG5_AMC+PY8 FxFx are consistent with the data, the latter at higher precision. The NNLOJET@NNLO prediction models this region well and with high precision, even though the fraction of events with at least three jets is larger than in the *high- p_T* phase space.

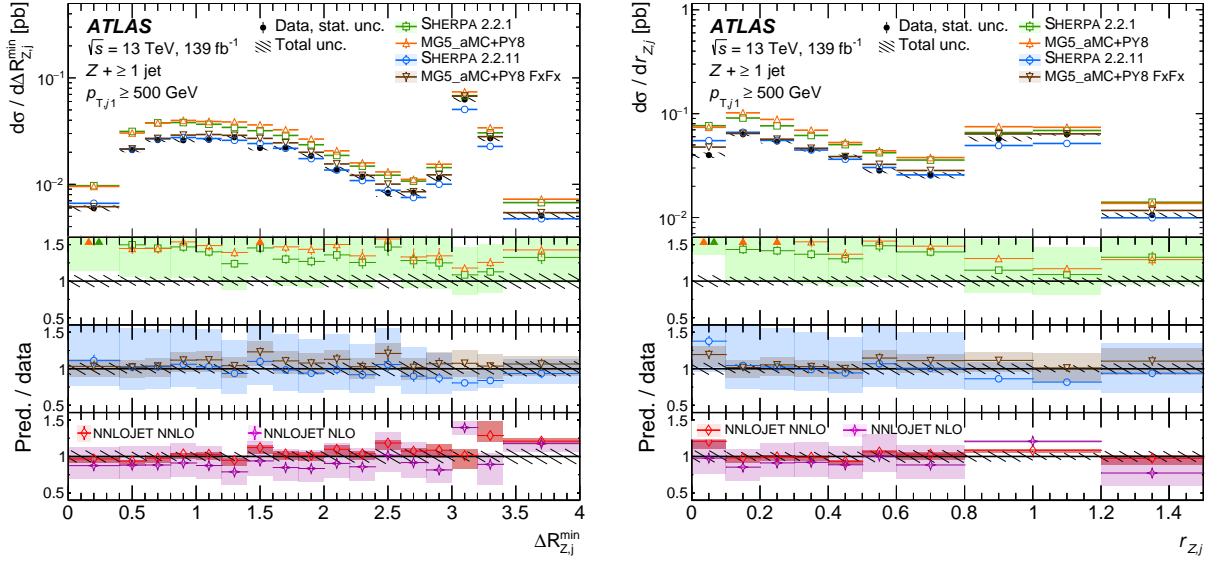


Figure 7: Differential cross section as a function of angular distance between the Z boson and the closest jet, $\Delta R_{Z,j}^{\min}$ (left) and of the ratio of Z-boson to closest-jet transverse momenta $r_{Z,j}$ (right) in the *high- p_T* region. For the NNLOJET predictions, the bins around $r_{Z,j} = 1$ are merged to be insensitive to the singularity in the fixed-order calculation. Further details are provided in the caption of Figure 5.

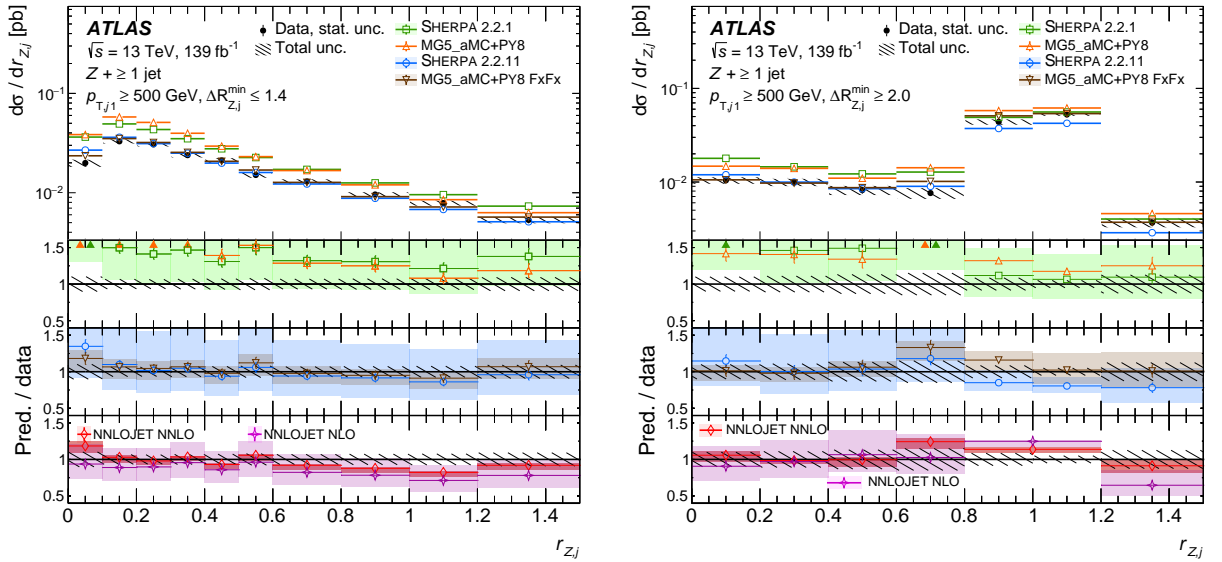


Figure 8: Differential cross section as a function of the ratio of Z-boson to closest-jet transverse momenta $r_{Z,j}$ in the *collinear* $\Delta R_{Z,j}^{\min} \leq 1.4$ region (left) and in the *back-to-back* $\Delta R_{Z,j}^{\min} \geq 2.0$ region (right). For the NNLOJET predictions, the bins around $r_{Z,j} = 1$ are merged to be insensitive to the singularity in the fixed-order calculation. Further details are provided in the caption of Figure 5.

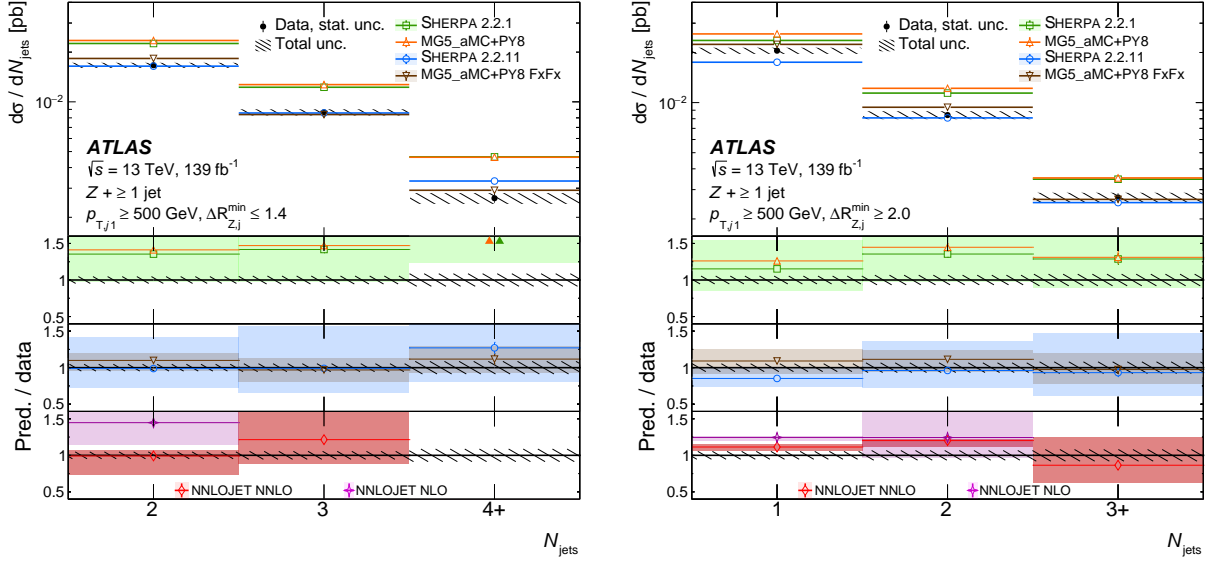


Figure 9: Differential cross section as a function of the jet multiplicity in the *collinear* $\Delta R_{Z,j}^{\min} \leq 1.4$ region (left) and in the *back-to-back* $\Delta R_{Z,j}^{\min} \geq 2.0$ region (right). In each case, the last bin is inclusive in higher jet multiplicities. In data, no events with exactly one jet are selected in the *collinear* region. Further details are provided in the caption of Figure 5.

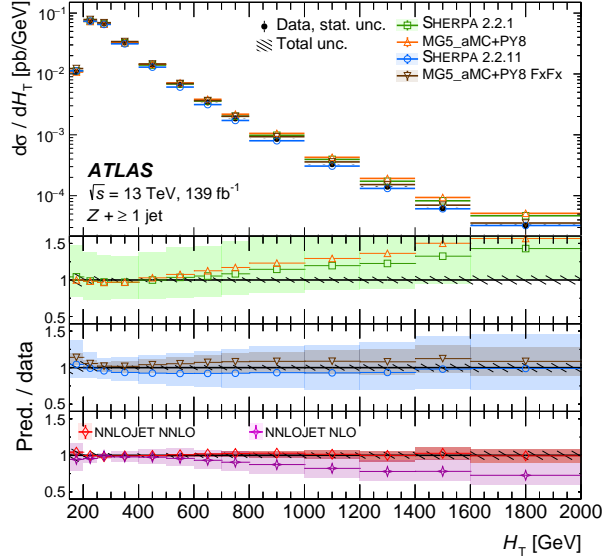


Figure 10: Differential cross section as a function of the transverse momenta scalar sum H_T in the *inclusive* region. Further details are provided in the caption of Figure 5.

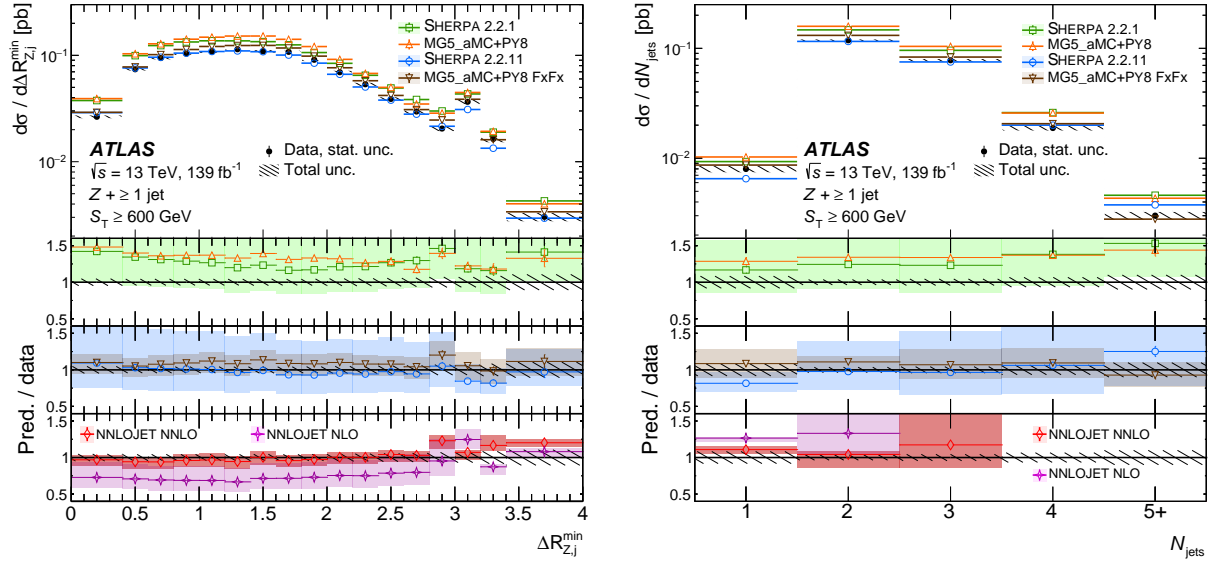


Figure 11: Differential cross section as a function of the angular distance $\Delta R_{Z,j}^{\min}$ between the Z boson and the closest jet (left) and of the jet multiplicity (right) in the $high-S_T$ region. In the jet-multiplicity distribution, the last bin is inclusive in higher jet multiplicities. Further details are provided in the caption of Figure 5.

9 Conclusions

This paper presents measurements of cross sections for a Z boson produced in association with high-transverse-momentum jets and decaying into a charged-lepton pair. The data were collected from pp collisions at $\sqrt{s} = 13$ TeV with the ATLAS detector at the LHC during 2015–2018 and correspond to an integrated luminosity of 139 fb^{-1} . Measurements were performed on events that contain a Z -boson candidate reconstructed from an e^+e^- pair or a $\mu^+\mu^-$ pair in association with hadronic jets defined as jets having transverse momentum greater than or equal to 100 GeV. Primarily, only the QCD component of Z + jets production is measured, treating the EW Zjj processes as a background. The paper focuses on selections with very high leading-jet p_T ($p_{T,j1} \geq 500$ GeV) and very high S_T ($S_T \geq 600$ GeV), which are used to study two populations of events – collinear events and back-to-back events – with distinct patterns in distributions of $\Delta R_{Z,j}^{\min}$, $r_{Z,j}$, and jet multiplicity.

The data distributions were unfolded to the particle level and compared with state-of-the-art generator predictions and fixed-order calculations. Both SHERPA 2.2.1 and MG5_AMC+PY8 CKKWL overestimate the cross sections for large values of $p_{T,j1}$, H_T and S_T . The predictions from MG5_AMC+PY8 FxFx, with matrix elements for up to three partons at NLO, offer a significant improvement over MG5_AMC+PY8 CKKWL (which models up to four partons at LO) and in general match the data with high precision. Similarly, SHERPA 2.2.11, with the addition of a fifth parton at LO in the matrix element, the addition of NLO virtual EW corrections, and a different treatment of unordered histories in the parton shower, shows a significant improvement over SHERPA 2.2.1 and agrees with the data. The NNLO calculations at fixed order from NNLOJET describe the data cross sections at a very high level of precision, including in high- p_T regions where a sizeable fraction of the events have more than two jets. The calculation exhibits a harder $p_{T,\ell\ell}$ spectrum than the data in a region where larger negative EW corrections are expected.

Acknowledgements

We thank CERN for the very successful operation of the LHC, as well as the support staff from our institutions without whom ATLAS could not be operated efficiently.

We acknowledge the support of ANPCyT, Argentina; YerPhI, Armenia; ARC, Australia; BMWFW and FWF, Austria; ANAS, Azerbaijan; CNPq and FAPESP, Brazil; NSERC, NRC and CFI, Canada; CERN; ANID, Chile; CAS, MOST and NSFC, China; Minciencias, Colombia; MEYS CR, Czech Republic; DNRF and DNSRC, Denmark; IN2P3-CNRS and CEA-DRF/IRFU, France; SRNSFG, Georgia; BMBF, HGF and MPG, Germany; GSRI, Greece; RGC and Hong Kong SAR, China; ISF and Benoziyo Center, Israel; INFN, Italy; MEXT and JSPS, Japan; CNRST, Morocco; NWO, Netherlands; RCN, Norway; MEiN, Poland; FCT, Portugal; MNE/IFA, Romania; MESTD, Serbia; MSSR, Slovakia; ARRS and MIZŠ, Slovenia; DSI/NRF, South Africa; MICINN, Spain; SRC and Wallenberg Foundation, Sweden; SERI, SNSF and Cantons of Bern and Geneva, Switzerland; MOST, Taiwan; TENMAK, Türkiye; STFC, United Kingdom; DOE and NSF, United States of America. In addition, individual groups and members have received support from BCKDF, CANARIE, Compute Canada and CRC, Canada; PRIMUS 21/SCI/017 and UNCE SCI/013, Czech Republic; COST, ERC, ERDF, Horizon 2020 and Marie Skłodowska-Curie Actions, European Union; Investissements d’Avenir Labex, Investissements d’Avenir Idex and ANR, France; DFG and AvH Foundation, Germany; Herakleitos, Thales and Aristeia programmes co-financed by EU-ESF and the Greek NSRF, Greece; BSF-NSF and MINERVA, Israel; Norwegian Financial Mechanism 2014–2021, Norway; NCN and NAWA, Poland; La Caixa Banking Foundation, CERCA Programme Generalitat de

Catalunya and PROMETEO and GenT Programmes Generalitat Valenciana, Spain; Göran Gustafssons Stiftelse, Sweden; The Royal Society and Leverhulme Trust, United Kingdom.

The crucial computing support from all WLCG partners is acknowledged gratefully, in particular from CERN, the ATLAS Tier-1 facilities at TRIUMF (Canada), NDGF (Denmark, Norway, Sweden), CC-IN2P3 (France), KIT/GridKA (Germany), INFN-CNAF (Italy), NL-T1 (Netherlands), PIC (Spain), ASGC (Taiwan), RAL (UK) and BNL (USA), the Tier-2 facilities worldwide and large non-WLCG resource providers. Major contributors of computing resources are listed in Ref. [[102](#)].

References

- [1] D. J. Gross and F. Wilczek, *Asymptotically Free Gauge Theories. I*, [Phys. Rev. D **8** \(1973\) 3633](#).
- [2] H. D. Politzer, *Asymptotic freedom: an approach to strong interactions*, [Phys. Rep. **14** \(1974\) 129](#).
- [3] M. Rubin, G. P. Salam and S. Sapeta, *Giant QCD K-factors beyond NLO*, [JHEP **09** \(2010\) 084](#), arXiv: [1006.2144 \[hep-ph\]](#).
- [4] J. R. Christiansen and S. Prestel, *Merging weak and QCD showers with matrix elements*, [Eur. Phys. J. C **76** \(2016\) 39](#), arXiv: [1510.01517 \[hep-ph\]](#).
- [5] R. Boughezal, C. Focke and X. Liu, *Jet vetoes versus giant K-factors in the exclusive Z + 1-jet cross section*, [Phys. Rev. D **92** \(2015\) 09400](#), arXiv: [1501.01059 \[hep-ph\]](#).
- [6] J. R. Christiansen and T. Sjöstrand, *Weak gauge boson radiation in parton showers*, [JHEP **04** \(2014\) 115](#), arXiv: [1401.5238 \[hep-ph\]](#).
- [7] ATLAS Collaboration, *Measurement of the associated production of a Higgs boson decaying into b-quarks with a vector boson at high transverse momentum in pp collisions at $\sqrt{s} = 13$ TeV with the ATLAS detector*, [Phys. Lett. B **816** \(2021\) 136204](#), arXiv: [2008.02508 \[hep-ex\]](#).
- [8] ATLAS Collaboration, *Measurement of the production cross section for a Higgs boson in association with a vector boson in the $H \rightarrow WW^* \rightarrow \ell\nu\ell\nu$ channel in pp collisions at $\sqrt{s} = 13$ TeV with the ATLAS detector*, [Phys. Lett. B **798** \(2019\) 134949](#), arXiv: [1903.10052 \[hep-ex\]](#).
- [9] ATLAS Collaboration, *Search for squarks and gluinos in final states with one isolated lepton, jets, and missing transverse momentum at $\sqrt{s} = 13$ TeV with the ATLAS detector*, [Eur. Phys. J. C **81** \(2021\) 600](#), arXiv: [2101.01629 \[hep-ex\]](#), Erratum: [Eur. Phys. J. C **81** \(2021\) 956](#).
- [10] ATLAS Collaboration, *Searches for electroweak production of supersymmetric particles with compressed mass spectra in $\sqrt{s} = 13$ TeV pp collisions with the ATLAS detector*, [Phys. Rev. D **101** \(2020\) 052005](#), arXiv: [1911.12606 \[hep-ex\]](#).
- [11] CMS Collaboration, *Search for a heavy vector resonance decaying to a Z boson and a Higgs boson in proton–proton collisions at $\sqrt{s} = 13$ TeV*, [Eur. Phys. J. C **81** \(2021\) 688](#), arXiv: [2102.08198 \[hep-ex\]](#).
- [12] ATLAS Collaboration, *Differential cross-section measurements for the electroweak production of dijets in association with a Z boson in proton–proton collisions at ATLAS*, [Eur. Phys. J. C **81** \(2021\) 163](#), arXiv: [2006.15458 \[hep-ex\]](#).
- [13] E. Maguire, L. Heinrich and G. Watt, *HEPData: a repository for high energy physics data*, [J. Phys. Conf. Ser. **898** \(2017\) 102006](#), ed. by R. Mount and C. Tull, arXiv: [1704.05473 \[hep-ex\]](#).
- [14] ATLAS Collaboration, *The ATLAS Experiment at the CERN Large Hadron Collider*, [JINST **3** \(2008\) S08003](#).
- [15] L. Evans and P. Bryant, *LHC Machine*, [JINST **3** \(2008\) S08001](#).
- [16] ATLAS Collaboration, *Measurement of W boson angular distributions in events with high transverse momentum jets at $\sqrt{s} = 8$ TeV using the ATLAS detector*, [Phys. Lett. B **765** \(2017\) 132](#), arXiv: [1609.07045 \[hep-ex\]](#).

- [17] CMS Collaboration, *Measurements of the differential cross sections of the production of Z +jets and γ +jets and of Z boson emission collinear with a jet in pp collisions at $\sqrt{s} = 13$ TeV*, [JHEP **05** \(2021\) 285](#), arXiv: [2102.02238 \[hep-ex\]](#).
- [18] E. Bothmann et al., *Event generation with Sherpa 2.2*, [SciPost Phys. **7** \(2019\) 034](#), arXiv: [1905.09127 \[hep-ph\]](#).
- [19] ATLAS Collaboration, *Modelling and computational improvements to the simulation of single vector-boson plus jet processes for the ATLAS experiment*, [JHEP **08** \(2021\) 089](#), arXiv: [2112.09588 \[hep-ex\]](#).
- [20] R. Frederix and S. Frixione, *Merging meets matching in MC@NLO*, [JHEP **12** \(2012\) 061](#), arXiv: [1209.6215 \[hep-ph\]](#).
- [21] T. Sjöstrand et al., *An introduction to PYTHIA 8.2*, [Comput. Phys. Commun. **191** \(2015\) 159](#), arXiv: [1410.3012 \[hep-ph\]](#).
- [22] R. Boughezal et al., *Z-Boson Production in Association with a Jet at Next-To-Next-To-Leading Order in Perturbative QCD*, [Phys. Rev. Lett. **116** \(2016\) 152001](#), arXiv: [1512.01291 \[hep-ph\]](#).
- [23] R. Boughezal, X. Liu and F. Petriello, *Phenomenology of the Z boson plus jet process at NNLO*, [Phys. Rev. D **94** \(2016\) 074015](#), arXiv: [1602.08140 \[hep-ph\]](#).
- [24] A. Gehrmann-De Ridder, T. Gehrmann, E. W. N. Glover, A. Huss and T. A. Morgan, *Precise QCD Predictions for the Production of a Z Boson in Association with a Hadronic Jet*, [Phys. Rev. Lett. **117** \(2016\) 022001](#), arXiv: [1507.02850 \[hep-ph\]](#).
- [25] A. Gehrmann-De Ridder, T. Gehrmann, E. W. N. Glover, A. Huss and T. A. Morgan, *The NNLO QCD corrections to Z boson production at large transverse momentum*, [JHEP **07** \(2016\) 133](#), arXiv: [1605.04295 \[hep-ph\]](#).
- [26] S. Kallweit, J. M. Lindert, P. Maierhöfer, S. Pozzorini and M. Schönherr, *NLO QCD+EW predictions for V + jets including off-shell vector-boson decays and multijet merging*, [JHEP **04** \(2016\) 021](#), arXiv: [1511.08692 \[hep-ph\]](#).
- [27] S. Kallweit, J. M. Lindert, P. Maierhöfer, S. Pozzorini and M. Schönherr, *NLO electroweak automation and precise predictions for W +multijet production at the LHC*, [JHEP **04** \(2015\) 012](#), arXiv: [1412.5157 \[hep-ph\]](#).
- [28] ATLAS Collaboration, *The ATLAS Collaboration Software and Firmware*, ATL-SOFT-PUB-2021-001, 2021, URL: <https://cds.cern.ch/record/2767187>.
- [29] ATLAS Collaboration, *Improved luminosity determination in pp collisions at $\sqrt{s} = 7$ TeV using the ATLAS detector at the LHC*, [Eur. Phys. J. C **73** \(2013\) 2518](#), arXiv: [1302.4393 \[hep-ex\]](#).
- [30] ATLAS Collaboration, *The ATLAS Simulation Infrastructure*, [Eur. Phys. J. C **70** \(2010\) 823](#), arXiv: [1005.4568 \[physics.ins-det\]](#).
- [31] S. Agostinelli et al., *GEANT4 – a simulation toolkit*, [Nucl. Instrum. Meth. A **506** \(2003\) 250](#).
- [32] T. Gleisberg and S. Höche, *Comix, a new matrix element generator*, [JHEP **12** \(2008\) 039](#), arXiv: [0808.3674 \[hep-ph\]](#).
- [33] F. Buccioni et al., *OpenLoops 2*, [Eur. Phys. J. C **79** \(2019\) 866](#), arXiv: [1907.13071 \[hep-ph\]](#).
- [34] F. Cascioli, P. Maierhöfer and S. Pozzorini, *Scattering Amplitudes with Open Loops*, [Phys. Rev. Lett. **108** \(2012\) 111601](#), arXiv: [1111.5206 \[hep-ph\]](#).

- [35] A. Denner, S. Dittmaier and L. Hofer,
COLLIER: A fortran-based complex one-loop library in extended regularizations,
Comput. Phys. Commun. **212** (2017) 220, arXiv: [1604.06792 \[hep-ph\]](#).
- [36] S. Schumann and F. Krauss,
A parton shower algorithm based on Catani–Seymour dipole factorisation, *JHEP* **03** (2008) 038,
arXiv: [0709.1027 \[hep-ph\]](#).
- [37] S. Höche, F. Krauss, M. Schönherr and F. Siegert,
A critical appraisal of NLO+PS matching methods, *JHEP* **09** (2012) 049,
arXiv: [1111.1220 \[hep-ph\]](#).
- [38] S. Höche, F. Krauss, M. Schönherr and F. Siegert,
QCD matrix elements + parton showers. The NLO case, *JHEP* **04** (2013) 027,
arXiv: [1207.5030 \[hep-ph\]](#).
- [39] S. Catani, F. Krauss, B. R. Webber and R. Kuhn, *QCD Matrix Elements + Parton Showers*,
JHEP **11** (2001) 063, arXiv: [hep-ph/0109231](#).
- [40] S. Höche, F. Krauss, S. Schumann and F. Siegert, *QCD matrix elements and truncated showers*,
JHEP **05** (2009) 053, arXiv: [0903.1219 \[hep-ph\]](#).
- [41] S. Catani, S. Dittmaier, M. H. Seymour and Z. Trócsányi,
The dipole formalism for next-to-leading order QCD calculations with massive partons,
Nucl. Phys. B **627** (2002) 189, arXiv: [hep-ph/0201036](#).
- [42] The NNPDF Collaboration, R. D. Ball et al., *Parton distributions for the LHC run II*,
JHEP **04** (2015) 040, arXiv: [1410.8849 \[hep-ph\]](#).
- [43] J. Alwall et al., *The automated computation of tree-level and next-to-leading order differential cross sections, and their matching to parton shower simulations*, *JHEP* **07** (2014) 079,
arXiv: [1405.0301 \[hep-ph\]](#).
- [44] ATLAS Collaboration, *ATLAS Pythia 8 tunes to 7 TeV data*, ATL-PHYS-PUB-2014-021, 2014,
URL: <https://cds.cern.ch/record/1966419>.
- [45] NNPDF Collaboration, R. D. Ball et al., *Parton distributions with LHC data*,
Nucl. Phys. B **867** (2013) 244, arXiv: [1207.1303 \[hep-ph\]](#).
- [46] T. Sjöstrand, S. Mrenna and P. Skands, *A brief introduction to PYTHIA 8.1*,
Comput. Phys. Commun. **178** (2008) 852, arXiv: [0710.3820 \[hep-ph\]](#).
- [47] L. Lönnblad, *Correcting the Colour-Dipole Cascade Model with Fixed Order Matrix Elements*,
JHEP **05** (2002) 046, arXiv: [hep-ph/0112284](#).
- [48] L. Lönnblad and S. Prestel, *Matching tree-level matrix elements with interleaved showers*,
JHEP **03** (2012) 019, arXiv: [1109.4829 \[hep-ph\]](#).
- [49] M. Bähr et al., *Herwig++ physics and manual*, *Eur. Phys. J. C* **58** (2008) 639,
arXiv: [0803.0883 \[hep-ph\]](#).
- [50] J. Bellm et al., *Herwig 7.0/Herwig++ 3.0 release note*, *Eur. Phys. J. C* **76** (2016) 196,
arXiv: [1512.01178 \[hep-ph\]](#).
- [51] J. Baglio et al., *VBFNLO: A parton level Monte Carlo for processes with electroweak bosons – Manual for Version 2.7.0*, 2011, arXiv: [1107.4038 \[hep-ph\]](#).

- [52] S. Frixione, G. Ridolfi and P. Nason,
A positive-weight next-to-leading-order Monte Carlo for heavy flavour hadroproduction,
JHEP **09** (2007) 126, arXiv: [0707.3088 \[hep-ph\]](#).
- [53] P. Nason, *A new method for combining NLO QCD with shower Monte Carlo algorithms*,
JHEP **11** (2004) 040, arXiv: [hep-ph/0409146](#).
- [54] S. Frixione, P. Nason and C. Oleari,
Matching NLO QCD computations with parton shower simulations: the POWHEG method,
JHEP **11** (2007) 070, arXiv: [0709.2092 \[hep-ph\]](#).
- [55] S. Alioli, P. Nason, C. Oleari and E. Re, *A general framework for implementing NLO calculations in shower Monte Carlo programs: the POWHEG BOX*, **JHEP** **06** (2010) 043,
arXiv: [1002.2581 \[hep-ph\]](#).
- [56] L. A. Harland-Lang, A. D. Martin, P. Motylinski and R. S. Thorne,
Parton distributions in the LHC era: MMHT 2014 PDFs, **Eur. Phys. J. C** **75** (2015) 204,
arXiv: [1412.3989 \[hep-ph\]](#).
- [57] ATLAS Collaboration, *Studies on top-quark Monte Carlo modelling for Top2016*,
ATL-PHYS-PUB-2016-020, 2016, URL: <https://cds.cern.ch/record/2216168>.
- [58] M. Beneke, P. Falgari, S. Klein and C. Schwinn,
Hadronic top-quark pair production with NNLL threshold resummation,
Nucl. Phys. B **855** (2012) 695, arXiv: [1109.1536 \[hep-ph\]](#).
- [59] M. Cacciari, M. Czakon, M. Mangano, A. Mitov and P. Nason, *Top-pair production at hadron colliders with next-to-next-to-leading logarithmic soft-gluon resummation*,
Phys. Lett. B **710** (2012) 612, arXiv: [1111.5869 \[hep-ph\]](#).
- [60] P. Bärnreuther, M. Czakon and A. Mitov, *Percent-Level-Precision Physics at the Tevatron: Next-to-Next-to-Leading Order QCD Corrections to $q\bar{q} \rightarrow t\bar{t} + X$* ,
Phys. Rev. Lett. **109** (2012) 132001, arXiv: [1204.5201 \[hep-ph\]](#).
- [61] M. Czakon and A. Mitov, *NNLO corrections to top-pair production at hadron colliders: the all-fermionic scattering channels*, **JHEP** **12** (2012) 054, arXiv: [1207.0236 \[hep-ph\]](#).
- [62] M. Czakon and A. Mitov,
NNLO corrections to top pair production at hadron colliders: the quark-gluon reaction,
JHEP **01** (2013) 080, arXiv: [1210.6832 \[hep-ph\]](#).
- [63] M. Czakon, P. Fiedler and A. Mitov,
Total Top-Quark Pair-Production Cross Section at Hadron Colliders Through $O(\alpha_S^4)$,
Phys. Rev. Lett. **110** (2013) 252004, arXiv: [1303.6254 \[hep-ph\]](#).
- [64] M. Czakon and A. Mitov,
Top++: A program for the calculation of the top-pair cross-section at hadron colliders,
Comput. Phys. Commun. **185** (2014) 2930, arXiv: [1112.5675 \[hep-ph\]](#).
- [65] S. Frixione, E. Laenen, P. Motylinski, C. White and B. R. Webber,
Single-top hadroproduction in association with a W boson, **JHEP** **07** (2008) 029,
arXiv: [0805.3067 \[hep-ph\]](#).
- [66] N. Kidonakis,
Two-loop soft anomalous dimensions for single top quark associated production with a W^- or H^- ,
Phys. Rev. D **82** (2010) 054018, arXiv: [1005.4451 \[hep-ph\]](#).

- [67] N. Kidonakis, ‘Top Quark Production’, *Proceedings, Helmholtz International Summer School on Physics of Heavy Quarks and Hadrons (HQ 2013)* (JINR, Dubna, Russia, 15th–28th July 2013) 139, arXiv: [1311.0283 \[hep-ph\]](#).
- [68] P. Kant et al., *HATHOR for single top-quark production: Updated predictions and uncertainty estimates for single top-quark production in hadronic collisions*, *Comput. Phys. Commun.* **191** (2015) 74, arXiv: [1406.4403 \[hep-ph\]](#).
- [69] M. Aliev et al., *HATHOR – HAdronic Top and Heavy quarks crOss section calculatoR*, *Comput. Phys. Commun.* **182** (2011) 1034, arXiv: [1007.1327 \[hep-ph\]](#).
- [70] D. J. Lange, *The EvtGen particle decay simulation package*, *Nucl. Instrum. Meth. A* **462** (2001) 152.
- [71] ATLAS Collaboration, *The Pythia 8 A3 tune description of ATLAS minimum bias and inelastic measurements incorporating the Donnachie–Landshoff diffractive model*, ATL-PHYS-PUB-2016-017, 2016, URL: <https://cds.cern.ch/record/2206965>.
- [72] ATLAS Collaboration, *Electron and photon performance measurements with the ATLAS detector using the 2015–2017 LHC proton-proton collision data*, *JINST* **14** (2019) P12006, arXiv: [1908.00005 \[hep-ex\]](#).
- [73] ATLAS Collaboration, *Muon reconstruction performance of the ATLAS detector in proton–proton collision data at $\sqrt{s} = 13$ TeV*, *Eur. Phys. J. C* **76** (2016) 292, arXiv: [1603.05598 \[hep-ex\]](#).
- [74] ATLAS Collaboration, *Muon reconstruction and identification efficiency in ATLAS using the full Run 2 pp collision data set at $\sqrt{s} = 13$ TeV*, *Eur. Phys. J. C* **81** (2021) 578, arXiv: [2012.00578 \[hep-ex\]](#).
- [75] ATLAS Collaboration, *ATLAS data quality operations and performance for 2015–2018 data-taking*, *JINST* **15** (2020) P04003, arXiv: [1911.04632 \[physics.ins-det\]](#).
- [76] ATLAS Collaboration, *Performance of primary vertex reconstruction in proton-proton collisions at $\sqrt{s} = 7$ TeV in the ATLAS experiment*, ATLAS-CONF-2010-069, 2010, URL: <https://cds.cern.ch/record/1281344>.
- [77] ATLAS Collaboration, *Performance of electron and photon triggers in ATLAS during LHC Run 2*, *Eur. Phys. J. C* **80** (2020) 47, arXiv: [1909.00761 \[hep-ex\]](#).
- [78] ATLAS Collaboration, *Performance of the ATLAS muon triggers in Run 2*, *JINST* **15** (2020) P09015, arXiv: [2004.13447 \[hep-ex\]](#).
- [79] ATLAS Collaboration, *The ATLAS inner detector trigger performance in pp collisions at 13 TeV during LHC Run 2*, *Eur. Phys. J. C* **82** (2022) 206, arXiv: [2107.02485 \[hep-ex\]](#).
- [80] ATLAS Collaboration, *Jet reconstruction and performance using particle flow with the ATLAS Detector*, *Eur. Phys. J. C* **77** (2017) 466, arXiv: [1703.10485 \[hep-ex\]](#).
- [81] M. Cacciari, G. P. Salam and G. Soyez, *The anti- k_t jet clustering algorithm*, *JHEP* **04** (2008) 063, arXiv: [0802.1189 \[hep-ph\]](#).
- [82] M. Cacciari, G. P. Salam and G. Soyez, *FastJet User Manual*, *Eur. Phys. J. C* **72** (2012) 1896, arXiv: [1111.6097 \[hep-ph\]](#).

- [83] ATLAS Collaboration, *Jet energy scale and resolution measured in proton–proton collisions at $\sqrt{s} = 13$ TeV with the ATLAS detector*, *Eur. Phys. J. C* **81** (2020) 689, arXiv: [2007.02645 \[hep-ex\]](#).
- [84] ATLAS Collaboration, *Measurement of the production cross section of jets in association with a Z boson in pp collisions at $\sqrt{s} = 7$ TeV with the ATLAS detector*, *JHEP* **07** (2013) 032, arXiv: [1304.7098 \[hep-ex\]](#).
- [85] ATLAS Collaboration, *Measurement of ZZ production in the $\ell\ell\nu\nu$ final state with the ATLAS detector in pp collisions at $\sqrt{s} = 13$ TeV*, *JHEP* **10** (2019) 127, arXiv: [1905.07163 \[hep-ex\]](#).
- [86] ATLAS Collaboration, *Measurement of fiducial and differential W^+W^- production cross-sections at $\sqrt{s} = 13$ TeV with the ATLAS detector*, *Eur. Phys. J. C* **79** (2019) 884, arXiv: [1905.04242 \[hep-ex\]](#).
- [87] ATLAS Collaboration, *Measurement of $W^\pm Z$ production cross sections and gauge boson polarisation in pp collisions at $\sqrt{s} = 13$ TeV with the ATLAS detector*, *Eur. Phys. J. C* **79** (2019) 535, arXiv: [1902.05759 \[hep-ex\]](#).
- [88] ATLAS Collaboration, *ZZ $\rightarrow \ell^+\ell^-\ell'^+\ell'^-$ cross-section measurements and search for anomalous triple gauge couplings in 13 TeV pp collisions with the ATLAS detector*, *Phys. Rev. D* **97** (2018) 032005, arXiv: [1709.07703 \[hep-ex\]](#).
- [89] ATLAS Collaboration, *Measurement of $WW/WZ \rightarrow \ell\nu qq'$ production with the hadronically decaying boson reconstructed as one or two jets in pp collisions at $\sqrt{s} = 8$ TeV with ATLAS, and constraints on anomalous gauge couplings*, *Eur. Phys. J. C* **77** (2017) 563, arXiv: [1706.01702 \[hep-ex\]](#).
- [90] G. D’Agostini, *A multidimensional unfolding method based on Bayes’ theorem*, *Nucl. Instrum. Meth. A* **362** (1995) 487, ISSN: 0168-9002.
- [91] T. Adye, ‘Unfolding algorithms and tests using RooUnfold’, *Proceedings, 2011 Workshop on Statistical Issues Related to Discovery Claims in Search Experiments and Unfolding (PHYSTAT 2011)* (CERN, Geneva, Switzerland, 17th–20th Jan. 2011) 313, arXiv: [1105.1160 \[physics.data-an\]](#).
- [92] ATLAS Collaboration, *Measurements of the production cross section of a Z boson in association with jets in pp collisions at $\sqrt{s} = 13$ TeV with the ATLAS detector*, *Eur. Phys. J. C* **77** (2017) 361, arXiv: [1702.05725 \[hep-ex\]](#).
- [93] J. Butterworth et al., *PDF4LHC recommendations for LHC Run II*, *J. Phys. G* **43** (2016) 023001, arXiv: [1510.03865 \[hep-ph\]](#).
- [94] S. Dulat et al., *New parton distribution functions from a global analysis of quantum chromodynamics*, *Phys. Rev. D* **93** (2016) 033006, arXiv: [1506.07443 \[hep-ph\]](#).
- [95] ATLAS Collaboration, *Electron reconstruction and identification in the ATLAS experiment using the 2015 and 2016 LHC proton–proton collision data at $\sqrt{s} = 13$ TeV*, *Eur. Phys. J. C* **79** (2019) 639, arXiv: [1902.04655 \[hep-ex\]](#).
- [96] ATLAS Collaboration, *Jet energy scale measurements and their systematic uncertainties in proton–proton collisions at $\sqrt{s} = 13$ TeV with the ATLAS detector*, *Phys. Rev. D* **96** (2017) 072002, arXiv: [1703.09665 \[hep-ex\]](#).
- [97] ATLAS Collaboration, *Jet energy resolution in proton–proton collisions at $\sqrt{s} = 7$ TeV recorded in 2010 with the ATLAS detector*, *Eur. Phys. J. C* **73** (2013) 2306, arXiv: [1210.6210 \[hep-ex\]](#).

- [98] ATLAS Collaboration, *Luminosity determination in pp collisions at $\sqrt{s} = 13$ TeV using the ATLAS detector at the LHC*, ATLAS-CONF-2019-021, 2019, URL: <https://cds.cern.ch/record/2677054>.
- [99] G. Avoni et al., *The new LUCID-2 detector for luminosity measurement and monitoring in ATLAS*, *JINST* **13** (2018) P07017.
- [100] L. Lyons, D. Gibaut and P. Clifford, *How to combine uncorrelated estimates of a single physical quantity*, *Nucl. Instrum. Meth. A* **270** (1988) 110.
- [101] E. Gerwick, T. Plehn, S. Schumann and P. Schichtel, *Scaling Patterns for QCD Jets*, *JHEP* **10** (2012) 162, arXiv: [1208.3676](https://arxiv.org/abs/1208.3676) [[hep-ph](https://arxiv.org/abs/1208.3676)].
- [102] ATLAS Collaboration, *ATLAS Computing Acknowledgements*, ATL-SOFT-PUB-2021-003, 2021, URL: <https://cds.cern.ch/record/2776662>.

10 HepData material

The following tables will be included in the HEPData entry ([link to entry](#)):

1. Differential cross section of $p_{T,\ell\ell}$ in the *inclusive* region
2. Differential cross section of $p_{T,j1}$ in the *inclusive* region
3. Differential cross section of jet multiplicity in the *inclusive* region
4. Differential cross section of jet multiplicity in the *high- p_T* region
5. Differential cross section of $\Delta R_{Z,j}^{\min}$ in the *high- p_T* region
6. Differential cross section of $r_{Z,j}$ in the *high- p_T* region
7. Differential cross section of $r_{Z,j}$ in the *collinear* region
8. Differential cross section of $r_{Z,j}$ in the *back-to-back* region
9. Differential cross section of jet multiplicity in the *collinear* region
10. Differential cross section of jet multiplicity in the *back-to-back* region
11. Differential cross section of H_T in the *inclusive* region
12. Differential cross section of $\Delta R_{Z,j}^{\min}$ in the *high- S_T* region
13. Differential cross section of jet multiplicity in the *high- S_T* region
14. Relative bin-by-bin systematic uncertainties of $p_{T,\ell\ell}$ in the *inclusive* region
15. Relative bin-by-bin systematic uncertainties of $p_{T,j1}$ in the *inclusive* region
16. Relative bin-by-bin systematic uncertainties of jet multiplicity in the *inclusive* region
17. Relative bin-by-bin systematic uncertainties of jet multiplicity in the *high- p_T* region
18. Relative bin-by-bin systematic uncertainties of $\Delta R_{Z,j}^{\min}$ in the *high- p_T* region
19. Relative bin-by-bin systematic uncertainties of $r_{Z,j}$ in the *high- p_T* region
20. Relative bin-by-bin systematic uncertainties of $r_{Z,j}$ in the *collinear* region
21. Relative bin-by-bin systematic uncertainties of $r_{Z,j}$ in the *back-to-back* region
22. Relative bin-by-bin systematic uncertainties of jet multiplicity in the *collinear* region
23. Relative bin-by-bin systematic uncertainties of jet multiplicity in the *back-to-back* region
24. Relative bin-by-bin systematic uncertainties of H_T in the *inclusive* region
25. Relative bin-by-bin systematic uncertainties of $\Delta R_{Z,j}^{\min}$ in the *high- S_T* region
26. Relative bin-by-bin systematic uncertainties of jet multiplicity in the *high- S_T* region
27. Bin-by-bin Born to dressed level leptons correction scale factor for $p_{T,\ell\ell}$ in the *inclusive* region
28. Bin-by-bin Born to dressed level leptons correction scale factor for $p_{T,j1}$ in the *inclusive* region

29. Bin-by-bin Born to dressed level leptons correction scale factor for the jet multiplicity in the *inclusive* region
30. Bin-by-bin Born to dressed level leptons correction scale factor for the jet multiplicity in the *high- p_T* region
31. Bin-by-bin Born to dressed level leptons correction scale factor for $\Delta R_{Z,j}^{\min}$ in the *high- p_T* region
32. Bin-by-bin Born to dressed level leptons correction scale factor for $r_{Z,j}$ in the *high- p_T* region
33. Bin-by-bin Born to dressed level leptons correction scale factor for $r_{Z,j}$ in the *collinear* region
34. Bin-by-bin Born to dressed level leptons correction scale factor for $r_{Z,j}$ in the *back-to-back* region
35. Bin-by-bin Born to dressed level leptons correction scale factor for the jet multiplicity in the *collinear* region
36. Bin-by-bin Born to dressed level leptons correction scale factor for the jet multiplicity in the *back-to-back* region
37. Bin-by-bin Born to dressed level leptons correction scale factor for H_T in the *inclusive* region
38. Bin-by-bin Born to dressed level leptons correction scale factor for $\Delta R_{Z,j}^{\min}$ in the *high- S_T* region
39. Bin-by-bin Born to dressed level leptons correction scale factor for the jet multiplicity in the *high- S_T* region
40. Bin-by-bin overlap removal correction scale factor for $p_{T,\ell\ell}$ in the *inclusive* region
41. Bin-by-bin overlap removal correction scale factor for $p_{T,j1}$ in the *inclusive* region
42. Bin-by-bin overlap removal correction scale factor for the jet multiplicity in the *inclusive* region
43. Bin-by-bin overlap removal correction scale factor for the jet multiplicity in the *high- p_T* region
44. Bin-by-bin overlap removal correction scale factor for $\Delta R_{Z,j}^{\min}$ in the *high- p_T* region
45. Bin-by-bin overlap removal correction scale factor for $r_{Z,j}$ in the *high- p_T* region
46. Bin-by-bin overlap removal correction scale factor for $r_{Z,j}$ in the *collinear* region
47. Bin-by-bin overlap removal correction scale factor for $r_{Z,j}$ in the *back-to-back* region
48. Bin-by-bin overlap removal correction scale factor for the jet multiplicity in the *collinear* region
49. Bin-by-bin overlap removal correction scale factor for the jet multiplicity in the *back-to-back* region
50. Bin-by-bin overlap removal correction scale factor for H_T in the *inclusive* region
51. Bin-by-bin overlap removal correction scale factor for $\Delta R_{Z,j}^{\min}$ in the *high- S_T* region
52. Bin-by-bin overlap removal correction scale factor for the jet multiplicity in the *high- S_T* region
53. Differential cross section of $p_{T,\ell\ell}$ in the *inclusive* region, where the EW Zjj contribution is not subtracted as background
54. Differential cross section of $p_{T,j1}$ in the *inclusive* region, where the EW Zjj contribution is not subtracted as background

55. Differential cross section of jet multiplicity in the *inclusive* region, where the EW Zjj contribution is not subtracted as background
56. Differential cross section of jet multiplicity in the *high- p_T* region, where the EW Zjj contribution is not subtracted as background
57. Differential cross section of $\Delta R_{Z,j}^{\min}$ in the *high- p_T* region, where the EW Zjj contribution is not subtracted as background
58. Differential cross section of $r_{Z,j}$ in the *high- p_T* region, where the EW Zjj contribution is not subtracted as background
59. Differential cross section of $r_{Z,j}$ in the *collinear* region, where the EW Zjj contribution is not subtracted as background
60. Differential cross section of $r_{Z,j}$ in the *back-to-back* region, where the EW Zjj contribution is not subtracted as background
61. Differential cross section of jet multiplicity in the *collinear* region, where the EW Zjj contribution is not subtracted as background
62. Differential cross section of jet multiplicity in the *back-to-back* region, where the EW Zjj contribution is not subtracted as background
63. Differential cross section of H_T in the *inclusive* region, where the EW Zjj contribution is not subtracted as background
64. Differential cross section of $\Delta R_{Z,j}^{\min}$ in the *high- S_T* region, where the EW Zjj contribution is not subtracted as background
65. Differential cross section of jet multiplicity in the *high- S_T* region, where the EW Zjj contribution is not subtracted as background
66. Relative bin-by-bin systematic uncertainties of $p_{T,\ell\ell}$ in the *inclusive* region, where the EW Zjj contribution is not subtracted as background
67. Relative bin-by-bin systematic uncertainties of $p_{T,j1}$ in the *inclusive* region, where the EW Zjj contribution is not subtracted as background
68. Relative bin-by-bin systematic uncertainties of jet multiplicity in the *inclusive* region, where the EW Zjj contribution is not subtracted as background
69. Relative bin-by-bin systematic uncertainties of jet multiplicity in the *high- p_T* region, where the EW Zjj contribution is not subtracted as background
70. Relative bin-by-bin systematic uncertainties of $\Delta R_{Z,j}^{\min}$ in the *high- p_T* region, where the EW Zjj contribution is not subtracted as background
71. Relative bin-by-bin systematic uncertainties of $r_{Z,j}$ in the *high- p_T* region, where the EW Zjj contribution is not subtracted as background
72. Relative bin-by-bin systematic uncertainties of $r_{Z,j}$ in the *collinear* region, where the EW Zjj contribution is not subtracted as background
73. Relative bin-by-bin systematic uncertainties of $r_{Z,j}$ in the *back-to-back* region, where the EW Zjj contribution is not subtracted as background

74. Relative bin-by-bin systematic uncertainties of jet multiplicity in the *collinear* region, where the EW Z_{jj} contribution is not subtracted as background
75. Relative bin-by-bin systematic uncertainties of jet multiplicity in the *back-to-back* region, where the EW Z_{jj} contribution is not subtracted as background
76. Relative bin-by-bin systematic uncertainties of H_T in the *inclusive* region, where the EW Z_{jj} contribution is not subtracted as background
77. Relative bin-by-bin systematic uncertainties of $\Delta R_{Z,j}^{\min}$ in the *high- S_T* region, where the EW Z_{jj} contribution is not subtracted as background
78. Relative bin-by-bin systematic uncertainties of jet multiplicity in the *high- S_T* region, where the EW Z_{jj} contribution is not subtracted as background

The ATLAS Collaboration

G. Aad ¹⁰¹, B. Abbott ¹¹⁹, D.C. Abbott ¹⁰², K. Abeling ⁵⁵, S.H. Abidi ²⁹, A. Aboulhorma ^{35e}, H. Abramowicz ¹⁵⁰, H. Abreu ¹⁴⁹, Y. Abulaiti ¹¹⁶, A.C. Abusleme Hoffman ^{136a}, B.S. Acharya ^{68a,68b,o}, B. Achkar ⁵⁵, L. Adam ⁹⁹, C. Adam Bourdarios ⁴, L. Adamczyk ^{84a}, L. Adamek ¹⁵⁴, S.V. Addepalli ²⁶, J. Adelman ¹¹⁴, A. Adiguzel ^{21c}, S. Adorni ⁵⁶, T. Adye ¹³³, A.A. Affolder ¹³⁵, Y. Afik ³⁶, M.N. Agaras ¹³, J. Agarwala ^{72a,72b}, A. Aggarwal ⁹⁹, C. Agheorghiesei ^{27c}, J.A. Aguilar-Saavedra ^{129f}, A. Ahmad ³⁶, F. Ahmadov ^{38,w}, W.S. Ahmed ¹⁰³, X. Ai ⁴⁸, G. Aielli ^{75a,75b}, I. Aizenberg ¹⁶⁷, M. Akbiyik ⁹⁹, T.P.A. Åkesson ⁹⁷, A.V. Akimov ³⁷, K. Al Khoury ⁴¹, G.L. Alberghi ^{23b}, J. Albert ¹⁶³, P. Albicocco ⁵³, M.J. Alconada Verzini ⁸⁹, S. Alderweireldt ⁵², M. Aleksa ³⁶, I.N. Aleksandrov ³⁸, C. Alexa ^{27b}, T. Alexopoulos ¹⁰, A. Alfonsi ¹¹³, F. Alfonsi ^{23b}, M. Alhroob ¹¹⁹, B. Ali ¹³¹, S. Ali ¹⁴⁷, M. Aliev ³⁷, G. Alimonti ^{70a}, C. Allaire ³⁶, B.M.M. Allbrooke ¹⁴⁵, P.P. Allport ²⁰, A. Aloisio ^{71a,71b}, F. Alonso ⁸⁹, C. Alpigiani ¹³⁷, E. Alunno Camelia ^{75a,75b}, M. Alvarez Estevez ⁹⁸, M.G. Alvigi ^{71a,71b}, Y. Amaral Coutinho ^{81b}, A. Ambler ¹⁰³, C. Amelung ³⁶, C.G. Ames ¹⁰⁸, D. Amidei ¹⁰⁵, S.P. Amor Dos Santos ^{129a}, S. Amoroso ⁴⁸, K.R. Amos ¹⁶¹, C.S. Amrouche ⁵⁶, V. Ananiev ¹²⁴, C. Anastopoulos ¹³⁸, N. Andari ¹³⁴, T. Andeen ¹¹, J.K. Anders ¹⁹, S.Y. Andreev ^{47a,47b}, A. Andreazza ^{70a,70b}, S. Angelidakis ⁹, A. Angerami ^{41,y}, A.V. Anisenkov ³⁷, A. Annovi ^{73a}, C. Antel ⁵⁶, M.T. Anthony ¹³⁸, E. Antipov ¹²⁰, M. Antonelli ⁵³, D.J.A. Antrim ^{17a}, F. Anulli ^{74a}, M. Aoki ⁸², J.A. Aparisi Pozo ¹⁶¹, M.A. Aparo ¹⁴⁵, L. Aperio Bella ⁴⁸, C. Appelt ¹⁸, N. Aranzabal ³⁶, V. Araujo Ferraz ^{81a}, C. Arcangeletti ⁵³, A.T.H. Arce ⁵¹, E. Arena ⁹¹, J-F. Arguin ¹⁰⁷, S. Argyropoulos ⁵⁴, J.-H. Arling ⁴⁸, A.J. Armbruster ³⁶, O. Arnaez ¹⁵⁴, H. Arnold ¹¹³, Z.P. Arrubarrena Tame ¹⁰⁸, G. Artoni ^{74a,74b}, H. Asada ¹¹⁰, K. Asai ¹¹⁷, S. Asai ¹⁵², N.A. Asbah ⁶¹, E.M. Asimakopoulou ¹⁵⁹, J. Assahsah ^{35d}, K. Assamagan ²⁹, R. Astalos ^{28a}, R.J. Atkin ^{33a}, M. Atkinson ¹⁶⁰, N.B. Atlay ¹⁸, H. Atmani ^{62b}, P.A. Atlasiddha ¹⁰⁵, K. Augsten ¹³¹, S. Auricchio ^{71a,71b}, A.D. Aurioi ²⁰, V.A. Austrup ¹⁶⁹, G. Avner ¹⁴⁹, G. Avolio ³⁶, K. Axiotis ⁵⁶, M.K. Ayoub ^{14c}, G. Azuelos ^{107,ac}, D. Babal ^{28a}, H. Bachacou ¹³⁴, K. Bachas ^{151,q}, A. Bachi ³⁴, F. Backman ^{47a,47b}, A. Badea ⁶¹, P. Bagnaia ^{74a,74b}, M. Bahmani ¹⁸, A.J. Bailey ¹⁶¹, V.R. Bailey ¹⁶⁰, J.T. Baines ¹³³, C. Bakalis ¹⁰, O.K. Baker ¹⁷⁰, P.J. Bakker ¹¹³, E. Bakos ¹⁵, D. Bakshi Gupta ⁸, S. Balaji ¹⁴⁶, R. Balasubramanian ¹¹³, E.M. Baldin ³⁷, P. Balek ¹³², E. Ballabene ^{70a,70b}, F. Balli ¹³⁴, L.M. Baltes ^{63a}, W.K. Balunas ³², J. Balz ⁹⁹, E. Banas ⁸⁵, M. Bandieramonte ¹²⁸, A. Bandyopadhyay ²⁴, S. Bansal ²⁴, L. Barak ¹⁵⁰, E.L. Barberio ¹⁰⁴, D. Barberis ^{57b,57a}, M. Barbero ¹⁰¹, G. Barbour ⁹⁵, K.N. Barends ^{33a}, T. Barillari ¹⁰⁹, M-S. Barisits ³⁶, J. Barkeloo ¹²², T. Barklow ¹⁴², R.M. Barnett ^{17a}, P. Baron ¹²¹, D.A. Baron Moreno ¹⁰⁰, A. Baroncelli ^{62a}, G. Barone ²⁹, A.J. Barr ¹²⁵, L. Barranco Navarro ^{47a,47b}, F. Barreiro ⁹⁸, J. Barreiro Guimarães da Costa ^{14a}, U. Barron ¹⁵⁰, M.G. Barros Teixeira ^{129a}, S. Barsov ³⁷, F. Bartels ^{63a}, R. Bartoldus ¹⁴², A.E. Barton ⁹⁰, P. Bartos ^{28a}, A. Basalae ⁴⁸, A. Basan ⁹⁹, M. Baselga ⁴⁹, I. Bashta ^{76a,76b}, A. Bassalat ^{66,z}, M.J. Basso ¹⁵⁴, C.R. Basson ¹⁰⁰, R.L. Bates ⁵⁹, S. Batlamous ^{35e}, J.R. Batley ³², B. Batool ¹⁴⁰, M. Battaglia ¹³⁵, M. Bauge ^{74a,74b}, P. Bauer ²⁴, A. Bayirli ^{21a}, J.B. Beacham ⁵¹, T. Beau ¹²⁶, P.H. Beauchemin ¹⁵⁷, F. Becherer ⁵⁴, P. Bechtel ²⁴, H.P. Beck ^{19,p}, K. Becker ¹⁶⁵, C. Becot ⁴⁸, A.J. Beddall ^{21d}, V.A. Bednyakov ³⁸, C.P. Bee ¹⁴⁴, L.J. Beemster ¹⁵, T.A. Beermann ³⁶, M. Begalli ^{81b,81d}, M. Begel ²⁹, A. Behera ¹⁴⁴, J.K. Behr ⁴⁸, C. Beirao Da Cruz E Silva ³⁶, J.F. Beirer ^{55,36}, F. Beisiegel ²⁴, M. Belfkir ^{115b}, G. Bella ¹⁵⁰, L. Bellagamba ^{23b}, A. Bellerive ³⁴, P. Bellos ²⁰, K. Beloborodov ³⁷, K. Belotskiy ³⁷, N.L. Belyaev ³⁷, D. Benckekroun ^{35a}, F. Bendebba ^{35a}, Y. Benhammou ¹⁵⁰, D.P. Benjamin ²⁹,

M. Benoit ²⁹, J.R. Bensinger ²⁶, S. Bentvelsen ¹¹³, L. Beresford ³⁶, M. Beretta ⁵³, D. Berge ¹⁸,
E. Bergeaas Kuutmann ¹⁵⁹, N. Berger ⁴, B. Bergmann ¹³¹, J. Beringer ^{17a}, S. Berlendis ⁷,
G. Bernardi ⁵, C. Bernius ¹⁴², F.U. Bernlochner ²⁴, T. Berry ⁹⁴, P. Berta ¹³², A. Berthold ⁵⁰,
I.A. Bertram ⁹⁰, O. Bessidskaia Bylund ¹⁶⁹, S. Bethke ¹⁰⁹, A. Betti ⁴⁴, A.J. Bevan ⁹³,
M. Bhamjee ^{33c}, S. Bhatta ¹⁴⁴, D.S. Bhattacharya ¹⁶⁴, P. Bhattarai ²⁶, V.S. Bhopatkar ⁶, R. Bi ¹²⁸,
R. Bi ^{29,af}, R.M. Bianchi ¹²⁸, O. Biebel ¹⁰⁸, R. Bielski ¹²², N.V. Biesuz ^{73a,73b}, M. Biglietti ^{76a},
T.R.V. Billoud ¹³¹, M. Bindi ⁵⁵, A. Bingul ^{21b}, C. Bini ^{74a,74b}, S. Biondi ^{23b,23a}, A. Biondini ⁹¹,
C.J. Birch-sykes ¹⁰⁰, G.A. Bird ^{20,133}, M. Birman ¹⁶⁷, T. Bisanz ³⁶, D. Biswas ^{168,k},
A. Bitadze ¹⁰⁰, K. Bjørke ¹²⁴, I. Bloch ⁴⁸, C. Blocker ²⁶, A. Blue ⁵⁹, U. Blumenschein ⁹³,
J. Blumenthal ⁹⁹, G.J. Bobbink ¹¹³, V.S. Bobrovnikov ³⁷, M. Boehler ⁵⁴, D. Bogavac ³⁶,
A.G. Bogdanchikov ³⁷, C. Bohm ^{47a}, V. Boisvert ⁹⁴, P. Bokan ⁴⁸, T. Bold ^{84a}, M. Bomben ⁵,
M. Bona ⁹³, M. Boonekamp ¹³⁴, C.D. Booth ⁹⁴, A.G. Borbély ⁵⁹, H.M. Borecka-Bielska ¹⁰⁷,
L.S. Borgna ⁹⁵, G. Borissov ⁹⁰, D. Bortoletto ¹²⁵, D. Boscherini ^{23b}, M. Bosman ¹³,
J.D. Bossio Sola ³⁶, K. Bouaouda ^{35a}, J. Boudreau ¹²⁸, E.V. Bouhova-Thacker ⁹⁰,
D. Boumediene ⁴⁰, R. Bouquet ⁵, A. Boveia ¹¹⁸, J. Boyd ³⁶, D. Boye ²⁹, I.R. Boyko ³⁸,
J. Bracinik ²⁰, N. Brahimy ^{62d,62c}, G. Brandt ¹⁶⁹, O. Brandt ³², F. Braren ⁴⁸, B. Brau ¹⁰²,
J.E. Brau ¹²², W.D. Breaden Madden ⁵⁹, K. Brendlinger ⁴⁸, R. Brenner ¹⁶⁷, L. Brenner ³⁶,
R. Brenner ¹⁵⁹, S. Bressler ¹⁶⁷, B. Brickwedde ⁹⁹, D. Britton ⁵⁹, D. Britzger ¹⁰⁹, I. Brock ²⁴,
G. Brooijmans ⁴¹, W.K. Brooks ^{136f}, E. Brost ²⁹, P.A. Bruckman de Renstrom ⁸⁵, B. Brüers ⁴⁸,
D. Bruncko ^{28b,*}, A. Bruni ^{23b}, G. Bruni ^{23b}, M. Bruschi ^{23b}, N. Brusino ^{74a,74b},
L. Bryngemark ¹⁴², T. Buanes ¹⁶, Q. Buat ¹³⁷, P. Buchholz ¹⁴⁰, A.G. Buckley ⁵⁹,
I.A. Budagov ^{38,*}, M.K. Bugge ¹²⁴, O. Bulekov ³⁷, B.A. Bullard ⁶¹, S. Burdin ⁹¹,
C.D. Burgard ⁴⁸, A.M. Burger ⁴⁰, B. Burghgrave ⁸, J.T.P. Burr ³², C.D. Burton ¹¹,
J.C. Burzynski ¹⁴¹, E.L. Busch ⁴¹, V. Büscher ⁹⁹, P.J. Bussey ⁵⁹, J.M. Butler ²⁵, C.M. Buttar ⁵⁹,
J.M. Butterworth ⁹⁵, W. Buttinger ¹³³, C.J. Buxo Vazquez ¹⁰⁶, A.R. Buzykaev ³⁷, G. Cabras ^{23b},
S. Cabrera Urbán ¹⁶¹, D. Caforio ⁵⁸, H. Cai ¹²⁸, Y. Cai ^{14a,14d}, V.M.M. Cairo ³⁶, O. Cakir ^{3a},
N. Calace ³⁶, P. Calafiura ^{17a}, G. Calderini ¹²⁶, P. Calfayan ⁶⁷, G. Callea ⁵⁹, L.P. Caloba ^{81b},
D. Calvet ⁴⁰, S. Calvet ⁴⁰, T.P. Calvet ¹⁰¹, M. Calvetti ^{73a,73b}, R. Camacho Toro ¹²⁶,
S. Camarda ³⁶, D. Camarero Munoz ⁹⁸, P. Camarri ^{75a,75b}, M.T. Camerlingo ^{76a,76b},
D. Cameron ¹²⁴, C. Camincher ¹⁶³, M. Campanelli ⁹⁵, A. Camplani ⁴², V. Canale ^{71a,71b},
A. Canesse ¹⁰³, M. Cano Bret ⁷⁹, J. Cantero ¹⁶¹, Y. Cao ¹⁶⁰, F. Capocasa ²⁶, M. Capua ^{43b,43a},
A. Carbone ^{70a,70b}, R. Cardarelli ^{75a}, J.C.J. Cardenas ⁸, F. Cardillo ¹⁶¹, T. Carli ³⁶,
G. Carlino ^{71a}, B.T. Carlson ^{128,r}, E.M. Carlson ^{163,155a}, L. Carminati ^{70a,70b}, M. Carnesale ^{74a,74b},
S. Caron ¹¹², E. Carquin ^{136f}, S. Carrá ^{70a,70b}, G. Carratta ^{23b,23a}, F. Carrio Argos ^{33g},
J.W.S. Carter ¹⁵⁴, T.M. Carter ⁵², M.P. Casado ^{13,h}, A.F. Casha ¹⁵⁴, E.G. Castiglia ¹⁷⁰,
F.L. Castillo ^{63a}, L. Castillo Garcia ¹³, V. Castillo Gimenez ¹⁶¹, N.F. Castro ^{129a,129e},
A. Catinaccio ³⁶, J.R. Catmore ¹²⁴, V. Cavaliere ²⁹, N. Cavalli ^{23b,23a}, V. Cavasinni ^{73a,73b},
E. Celebi ^{21a}, F. Celli ¹²⁵, M.S. Centonze ^{69a,69b}, K. Cerny ¹²¹, A.S. Cerqueira ^{81a}, A. Cerri ¹⁴⁵,
L. Cerrito ^{75a,75b}, F. Cerutti ^{17a}, A. Cervelli ^{23b}, S.A. Cetin ^{21d}, Z. Chadi ^{35a},
D. Chakraborty ¹¹⁴, M. Chala ^{129f}, J. Chan ¹⁶⁸, W.S. Chan ¹¹³, W.Y. Chan ¹⁵²,
J.D. Chapman ³², B. Chargeishvili ^{148b}, D.G. Charlton ²⁰, T.P. Charman ⁹³, M. Chatterjee ¹⁹,
S. Chekanov ⁶, S.V. Chekulaev ^{155a}, G.A. Chelkov ^{38,a}, A. Chen ¹⁰⁵, B. Chen ¹⁵⁰, B. Chen ¹⁶³,
C. Chen ^{62a}, H. Chen ^{14c}, H. Chen ²⁹, J. Chen ^{62c}, J. Chen ²⁶, S. Chen ¹⁵², S.J. Chen ^{14c},
X. Chen ^{62c}, X. Chen ^{14b,ab}, Y. Chen ^{62a}, C.L. Cheng ¹⁶⁸, H.C. Cheng ^{64a}, A. Cheplakov ³⁸,
E. Cheremushkina ⁴⁸, E. Cherepanova ¹¹³, R. Cherkaoui El Moursli ^{35e}, E. Cheu ⁷, K. Cheung ⁶⁵,
L. Chevalier ¹³⁴, V. Chiarella ⁵³, G. Chiarelli ^{73a}, G. Chiodini ^{69a}, A.S. Chisholm ²⁰,
A. Chitan ^{27b}, Y.H. Chiu ¹⁶³, M.V. Chizhov ³⁸, K. Choi ¹¹, A.R. Chomont ^{74a,74b}, Y. Chou ¹⁰²,

E.Y.S. Chow [id113](#), T. Chowdhury [id33g](#), L.D. Christopher [id33g](#), K.L. Chu^{64a}, M.C. Chu [id64a](#),
 X. Chu [id14a,14d](#), J. Chudoba [id130](#), J.J. Chwastowski [id85](#), D. Cieri [id109](#), K.M. Ciesla [id84a](#), V. Cindro [id92](#),
 A. Ciocio [id17a](#), F. Cirotto [id71a,71b](#), Z.H. Citron [id167,1](#), M. Citterio [id70a](#), D.A. Ciubotaru^{27b},
 B.M. Ciungu [id154](#), A. Clark [id56](#), P.J. Clark [id52](#), J.M. Clavijo Columbie [id48](#), S.E. Clawson [id100](#),
 C. Clement [id47a,47b](#), J. Clercx [id48](#), L. Clissa [id23b,23a](#), Y. Coadou [id101](#), M. Cobal [id68a,68c](#),
 A. Coccaro [id57b](#), R.F. Coelho Barrue [id129a](#), R. Coelho Lopes De Sa [id102](#), S. Coelli [id70a](#), H. Cohen [id150](#),
 A.E.C. Coimbra [id70a,70b](#), B. Cole [id41](#), J. Collot [id60](#), P. Conde Muiño [id129a,129g](#), S.H. Connell [id33c](#),
 I.A. Connelly [id59](#), E.I. Conroy [id125](#), F. Conventi [id71a,ad](#), H.G. Cooke [id20](#), A.M. Cooper-Sarkar [id125](#),
 F. Cormier [id162](#), L.D. Corpe [id36](#), M. Corradi [id74a,74b](#), E.E. Corrigan [id97](#), F. Corriveau [id103,v](#),
 A. Cortes-Gonzalez [id18](#), M.J. Costa [id161](#), F. Costanza [id4](#), D. Costanzo [id138](#), B.M. Cote [id118](#),
 G. Cowan [id94](#), J.W. Cowley [id32](#), K. Cranmer [id116](#), S. Crépe-Renaudin [id60](#), F. Crescioli [id126](#),
 M. Cristinziani [id140](#), M. Cristoforetti [id77a,77b,c](#), V. Croft [id157](#), G. Crosetti [id43b,43a](#), A. Cueto [id36](#),
 T. Cuhadar Donszelmann [id158](#), H. Cui [id14a,14d](#), Z. Cui [id7](#), A.R. Cukierman [id142](#), W.R. Cunningham [id59](#),
 F. Curcio [id43b,43a](#), P. Czodrowski [id36](#), M.M. Czurylo [id63b](#), M.J. Da Cunha Sargedas De Sousa [id62a](#),
 J.V. Da Fonseca Pinto [id81b](#), C. Da Via [id100](#), W. Dabrowski [id84a](#), T. Dado [id49](#), S. Dahbi [id33g](#),
 T. Dai [id105](#), C. Dallapiccola [id102](#), M. Dam [id42](#), G. D'amen [id29](#), V. D'Amico [id76a,76b](#), J. Damp [id99](#),
 J.R. Dandoy [id127](#), M.F. Daneri [id30](#), M. Danninger [id141](#), V. Dao [id36](#), G. Darbo [id57b](#), S. Darmora [id6](#),
 S.J. Das [id29](#), A. Dattagupta [id122](#), S. D'Auria [id70a,70b](#), C. David [id155b](#), T. Davidek [id132](#), D.R. Davis [id51](#),
 B. Davis-Purcell [id34](#), I. Dawson [id93](#), K. De [id8](#), R. De Asmundis [id71a](#), M. De Beurs [id113](#),
 S. De Castro [id23b,23a](#), N. De Groot [id112](#), P. de Jong [id113](#), H. De la Torre [id106](#), A. De Maria [id14c](#),
 A. De Salvo [id74a](#), U. De Sanctis [id75a,75b](#), M. De Santis [id75a,75b](#), A. De Santo [id145](#),
 J.B. De Vivie De Regie [id60](#), D.V. Dedovich³⁸, J. Degens [id113](#), A.M. Deiana [id44](#), F. Del Corso [id23b,23a](#),
 J. Del Peso [id98](#), F. Del Rio [id63a](#), F. Deliot [id134](#), C.M. Delitzsch [id49](#), M. Della Pietra [id71a,71b](#),
 D. Della Volpe [id56](#), A. Dell'Acqua [id36](#), L. Dell'Asta [id70a,70b](#), M. Delmastro [id4](#), P.A. Delsart [id60](#),
 S. Demers [id170](#), M. Demichev [id38](#), S.P. Denisov [id37](#), L. D'Eramo [id114](#), D. Derendarz [id85](#),
 F. Derue [id126](#), P. Dervan [id91](#), K. Desch [id24](#), K. Dette [id154](#), C. Deutsch [id24](#), P.O. Deviveiros [id36](#),
 F.A. Di Bello [id74a,74b](#), A. Di Ciaccio [id75a,75b](#), L. Di Ciaccio [id4](#), A. Di Domenico [id74a,74b](#),
 C. Di Donato [id71a,71b](#), A. Di Girolamo [id36](#), G. Di Gregorio [id73a,73b](#), A. Di Luca [id77a,77b](#),
 B. Di Micco [id76a,76b](#), R. Di Nardo [id76a,76b](#), C. Diaconu [id101](#), F.A. Dias [id113](#), T. Dias Do Vale [id141](#),
 M.A. Diaz [id136a,136b](#), F.G. Diaz Capriles [id24](#), M. Didenko [id161](#), E.B. Diehl [id105](#), L. Diehl [id54](#),
 S. Díez Cornell [id48](#), C. Diez Pardos [id140](#), C. Dimitriadi [id24,159](#), A. Dimitrievska [id17a](#), W. Ding [id14b](#),
 J. Dingfelder [id24](#), I-M. Dinu [id27b](#), S.J. Dittmeier [id63b](#), F. Dittus [id36](#), F. Djama [id101](#), T. Djobava [id148b](#),
 J.I. Djuvsland [id16](#), D. Dodsworth [id26](#), C. Doglioni [id100,97](#), J. Dolejsi [id132](#), Z. Dolezal [id132](#),
 M. Donadelli [id81c](#), B. Dong [id62c](#), J. Donini [id40](#), A. D'Onofrio [id14c](#), M. D'Onofrio [id91](#), J. Dopke [id133](#),
 A. Doria [id71a](#), M.T. Dova [id89](#), A.T. Doyle [id59](#), M.A. Draguet [id125](#), E. Drechsler [id141](#), E. Dreyer [id167](#),
 I. Drivas-koulouris [id10](#), A.S. Drobac [id157](#), D. Du [id62a](#), T.A. du Pree [id113](#), F. Dubinin [id37](#),
 M. Dubovsky [id28a](#), E. Duchovni [id167](#), G. Duckeck [id108](#), O.A. Ducu [id36](#), D. Duda [id109](#), A. Dudarev [id36](#),
 M. D'uffizi [id100](#), L. Dufлот [id66](#), M. Dührssen [id36](#), C. Dülsen [id169](#), A.E. Dumitriu [id27b](#), M. Dunford [id63a](#),
 S. Dungs [id49](#), K. Dunne [id47a,47b](#), A. Duperrin [id101](#), H. Duran Yildiz [id3a](#), M. Düren [id58](#),
 A. Durglishvili [id148b](#), B.L. Dwyer [id114](#), G.I. Dyckes [id17a](#), M. Dyndal [id84a](#), S. Dysch [id100](#),
 B.S. Dziedzic [id85](#), Z.O. Earnshaw [id145](#), B. Eckerova [id28a](#), M.G. Eggleston⁵¹,
 E. Egidio Purcino De Souza [id81b](#), L.F. Ehrke [id56](#), G. Eigen [id16](#), K. Einsweiler [id17a](#), T. Ekelof [id159](#),
 P.A. Ekman [id97](#), Y. El Ghazali [id35b](#), H. El Jarrari [id35e,147](#), A. El Moussaouy [id35a](#), V. Ellajosyula [id159](#),
 M. Ellert [id159](#), F. Ellinghaus [id169](#), A.A. Elliot [id93](#), N. Ellis [id36](#), J. Elmsheuser [id29](#), M. Elsing [id36](#),
 D. Emelianov [id133](#), A. Emerman [id41](#), Y. Enari [id152](#), I. Ene [id17a](#), S. Epari [id13](#), J. Erdmann [id49](#),
 A. Ereditato [id19](#), P.A. Erland [id85](#), M. Errenst [id169](#), M. Escalier [id66](#), C. Escobar [id161](#), E. Etzion [id150](#),
 G. Evans [id129a](#), H. Evans [id67](#), M.O. Evans [id145](#), A. Ezhilov [id37](#), S. Ezzarqtouni [id35a](#), F. Fabbri [id59](#),

L. Fabbri [ID23b,23a](#), G. Facini [ID95](#), V. Fadeyev [ID135](#), R.M. Fakhruddinov [ID37](#), S. Falciano [ID74a](#),
 P.J. Falke [ID24](#), S. Falke [ID36](#), J. Faltova [ID132](#), Y. Fan [ID14a](#), Y. Fang [ID14a,14d](#), G. Fanourakis [ID46](#),
 M. Fanti [ID70a,70b](#), M. Faraj [ID68a,68b](#), A. Farbin [ID8](#), A. Farilla [ID76a](#), T. Faroque [ID106](#), S.M. Farrington [ID52](#),
 F. Fassi [ID35e](#), D. Fassouliotis [ID9](#), M. Faucci Giannelli [ID75a,75b](#), W.J. Fawcett [ID32](#), L. Fayard [ID66](#),
 O.L. Fedin [ID37,a](#), G. Fedotov [ID37](#), M. Feickert [ID160](#), L. Feligioni [ID101](#), A. Fell [ID138](#), D.E. Fellers [ID122](#),
 C. Feng [ID62b](#), M. Feng [ID14b](#), M.J. Fenton [ID158](#), A.B. Fenyuk [ID37](#), L. Ferencz [ID48](#), S.W. Ferguson [ID45](#),
 J.A. Fernandez Pretel [ID54](#), J. Ferrando [ID48](#), A. Ferrari [ID159](#), P. Ferrari [ID113](#), R. Ferrari [ID72a](#),
 D. Ferrere [ID56](#), C. Ferretti [ID105](#), F. Fiedler [ID99](#), A. Filipčič [ID92](#), E.K. Filmer [ID1](#), F. Filthaut [ID112](#),
 M.C.N. Fiolhais [ID129a,129c,b](#), L. Fiorini [ID161](#), F. Fischer [ID140](#), W.C. Fisher [ID106](#), T. Fitschen [ID20,66](#),
 I. Fleck [ID140](#), P. Fleischmann [ID105](#), T. Flick [ID169](#), L. Flores [ID127](#), M. Flores [ID33d](#),
 L.R. Flores Castillo [ID64a](#), F.M. Follega [ID77a,77b](#), N. Fomin [ID16](#), J.H. Foo [ID154](#), B.C. Forland [ID67](#),
 A. Formica [ID134](#), A.C. Forti [ID100](#), E. Fortin [ID101](#), A.W. Fortman [ID61](#), M.G. Foti [ID17a](#), L. Fountas [ID9](#),
 D. Fournier [ID66](#), H. Fox [ID90](#), P. Francavilla [ID73a,73b](#), S. Francescato [ID61](#), M. Franchini [ID23b,23a](#),
 S. Franchino [ID63a](#), D. Francis [ID36](#), L. Franco [ID112](#), L. Franconi [ID19](#), M. Franklin [ID61](#), G. Frattari [ID26](#),
 A.C. Freegard [ID93](#), P.M. Freeman [ID20](#), W.S. Freund [ID81b](#), N. Fritzsche [ID50](#), A. Froch [ID54](#),
 D. Froidevaux [ID36](#), J.A. Frost [ID125](#), Y. Fu [ID62a](#), M. Fujimoto [ID117](#), E. Fullana Torregrosa [ID161,*](#),
 J. Fuster [ID161](#), A. Gabrielli [ID23b,23a](#), A. Gabrielli [ID36](#), P. Gadow [ID48](#), G. Gagliardi [ID57b,57a](#),
 L.G. Gagnon [ID17a](#), G.E. Gallardo [ID125](#), E.J. Gallas [ID125](#), B.J. Gallop [ID133](#), R. Gamboa Goni [ID93](#),
 K.K. Gan [ID118](#), S. Ganguly [ID152](#), J. Gao [ID62a](#), Y. Gao [ID52](#), F.M. Garay Walls [ID136a,136b](#), B. Garcia [ID29,af](#),
 C. García [ID161](#), J.E. García Navarro [ID161](#), J.A. García Pascual [ID14a](#), M. Garcia-Sciveres [ID17a](#),
 R.W. Gardner [ID39](#), D. Garg [ID79](#), R.B. Garg [ID142](#), S. Gargiulo [ID54](#), C.A. Garner [ID154](#), V. Garonne [ID29](#),
 S.J. Gasiorowski [ID137](#), P. Gaspar [ID81b](#), G. Gaudio [ID72a](#), P. Gauzzi [ID74a,74b](#), I.L. Gavrilenko [ID37](#),
 A. Gavrilyuk [ID37](#), C. Gay [ID162](#), G. Gaycken [ID48](#), E.N. Gazis [ID10](#), A.A. Geanta [ID27b](#), C.M. Gee [ID135](#),
 J. Geisen [ID97](#), M. Geisen [ID99](#), C. Gemme [ID57b](#), M.H. Genest [ID60](#), S. Gentile [ID74a,74b](#), S. George [ID94](#),
 W.F. George [ID20](#), T. Geralis [ID46](#), L.O. Gerlach [ID55](#), P. Gessinger-Befurt [ID36](#), M. Ghasemi Bostanabad [ID163](#),
 M. Ghneimat [ID140](#), A. Ghosal [ID140](#), A. Ghosh [ID158](#), A. Ghosh [ID7](#), B. Giacobbe [ID23b](#), S. Giagu [ID74a,74b](#),
 N. Giangiacomi [ID154](#), P. Giannetti [ID73a](#), A. Giannini [ID62a](#), S.M. Gibson [ID94](#), M. Gignac [ID135](#),
 D.T. Gil [ID84b](#), A.K. Gilbert [ID84a](#), B.J. Gilbert [ID41](#), D. Gillberg [ID34](#), G. Gilles [ID113](#), N.E.K. Gillwald [ID48](#),
 L. Ginabat [ID126](#), D.M. Gingrich [ID2,ac](#), M.P. Giordani [ID68a,68c](#), P.F. Giraud [ID134](#), G. Giugliarelli [ID68a,68c](#),
 D. Giugni [ID70a](#), F. Giuli [ID36](#), I. Gkialas [ID9,i](#), L.K. Gladilin [ID37](#), C. Glasman [ID98](#), G.R. Gledhill [ID122](#),
 M. Glisic [ID122](#), I. Gnesi [ID43b,e](#), Y. Go [ID29,af](#), M. Goblirsch-Kolb [ID26](#), D. Godin [ID107](#), S. Goldfarb [ID104](#),
 T. Golling [ID56](#), M.G.D. Gololo [ID33g](#), D. Golubkov [ID37](#), J.P. Gombas [ID106](#), A. Gomes [ID129a,129b](#),
 G. Gomes Da Silva [ID140](#), A.J. Gomez Delegido [ID161](#), R. Goncalves Gama [ID55](#), R. Gonçalves [ID129a,129c](#),
 G. Gonella [ID122](#), L. Gonella [ID20](#), A. Gongadze [ID38](#), F. Gonnella [ID20](#), J.L. Gonski [ID41](#),
 S. González de la Hoz [ID161](#), S. Gonzalez Fernandez [ID13](#), R. Gonzalez Lopez [ID91](#),
 C. Gonzalez Renteria [ID17a](#), R. Gonzalez Suarez [ID159](#), S. Gonzalez-Sevilla [ID56](#),
 G.R. Gonzalvo Rodriguez [ID161](#), R.Y. González Andana [ID52](#), L. Goossens [ID36](#), N.A. Gorasia [ID20](#),
 P.A. Gorbounov [ID37](#), B. Gorini [ID36](#), E. Gorini [ID69a,69b](#), A. Gorišek [ID92](#), A.T. Goshaw [ID51](#),
 M.I. Gostkin [ID38](#), C.A. Gottardo [ID112](#), M. Goughri [ID35b](#), V. Goumarre [ID48](#), A.G. Goussiou [ID137](#),
 N. Govender [ID33c](#), C. Goy [ID4](#), I. Grabowska-Bold [ID84a](#), K. Graham [ID34](#), E. Gramstad [ID124](#),
 S. Grancagnolo [ID18](#), M. Grandi [ID145](#), V. Gratchev [ID37,*](#), P.M. Gravila [ID27f](#), F.G. Gravili [ID69a,69b](#),
 H.M. Gray [ID17a](#), M. Greco [ID69a,69b](#), C. Grefe [ID24](#), I.M. Gregor [ID48](#), P. Grenier [ID142](#), C. Grieco [ID13](#),
 A.A. Grillo [ID135](#), K. Grimm [ID31,m](#), S. Grinstein [ID13,t](#), J.-F. Grivaz [ID66](#), E. Gross [ID167](#),
 J. Grosse-Knetter [ID55](#), C. Grud [ID105](#), A. Grummer [ID111](#), J.C. Grundy [ID125](#), L. Guan [ID105](#), W. Guan [ID168](#),
 C. Gubbels [ID162](#), J.G.R. Guerrero Rojas [ID161](#), G. Guerrieri [ID68a,68c](#), F. Guescini [ID109](#), R. Gugel [ID99](#),
 J.A.M. Guhit [ID105](#), A. Guida [ID48](#), T. Guillemin [ID4](#), E. Guilloton [ID165,133](#), S. Guindon [ID36](#),
 F. Guo [ID14a,14d](#), J. Guo [ID62c](#), L. Guo [ID66](#), Y. Guo [ID105](#), R. Gupta [ID48](#), S. Gurbuz [ID24](#), S.S. Gurdasani [ID54](#),

G. Gustavino ³⁶, M. Guth ⁵⁶, P. Gutierrez ¹¹⁹, L.F. Gutierrez Zagazeta ¹²⁷, C. Gutschow ⁹⁵, C. Guyot ¹³⁴, C. Gwenlan ¹²⁵, C.B. Gwilliam ⁹¹, E.S. Haaland ¹²⁴, A. Haas ¹¹⁶, M. Habedank ⁴⁸, C. Haber ^{17a}, H.K. Hadavand ⁸, A. Hadeef ⁹⁹, S. Hadzic ¹⁰⁹, M. Haleem ¹⁶⁴, J. Haley ¹²⁰, J.J. Hall ¹³⁸, G.D. Hallewell ¹⁰¹, L. Halser ¹⁹, K. Hamano ¹⁶³, H. Hamdaoui ^{35e}, M. Hamer ²⁴, G.N. Hamity ⁵², J. Han ^{62b}, K. Han ^{62a}, L. Han ^{14c}, L. Han ^{62a}, S. Han ^{17a}, Y.F. Han ¹⁵⁴, K. Hanagaki ⁸², M. Hance ¹³⁵, D.A. Hangal ^{41,y}, M.D. Hank ³⁹, R. Hankache ¹⁰⁰, J.B. Hansen ⁴², J.D. Hansen ⁴², P.H. Hansen ⁴², K. Hara ¹⁵⁶, D. Harada ⁵⁶, T. Harenberg ¹⁶⁹, S. Harkusha ³⁷, Y.T. Harris ¹²⁵, P.F. Harrison ¹⁶⁵, N.M. Hartman ¹⁴², N.M. Hartmann ¹⁰⁸, Y. Hasegawa ¹³⁹, A. Hasib ⁵², S. Haug ¹⁹, R. Hauser ¹⁰⁶, M. Havranek ¹³¹, C.M. Hawkes ²⁰, R.J. Hawkings ³⁶, S. Hayashida ¹¹⁰, D. Hayden ¹⁰⁶, C. Hayes ¹⁰⁵, R.L. Hayes ¹⁶², C.P. Hays ¹²⁵, J.M. Hays ⁹³, H.S. Hayward ⁹¹, F. He ^{62a}, Y. He ¹⁵³, Y. He ¹²⁶, M.P. Heath ⁵², V. Hedberg ⁹⁷, A.L. Heggelund ¹²⁴, N.D. Hehir ⁹³, C. Heidegger ⁵⁴, K.K. Heidegger ⁵⁴, W.D. Heidorn ⁸⁰, J. Heilman ³⁴, S. Heim ⁴⁸, T. Heim ^{17a}, J.G. Heinlein ¹²⁷, J.J. Heinrich ¹²², L. Heinrich ³⁶, J. Hejbal ¹³⁰, L. Helary ⁴⁸, A. Held ¹¹⁶, S. Hellesund ¹²⁴, C.M. Helling ¹⁶², S. Hellman ^{47a,47b}, C. Helsens ³⁶, R.C.W. Henderson ⁹⁰, L. Henkelmann ³², A.M. Henriques Correia ³⁶, H. Herde ¹⁴², Y. Hernández Jiménez ¹⁴⁴, H. Herr ⁹⁹, M.G. Herrmann ¹⁰⁸, T. Herrmann ⁵⁰, G. Herten ⁵⁴, R. Hertenberger ¹⁰⁸, L. Hervas ³⁶, N.P. Hessey ^{155a}, H. Hibi ⁸³, E. Higón-Rodríguez ¹⁶¹, S.J. Hillier ²⁰, I. Hinchliffe ^{17a}, F. Hinterkeuser ²⁴, M. Hirose ¹²³, S. Hirose ¹⁵⁶, D. Hirschbuehl ¹⁶⁹, T.G. Hitchings ¹⁰⁰, B. Hiti ⁹², J. Hobbs ¹⁴⁴, R. Hobincu ^{27e}, N. Hod ¹⁶⁷, M.C. Hodgkinson ¹³⁸, B.H. Hodgkinson ³², A. Hoecker ³⁶, J. Hofer ⁴⁸, D. Hohn ⁵⁴, T. Holm ²⁴, M. Holzbock ¹⁰⁹, L.B.A.H. Hommels ³², B.P. Honan ¹⁰⁰, J. Hong ^{62c}, T.M. Hong ¹²⁸, Y. Hong ⁵⁵, J.C. Honig ⁵⁴, A. Hönle ¹⁰⁹, B.H. Hooberman ¹⁶⁰, W.H. Hopkins ⁶, Y. Horii ¹¹⁰, S. Hou ¹⁴⁷, A.S. Howard ⁹², J. Howarth ⁵⁹, J. Hoya ⁸⁹, M. Hrabovsky ¹²¹, A. Hrynevich ³⁷, T. Hryn'ova ⁴, P.J. Hsu ⁶⁵, S.-C. Hsu ¹³⁷, Q. Hu ^{41,y}, Y.F. Hu ^{14a,14d,ae}, D.P. Huang ⁹⁵, S. Huang ^{64b}, X. Huang ^{14c}, Y. Huang ^{62a}, Y. Huang ^{14a}, Z. Huang ¹⁰⁰, Z. Hubacek ¹³¹, M. Huebner ²⁴, F. Huegging ²⁴, T.B. Huffman ¹²⁵, M. Huhtinen ³⁶, S.K. Huiberts ¹⁶, R. Hulsken ¹⁰³, N. Huseynov ^{12,a}, J. Huston ¹⁰⁶, J. Huth ⁶¹, R. Hyneman ¹⁴², S. Hyrych ^{28a}, G. Iacobucci ⁵⁶, G. Iakovidis ²⁹, I. Ibragimov ¹⁴⁰, L. Iconomidou-Fayard ⁶⁶, P. Inengo ^{71a,71b}, R. Iguchi ¹⁵², T. Iizawa ⁵⁶, Y. Ikegami ⁸², A. Ilg ¹⁹, N. Ilic ¹⁵⁴, H. Imam ^{35a}, T. Ingebretsen Carlson ^{47a,47b}, G. Introzzi ^{72a,72b}, M. Iodice ^{76a}, V. Ippolito ^{74a,74b}, M. Ishino ¹⁵², W. Islam ¹⁶⁸, C. Issever ^{18,48}, S. Istin ^{21a,ag}, H. Ito ¹⁶⁶, J.M. Iturbe Ponce ^{64a}, R. Iuppa ^{77a,77b}, A. Ivina ¹⁶⁷, J.M. Izen ⁴⁵, V. Izzo ^{71a}, P. Jacka ^{130,131}, P. Jackson ¹, R.M. Jacobs ⁴⁸, B.P. Jaeger ¹⁴¹, C.S. Jagfeld ¹⁰⁸, G. Jäkel ¹⁶⁹, K. Jakobs ⁵⁴, T. Jakoubek ¹⁶⁷, J. Jamieson ⁵⁹, K.W. Janas ^{84a}, G. Jarlskog ⁹⁷, A.E. Jaspán ⁹¹, T. Javůrek ³⁶, M. Javurkova ¹⁰², F. Jeanneau ¹³⁴, L. Jeanty ¹²², J. Jejelava ^{148a,x}, P. Jenni ^{54,f}, C.E. Jessiman ³⁴, S. Jézéquel ⁴, J. Jia ¹⁴⁴, X. Jia ⁶¹, X. Jia ^{14a,14d}, Z. Jia ^{14c}, Y. Jiang ^{62a}, S. Jiggins ⁵², J. Jimenez Pena ¹⁰⁹, S. Jin ^{14c}, A. Jinaru ^{27b}, O. Jinnouchi ¹⁵³, H. Jivan ^{33g}, P. Johansson ¹³⁸, K.A. Johns ⁷, C.A. Johnson ⁶⁷, D.M. Jones ³², E. Jones ¹⁶⁵, R.W.L. Jones ⁹⁰, T.J. Jones ⁹¹, J. Jovicevic ¹⁵, X. Ju ^{17a}, J.J. Junggeburth ³⁶, A. Juste Rozas ^{13,t}, S. Kabana ^{136e}, A. Kaczmarska ⁸⁵, M. Kado ^{74a,74b}, H. Kagan ¹¹⁸, M. Kagan ¹⁴², A. Kahn ⁴¹, A. Kahn ¹²⁷, C. Kahra ⁹⁹, T. Kaji ¹⁶⁶, E. Kajomovitz ¹⁴⁹, N. Kakati ¹⁶⁷, C.W. Kalderon ²⁹, A. Kamenshchikov ¹⁵⁴, N.J. Kang ¹³⁵, Y. Kano ¹¹⁰, D. Kar ^{33g}, K. Karava ¹²⁵, M.J. Kareem ^{155b}, E. Karentzos ⁵⁴, I. Karkanias ¹⁵¹, S.N. Karpov ³⁸, Z.M. Karpova ³⁸, V. Kartvelishvili ⁹⁰, A.N. Karyukhin ³⁷, E. Kasimi ¹⁵¹, C. Kato ^{62d}, J. Katzy ⁴⁸, S. Kaur ³⁴, K. Kawade ¹³⁹, K. Kawagoe ⁸⁸, T. Kawaguchi ¹¹⁰, T. Kawamoto ¹³⁴, G. Kawamura ⁵⁵, E.F. Kay ¹⁶³, F.I. Kaya ¹⁵⁷, S. Kazakos ¹³, V.F. Kazanin ³⁷, Y. Ke ¹⁴⁴, J.M. Keaveney ^{33a}, R. Keeler ¹⁶³, G.V. Kehris ⁶¹, J.S. Keller ³⁴, A.S. Kelly ⁹⁵, D. Kelsey ¹⁴⁵, J.J. Kempster ²⁰, J. Kendrick ²⁰, K.E. Kennedy ⁴¹, O. Kepka ¹³⁰,

B.P. Kerridge ¹⁶⁵, S. Kersten ¹⁶⁹, B.P. Kerševan ⁹², L. Keszeghova ^{28a}, S. Ketabchi Haghighat ¹⁵⁴,
 M. Khandoga ¹²⁶, A. Khanov ¹²⁰, A.G. Kharlamov ³⁷, T. Kharlamova ³⁷, E.E. Khoda ¹³⁷,
 T.J. Khoo ¹⁸, G. Khoriali ¹⁶⁴, J. Khubua ^{148b}, Y.A.R. Khwaira ⁶⁶, M. Kiehn ³⁶,
 A. Kilgallon ¹²², D.W. Kim ^{47a,47b}, E. Kim ¹⁵³, Y.K. Kim ³⁹, N. Kimura ⁹⁵, A. Kirchhoff ⁵⁵,
 D. Kirchmeier ⁵⁰, C. Kirfel ²⁴, J. Kirk ¹³³, A.E. Kiryunin ¹⁰⁹, T. Kishimoto ¹⁵², D.P. Kisliuk ¹⁵⁴,
 C. Kitsaki ¹⁰, O. Kivernyk ²⁴, M. Klassen ^{63a}, C. Klein ³⁴, L. Klein ¹⁶⁴, M.H. Klein ¹⁰⁵,
 M. Klein ⁹¹, U. Klein ⁹¹, P. Klimek ³⁶, A. Klimentov ²⁹, F. Klimpel ¹⁰⁹, T. Klingl ²⁴,
 T. Klioutchnikova ³⁶, F.F. Klitzner ¹⁰⁸, P. Kluit ¹¹³, S. Kluth ¹⁰⁹, E. Kneringer ⁷⁸,
 T.M. Knight ¹⁵⁴, A. Knue ⁵⁴, D. Kobayashi⁸⁸, R. Kobayashi ⁸⁶, M. Kocian ¹⁴², T. Kodama¹⁵²,
 P. Kodyš ¹³², D.M. Koeck ¹⁴⁵, P.T. Koenig ²⁴, T. Koffas ³⁴, N.M. Köhler ³⁶, M. Kolb ¹³⁴,
 I. Koletsou ⁴, T. Komarek ¹²¹, K. Köneke ⁵⁴, A.X.Y. Kong ¹, T. Kono ¹¹⁷, N. Konstantinidis ⁹⁵,
 B. Konya ⁹⁷, R. Kopeliansky ⁶⁷, S. Koperny ^{84a}, K. Korcyl ⁸⁵, K. Kordas ¹⁵¹, G. Koren ¹⁵⁰,
 A. Korn ⁹⁵, S. Korn ⁵⁵, I. Korolkov ¹³, N. Korotkova ³⁷, B. Kortman ¹¹³, O. Kortner ¹⁰⁹,
 S. Kortner ¹⁰⁹, W.H. Kostecka ¹¹⁴, V.V. Kostyukhin ¹⁴⁰, A. Kotsokechagia ⁶⁶, A. Kotwal ⁵¹,
 A. Koulouris ³⁶, A. Kourkoumeli-Charalampidi ^{72a,72b}, C. Kourkoumelis ⁹, E. Kourlitis ⁶,
 O. Kovanda ¹⁴⁵, R. Kowalewski ¹⁶³, W. Kozanecki ¹³⁴, A.S. Kozhin ³⁷, V.A. Kramarenko ³⁷,
 G. Kramberger ⁹², P. Kramer ⁹⁹, M.W. Krasny ¹²⁶, A. Krasznahorkay ³⁶, J.A. Kremer ⁹⁹,
 T. Kresse ⁵⁰, J. Kretschmar ⁹¹, K. Kreul ¹⁸, P. Krieger ¹⁵⁴, F. Krieter ¹⁰⁸,
 S. Krishnamurthy ¹⁰², A. Krishnan ^{63b}, M. Krivos ¹³², K. Krizka ^{17a}, K. Kroeninger ⁴⁹,
 H. Kroha ¹⁰⁹, J. Kroll ¹³⁰, J. Kroll ¹²⁷, K.S. Krowpman ¹⁰⁶, U. Kruchonak ³⁸, H. Krüger ²⁴,
 N. Krumnack⁸⁰, M.C. Kruse ⁵¹, J.A. Krzysiak ⁸⁵, A. Kubota ¹⁵³, O. Kuchinskaja ³⁷, S. Kuday ^{3a},
 D. Kuechler ⁴⁸, J.T. Kuechler ⁴⁸, S. Kuehn ³⁶, T. Kuhl ⁴⁸, V. Kukhtin ³⁸, Y. Kulchitsky ^{37,a},
 S. Kuleshov ^{136d,136b}, M. Kumar ^{33g}, N. Kumari ¹⁰¹, M. Kuna ⁶⁰, A. Kupco ¹³⁰, T. Kupfer⁴⁹,
 A. Kupich ³⁷, O. Kuprash ⁵⁴, H. Kurashige ⁸³, L.L. Kurchaninov ^{155a}, Y.A. Kurochkin ³⁷,
 A. Kurova ³⁷, E.S. Kuwertz ³⁶, M. Kuze ¹⁵³, A.K. Kvam ¹⁰², J. Kvita ¹²¹, T. Kwan ¹⁰³,
 K.W. Kwok ^{64a}, C. Lacasta ¹⁶¹, F. Lacava ^{74a,74b}, H. Lacker ¹⁸, D. Lacour ¹²⁶, N.N. Lad ⁹⁵,
 E. Ladygin ³⁸, B. Laforge ¹²⁶, T. Lagouri ^{136e}, S. Lai ⁵⁵, I.K. Lakomic ^{84a}, N. Lalloue ⁶⁰,
 J.E. Lambert ¹¹⁹, S. Lammers ⁶⁷, W. Lampl ⁷, C. Lampoudis ¹⁵¹, A.N. Lancaster ¹¹⁴,
 E. Lançon ²⁹, U. Landgraf ⁵⁴, M.P.J. Landon ⁹³, V.S. Lang ⁵⁴, R.J. Langenberg ¹⁰²,
 A.J. Lankford ¹⁵⁸, F. Lanni ²⁹, K. Lantzsch ²⁴, A. Lanza ^{72a}, A. Lapertosa ^{57b,57a},
 J.F. Laporte ¹³⁴, T. Lari ^{70a}, F. Lasagni Manghi ^{23b}, M. Lassnig ³⁶, V. Latonova ¹³⁰, T.S. Lau ^{64a},
 A. Laudrain ⁹⁹, A. Laurier ³⁴, S.D. Lawlor ⁹⁴, Z. Lawrence ¹⁰⁰, M. Lazzaroni ^{70a,70b}, B. Le¹⁰⁰,
 B. Leban ⁹², A. Lebedev ⁸⁰, M. LeBlanc ³⁶, T. LeCompte ⁶, F. Ledroit-Guillon ⁶⁰, A.C.A. Lee⁹⁵,
 G.R. Lee ¹⁶, L. Lee ⁶¹, S.C. Lee ¹⁴⁷, S. Lee ^{47a,47b}, L.L. Leeuw ^{33c}, H.P. Lefebvre ⁹⁴,
 M. Lefebvre ¹⁶³, C. Leggett ^{17a}, K. Lehmann ¹⁴¹, G. Lehmann Miotto ³⁶, W.A. Leight ¹⁰²,
 A. Leisos ^{151,s}, M.A.L. Leite ^{81c}, C.E. Leitgeb ⁴⁸, R. Leitner ¹³², K.J.C. Leney ⁴⁴, T. Lenz ²⁴,
 S. Leone ^{73a}, C. Leonidopoulos ⁵², A. Leopold ¹⁴³, C. Leroy ¹⁰⁷, R. Les ¹⁰⁶, C.G. Lester ³²,
 M. Levchenko ³⁷, J. Levêque ⁴, D. Levin ¹⁰⁵, L.J. Levinson ¹⁶⁷, D.J. Lewis ²⁰, B. Li ^{14b},
 B. Li ^{62b}, C. Li ^{62a}, C-Q. Li ^{62c,62d}, H. Li ^{62a}, H. Li ^{62b}, H. Li ^{14c}, H. Li ^{62b}, J. Li ^{62c},
 K. Li ¹³⁷, L. Li ^{62c}, M. Li ^{14a,14d}, Q.Y. Li ^{62a}, S. Li ^{62d,62c,d}, T. Li ^{62b}, X. Li ¹⁰³, Z. Li ^{62b},
 Z. Li ¹²⁵, Z. Li ¹⁰³, Z. Li ⁹¹, Z. Liang ^{14a}, M. Liberatore ⁴⁸, B. Liberti ^{75a}, K. Lie ^{64c},
 J. Lieber Marin ^{81b}, K. Lin ¹⁰⁶, R.A. Linck ⁵⁷, R.E. Lindley ⁷, J.H. Lindon ², A. Linss ⁴⁸,
 E. Lipeles ¹²⁷, A. Lipniacka ¹⁶, T.M. Liss ^{160,aa}, A. Lister ¹⁶², J.D. Little ⁴, B. Liu ^{14a},
 B.X. Liu ¹⁴¹, D. Liu ^{62d,62c}, J.B. Liu ^{62a}, J.K.K. Liu ³², K. Liu ^{62d,62c}, M. Liu ^{62a},
 M.Y. Liu ^{62a}, P. Liu ^{14a}, Q. Liu ^{62d,137,62c}, X. Liu ^{62a}, Y. Liu ⁴⁸, Y. Liu ^{14c,14d}, Y.L. Liu ¹⁰⁵,
 Y.W. Liu ^{62a}, M. Livan ^{72a,72b}, J. Llorente Merino ¹⁴¹, S.L. Lloyd ⁹³, E.M. Lobodzinska ⁴⁸,
 P. Loch ⁷, S. Loffredo ^{75a,75b}, T. Lohse ¹⁸, K. Lohwasser ¹³⁸, M. Lokajicek ¹³⁰, J.D. Long ¹⁶⁰,





















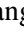
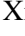

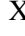






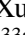
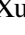




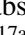


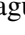
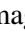
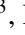
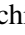

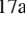
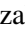

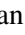

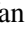
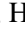


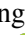
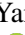


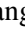












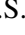
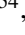
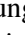
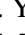






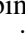
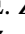
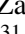

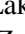


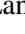
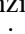
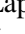

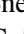
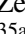
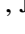

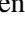
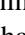
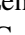
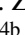


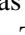
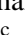

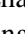
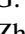



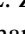


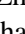
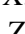


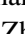
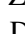


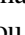
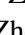
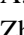


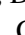
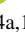
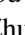
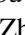
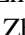
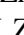
I. Longarini ^{74a,74b}, L. Longo ^{69a,69b}, R. Longo ¹⁶⁰, I. Lopez Paz ³⁶, A. Lopez Solis ⁴⁸,
 J. Lorenz ¹⁰⁸, N. Lorenzo Martinez ⁴, A.M. Lory ¹⁰⁸, A. Lösle ⁵⁴, X. Lou ^{47a,47b}, X. Lou ^{14a,14d},
 A. Lounis ⁶⁶, J. Love ⁶, P.A. Love ⁹⁰, J.J. Lozano Bahilo ¹⁶¹, G. Lu ^{14a,14d}, M. Lu ⁷⁹,
 S. Lu ¹²⁷, Y.J. Lu ⁶⁵, H.J. Lubatti ¹³⁷, C. Luci ^{74a,74b}, F.L. Lucio Alves ^{14c}, A. Lucotte ⁶⁰,
 F. Luehring ⁶⁷, I. Luise ¹⁴⁴, O. Lukianchuk ⁶⁶, O. Lundberg ¹⁴³, B. Lund-Jensen ¹⁴³,
 N.A. Luongo ¹²², M.S. Lutz ¹⁵⁰, D. Lynn ²⁹, H. Lyons ⁹¹, R. Lysak ¹³⁰, E. Lytken ⁹⁷, F. Lyu ^{14a},
 V. Lyubushkin ³⁸, T. Lyubushkina ³⁸, H. Ma ²⁹, L.L. Ma ^{62b}, Y. Ma ⁹⁵, D.M. Mac Donell ¹⁶³,
 G. Maccarrone ⁵³, J.C. MacDonald ¹³⁸, R. Madar ⁴⁰, W.F. Mader ⁵⁰, J. Maeda ⁸³, T. Maeno ²⁹,
 M. Maerker ⁵⁰, V. Magerl ⁵⁴, J. Magro ^{68a,68c}, H. Maguire ¹³⁸, D.J. Mahon ⁴¹,
 C. Maidantchik ^{81b}, A. Maio ^{129a,129b,129d}, K. Maj ^{84a}, O. Majersky ^{28a}, S. Majewski ¹²²,
 N. Makovec ⁶⁶, V. Maksimovic ¹⁵, B. Malaescu ¹²⁶, Pa. Malecki ⁸⁵, V.P. Maleev ³⁷,
 F. Malek ⁶⁰, D. Malito ^{43b,43a}, U. Mallik ⁷⁹, C. Malone ³², S. Maltezos ¹⁰, S. Malyukov ³⁸,
 J. Mamuzic ¹³, G. Mancini ⁵³, G. Manco ^{72a,72b}, J.P. Mandalia ⁹³, I. Mandić ⁹²,
 L. Manhaes de Andrade Filho ^{81a}, I.M. Maniatis ¹⁵¹, M. Manisha ¹³⁴, J. Manjarres Ramos ⁵⁰,
 D.C. Mankad ¹⁶⁷, K.H. Mankinen ⁹⁷, A. Mann ¹⁰⁸, A. Manousos ⁷⁸, B. Mansoulie ¹³⁴,
 S. Manzoni ³⁶, A. Marantis ¹⁵¹, G. Marchiori ⁵, M. Marcisovsky ¹³⁰, L. Marcoccia ^{75a,75b},
 C. Marcon ⁹⁷, M. Marinescu ²⁰, M. Marjanovic ¹¹⁹, Z. Marshall ^{17a}, S. Marti-Garcia ¹⁶¹,
 T.A. Martin ¹⁶⁵, V.J. Martin ⁵², B. Martin dit Latour ¹⁶, L. Martinelli ^{74a,74b}, M. Martinez ^{13,t},
 P. Martinez Agullo ¹⁶¹, V.I. Martinez Outschoorn ¹⁰², P. Martinez Suarez ¹³, S. Martin-Haugh ¹³³,
 V.S. Martoiu ^{27b}, A.C. Martyniuk ⁹⁵, A. Marzin ³⁶, S.R. Maschek ¹⁰⁹, L. Masetti ⁹⁹,
 T. Mashimo ¹⁵², J. Masik ¹⁰⁰, A.L. Maslennikov ³⁷, L. Massa ^{23b}, P. Massarotti ^{71a,71b},
 P. Mastrandrea ^{73a,73b}, A. Mastroberardino ^{43b,43a}, T. Masubuchi ¹⁵², T. Mathisen ¹⁵⁹,
 A. Matic ¹⁰⁸, N. Matsuzawa ¹⁵², J. Maurer ^{27b}, B. Maček ⁹², D.A. Maximov ³⁷, R. Mazini ¹⁴⁷,
 I. Maznas ¹⁵¹, M. Mazza ¹⁰⁶, S.M. Mazza ¹³⁵, C. Mc Ginn ^{29,af}, J.P. Mc Gowan ¹⁰³,
 S.P. Mc Kee ¹⁰⁵, T.G. McCarthy ¹⁰⁹, W.P. McCormack ^{17a}, E.F. McDonald ¹⁰⁴,
 A.E. McDougall ¹¹³, J.A. Mcfayden ¹⁴⁵, G. Mchedlize ^{148b}, R.P. Mckenzie ^{33g},
 T.C. McLachlan ⁴⁸, D.J. McLaughlin ⁹⁵, K.D. McLean ¹⁶³, S.J. McMahon ¹³³, P.C. McNamara ¹⁰⁴,
 R.A. McPherson ^{163,v}, J.E. Mdhululi ^{33g}, S. Meehan ³⁶, T. Megy ⁴⁰, S. Mehlhase ¹⁰⁸,
 A. Mehta ⁹¹, B. Meirose ⁴⁵, D. Melini ¹⁴⁹, B.R. Mellado Garcia ^{33g}, A.H. Melo ⁵⁵,
 F. Meloni ⁴⁸, E.D. Mendes Gouveia ^{129a}, A.M. Mendes Jacques Da Costa ²⁰, H.Y. Meng ¹⁵⁴,
 L. Meng ⁹⁰, S. Menke ¹⁰⁹, M. Mentink ³⁶, E. Meoni ^{43b,43a}, C. Merlassino ¹²⁵,
 L. Merola ^{71a,71b}, C. Meroni ^{70a}, G. Merz ¹⁰⁵, O. Meshkov ³⁷, J.K.R. Meshreki ¹⁴⁰, J. Metcalfe ⁶,
 A.S. Mete ⁶, C. Meyer ⁶⁷, J-P. Meyer ¹³⁴, M. Michetti ¹⁸, R.P. Middleton ¹³³, L. Mijović ⁵²,
 G. Mikenberg ¹⁶⁷, M. Mikestikova ¹³⁰, M. Mikuž ⁹², H. Mildner ¹³⁸, A. Milic ¹⁵⁴,
 C.D. Milke ⁴⁴, D.W. Miller ³⁹, L.S. Miller ³⁴, A. Milov ¹⁶⁷, D.A. Milstead ^{47a,47b}, T. Min ^{14c},
 A.A. Minaenko ³⁷, I.A. Minashvili ^{148b}, L. Mince ⁵⁹, A.I. Mincer ¹¹⁶, B. Mindur ^{84a},
 M. Mineev ³⁸, Y. Minegishi ¹⁵², Y. Mino ⁸⁶, L.M. Mir ¹³, M. Miralles Lopez ¹⁶¹,
 M. Mironova ¹²⁵, T. Mitani ¹⁶⁶, A. Mitra ¹⁶⁵, V.A. Mitsou ¹⁶¹, O. Miu ¹⁵⁴, P.S. Miyagawa ⁹³,
 Y. Miyazaki ⁸⁸, A. Mizukami ⁸², J.U. Mjörnmark ⁹⁷, T. Mkrtchyan ^{63a}, M. Mlynarikova ¹¹⁴,
 T. Moa ^{47a,47b}, S. Mobius ⁵⁵, K. Mochizuki ¹⁰⁷, P. Moder ⁴⁸, P. Mogg ¹⁰⁸,
 A.F. Mohammed ^{14a,14d}, S. Mohapatra ⁴¹, G. Mokgatitwane ^{33g}, B. Mondal ¹⁴⁰, S. Mondal ¹³¹,
 K. Mönig ⁴⁸, E. Monnier ¹⁰¹, L. Monsonis Romero ¹⁶¹, J. Montejo Berlingen ³⁶, M. Montella ¹¹⁸,
 F. Monticelli ⁸⁹, N. Morange ⁶⁶, A.L. Moreira De Carvalho ^{129a}, M. Moreno Llácer ¹⁶¹,
 C. Moreno Martinez ¹³, P. Morettini ^{57b}, S. Morgenstern ¹⁶⁵, M. Morii ⁶¹, M. Morinaga ¹⁵²,
 V. Morisbak ¹²⁴, A.K. Morley ³⁶, F. Morodei ^{74a,74b}, L. Morvaj ³⁶, P. Moschovakos ³⁶,
 B. Moser ³⁶, M. Mosidze ^{148b}, T. Moskalets ⁵⁴, P. Moskvitina ¹¹², J. Moss ^{31,n}, E.J.W. Moyse ¹⁰²,
 S. Muanza ¹⁰¹, J. Mueller ¹²⁸, D. Muenstermann ⁹⁰, R. Müller ¹⁹, G.A. Mullier ⁹⁷, J.J. Mullin ¹²⁷,

D.P. Mungo [ID 70a,70b](#), J.L. Munoz Martinez [ID 13](#), D. Munoz Perez [ID 161](#), F.J. Munoz Sanchez [ID 100](#),
 M. Murin [ID 100](#), W.J. Murray [ID 165,133](#), A. Murrone [ID 70a,70b](#), J.M. Muse [ID 119](#), M. Muškinja [ID 17a](#),
 C. Mwewa [ID 29](#), A.G. Myagkov [ID 37,a](#), A.J. Myers [ID 8](#), A.A. Myers [ID 128](#), G. Myers [ID 67](#), M. Myska [ID 131](#),
 B.P. Nachman [ID 17a](#), O. Nackenhorst [ID 49](#), A.Nag Nag [ID 50](#), K. Nagai [ID 125](#), K. Nagano [ID 82](#),
 J.L. Nagle [ID 29,af](#), E. Nagy [ID 101](#), A.M. Nairz [ID 36](#), Y. Nakahama [ID 82](#), K. Nakamura [ID 82](#), H. Nanjo [ID 123](#),
 R. Narayan [ID 44](#), E.A. Narayanan [ID 111](#), I. Naryshkin [ID 37](#), M. Naseri [ID 34](#), C. Nass [ID 24](#), G. Navarro [ID 22a](#),
 J. Navarro-Gonzalez [ID 161](#), R. Nayak [ID 150](#), P.Y. Nechaeva [ID 37](#), F. Nechansky [ID 48](#), T.J. Neep [ID 20](#),
 A. Negri [ID 72a,72b](#), M. Negrini [ID 23b](#), C. Nellist [ID 112](#), C. Nelson [ID 103](#), K. Nelson [ID 105](#), S. Nemecek [ID 130](#),
 M. Nessi [ID 36,g](#), M.S. Neubauer [ID 160](#), F. Neuhaus [ID 99](#), J. Neundorf [ID 48](#), R. Newhouse [ID 162](#),
 P.R. Newman [ID 20](#), C.W. Ng [ID 128](#), Y.S. Ng [ID 18](#), Y.W.Y. Ng [ID 158](#), B. Ngair [ID 35e](#), H.D.N. Nguyen [ID 107](#),
 R.B. Nickerson [ID 125](#), R. Nicolaidou [ID 134](#), J. Nielsen [ID 135](#), M. Niemeyer [ID 55](#), N. Nikiforou [ID 36](#),
 V. Nikolaenko [ID 37,a](#), I. Nikolic-Audit [ID 126](#), K. Nikolopoulos [ID 20](#), P. Nilsson [ID 29](#), H.R. Nindhito [ID 56](#),
 A. Nisati [ID 74a](#), N. Nishu [ID 2](#), R. Nisius [ID 109](#), J-E. Nitschke [ID 50](#), E.K. Nkadameng [ID 33g](#),
 S.J. Noacco Rosende [ID 89](#), T. Nobe [ID 152](#), D.L. Noel [ID 32](#), Y. Noguchi [ID 86](#), T. Nommensen [ID 146](#),
 M.A. Nomura [ID 29](#), M.B. Norfolk [ID 138](#), R.R.B. Norisam [ID 95](#), B.J. Norman [ID 34](#), J. Novak [ID 92](#), T. Novak [ID 48](#),
 O. Novgorodova [ID 50](#), L. Novotny [ID 131](#), R. Novotny [ID 111](#), L. Nozka [ID 121](#), K. Ntekas [ID 158](#), E. Nurse [ID 95](#),
 F.G. Oakham [ID 34,ac](#), J. Ocariz [ID 126](#), A. Ochi [ID 83](#), I. Ochoa [ID 129a](#), S. Oda [ID 88](#), S. Oerdek [ID 159](#),
 A. Ogrodnik [ID 84a](#), A. Oh [ID 100](#), C.C. Ohm [ID 143](#), H. Oide [ID 153](#), R. Oishi [ID 152](#), M.L. Ojeda [ID 48](#),
 Y. Okazaki [ID 86](#), M.W. O'Keefe [ID 91](#), Y. Okumura [ID 152](#), A. Olariu [ID 27b](#), L.F. Oleiro Seabra [ID 129a](#),
 S.A. Olivares Pino [ID 136e](#), D. Oliveira Damazio [ID 29](#), D. Oliveira Goncalves [ID 81a](#), J.L. Oliver [ID 158](#),
 M.J.R. Olsson [ID 158](#), A. Olszewski [ID 85](#), J. Olszowska [ID 85,*](#), Ö.O. Öncel [ID 54](#), D.C. O'Neil [ID 141](#),
 A.P. O'Neill [ID 19](#), A. Onofre [ID 129a,129e](#), P.U.E. Onyisi [ID 11](#), M.J. Oreglia [ID 39](#), G.E. Orellana [ID 89](#),
 D. Orestano [ID 76a,76b](#), N. Orlando [ID 13](#), R.S. Orr [ID 154](#), V. O'Shea [ID 59](#), R. Ospanov [ID 62a](#),
 G. Otero y Garzon [ID 30](#), H. Otono [ID 88](#), P.S. Ott [ID 63a](#), G.J. Ottino [ID 17a](#), M. Ouchrif [ID 35d](#),
 J. Ouellette [ID 29,af](#), F. Ould-Saada [ID 124](#), M. Owen [ID 59](#), R.E. Owen [ID 133](#), K.Y. Oyulmaz [ID 21a](#),
 V.E. Ozcan [ID 21a](#), N. Ozturk [ID 8](#), S. Ozturk [ID 21d](#), J. Pacalt [ID 121](#), H.A. Pacey [ID 32](#), K. Pachal [ID 51](#),
 A. Pacheco Pages [ID 13](#), C. Padilla Aranda [ID 13](#), G. Padovano [ID 74a,74b](#), S. Pagan Griso [ID 17a](#),
 G. Palacino [ID 67](#), A. Palazzo [ID 69a,69b](#), S. Palazzo [ID 52](#), S. Palestini [ID 36](#), M. Palka [ID 84b](#), J. Pan [ID 170](#),
 T. Pan [ID 64a](#), D.K. Panchal [ID 11](#), C.E. Pandini [ID 113](#), J.G. Panduro Vazquez [ID 94](#), P. Pani [ID 48](#),
 G. Panizzo [ID 68a,68c](#), L. Paolozzi [ID 56](#), C. Papadatos [ID 107](#), S. Parajuli [ID 44](#), A. Paramonov [ID 6](#),
 C. Paraskevopoulos [ID 10](#), D. Paredes Hernandez [ID 64b](#), T.H. Park [ID 154](#), M.A. Parker [ID 32](#), F. Parodi [ID 57b,57a](#),
 E.W. Parrish [ID 114](#), V.A. Parrish [ID 52](#), J.A. Parsons [ID 41](#), U. Parzefall [ID 54](#), B. Pascual Dias [ID 107](#),
 L. Pascual Dominguez [ID 150](#), V.R. Pascuzzi [ID 17a](#), F. Pasquali [ID 113](#), E. Pasqualucci [ID 74a](#), S. Passaggio [ID 57b](#),
 F. Pastore [ID 94](#), P. Pasuwan [ID 47a,47b](#), J.R. Pater [ID 100](#), J. Patton [ID 91](#), T. Pauly [ID 36](#), J. Pearkes [ID 142](#),
 M. Pedersen [ID 124](#), R. Pedro [ID 129a](#), S.V. Peleganchuk [ID 37](#), O. Penc [ID 130](#), C. Peng [ID 64b](#), H. Peng [ID 62a](#),
 M. Penzin [ID 37](#), B.S. Peralva [ID 81a,81d](#), A.P. Pereira Peixoto [ID 60](#), L. Pereira Sanchez [ID 47a,47b](#),
 D.V. Perepelitsa [ID 29,af](#), E. Perez Codina [ID 155a](#), M. Perganti [ID 10](#), L. Perini [ID 70a,70b,*](#), H. Pernegger [ID 36](#),
 S. Perrella [ID 36](#), A. Perrevoort [ID 112](#), O. Perrin [ID 40](#), K. Peters [ID 48](#), R.F.Y. Peters [ID 100](#), B.A. Petersen [ID 36](#),
 T.C. Petersen [ID 42](#), E. Petit [ID 101](#), V. Petousis [ID 131](#), C. Petridou [ID 151](#), A. Petrukhin [ID 140](#), M. Pettee [ID 17a](#),
 N.E. Pettersson [ID 36](#), A. Petukhov [ID 37](#), K. Petukhova [ID 132](#), A. Peyaud [ID 134](#), R. Pezoa [ID 136f](#),
 L. Pezzotti [ID 36](#), G. Pezzullo [ID 170](#), T. Pham [ID 104](#), P.W. Phillips [ID 133](#), M.W. Phipps [ID 160](#),
 G. Piacquadio [ID 144](#), E. Pianori [ID 17a](#), F. Piazza [ID 70a,70b](#), R. Piegai [ID 30](#), D. Pietreanu [ID 27b](#),
 A.D. Pilkington [ID 100](#), M. Pinamonti [ID 68a,68c](#), J.L. Pinfeld [ID 2](#), B.C. Pinheiro Pereira [ID 129a](#),
 C. Pitman Donaldson [ID 95](#), D.A. Pizzi [ID 34](#), L. Pizzimento [ID 75a,75b](#), A. Pizzini [ID 113](#), M.-A. Pleier [ID 29](#),
 V. Plesanovs [ID 54](#), V. Pleskot [ID 132](#), E. Plotnikova [ID 38](#), G. Poddar [ID 4](#), R. Poettgen [ID 97](#), R. Poggi [ID 56](#),
 L. Poggioli [ID 126](#), I. Pogrebnyak [ID 106](#), D. Pohl [ID 24](#), I. Pokharel [ID 55](#), S. Polacek [ID 132](#), G. Polesello [ID 72a](#),
 A. Poley [ID 141,155a](#), R. Polifka [ID 131](#), A. Polini [ID 23b](#), C.S. Pollard [ID 125](#), Z.B. Pollock [ID 118](#),

V. Polychronakos ²⁹, D. Ponomarenko ³⁷, L. Pontecorvo ³⁶, S. Popa ^{27a}, G.A. Popeneciu ^{27d}, D.M. Portillo Quintero ^{155a}, S. Pospisil ¹³¹, P. Postolache ^{27c}, K. Potamianos ¹²⁵, I.N. Potrap ³⁸, C.J. Potter ³², H. Potti ¹, T. Poulsen ⁴⁸, J. Poveda ¹⁶¹, G. Pownall ⁴⁸, M.E. Pozo Astigarraga ³⁶, A. Prades Ibanez ¹⁶¹, M.M. Prapa ⁴⁶, D. Price ¹⁰⁰, M. Primavera ^{69a}, M.A. Principe Martin ⁹⁸, M.L. Proffitt ¹³⁷, N. Proklova ³⁷, K. Prokofiev ^{64c}, G. Proto ^{75a,75b}, S. Protopopescu ²⁹, J. Proudfoot ⁶, M. Przybycien ^{34a}, J.E. Puddefoot ¹³⁸, D. Pudzha ³⁷, P. Puzo ⁶⁶, D. Pyatiizbyantseva ³⁷, J. Qian ¹⁰⁵, Y. Qin ¹⁰⁰, T. Qiu ⁹³, A. Quadt ⁵⁵, M. Queitsch-Maitland ²⁴, G. Rabanal Bolanos ⁶¹, D. Rafanoharana ⁵⁴, F. Ragusa ^{70a,70b}, J.L. Rainbolt ³⁹, J.A. Raine ⁵⁶, S. Rajagopalan ²⁹, E. Ramakoti ³⁷, K. Ran ^{14a,14d}, V. Raskina ¹²⁶, D.F. Rassloff ^{63a}, S. Rave ⁹⁹, B. Ravina ⁵⁹, I. Ravinovich ¹⁶⁷, M. Raymond ³⁶, A.L. Read ¹²⁴, N.P. Readioff ¹³⁸, D.M. Rebuzzi ^{72a,72b}, G. Redlinger ²⁹, K. Reeves ⁴⁵, J.A. Reidelsturz ¹⁶⁹, D. Reikher ¹⁵⁰, A. Reiss ⁹⁹, A. Rej ¹⁴⁰, C. Rembser ³⁶, A. Renardi ⁴⁸, M. Renda ^{27b}, M.B. Rendel ¹⁰⁹, A.G. Rennie ⁵⁹, S. Resconi ^{70a}, M. Ressegotti ^{57b,57a}, E.D. Resseguie ^{17a}, S. Rettie ⁹⁵, B. Reynolds ¹¹⁸, E. Reynolds ^{17a}, M. Rezaei Estabragh ¹⁶⁹, O.L. Rezanova ³⁷, P. Reznicek ¹³², E. Ricci ^{77a,77b}, R. Richter ¹⁰⁹, S. Richter ^{47a,47b}, E. Richter-Was ^{84b}, M. Ridel ¹²⁶, P. Rieck ¹¹⁶, P. Riedler ³⁶, M. Rijssenbeek ¹⁴⁴, A. Rimoldi ^{72a,72b}, M. Rimoldi ⁴⁸, L. Rinaldi ^{23b,23a}, T.T. Rinn ²⁹, M.P. Rinnagel ¹⁰⁸, G. Ripellino ¹⁴³, I. Riu ¹³, P. Rivadeneira ⁴⁸, J.C. Rivera Vergara ¹⁶³, F. Rizatdinova ¹²⁰, E. Rizvi ⁹³, C. Rizzi ⁵⁶, B.A. Roberts ¹⁶⁵, B.R. Roberts ^{17a}, S.H. Robertson ^{103,v}, M. Robin ⁴⁸, D. Robinson ³², C.M. Robles Gajardo ^{136f}, M. Robles Manzano ⁹⁹, A. Robson ⁵⁹, A. Rocchi ^{75a,75b}, C. Roda ^{73a,73b}, S. Rodriguez Bosca ^{63a}, Y. Rodriguez Garcia ^{22a}, A. Rodriguez Rodriguez ⁵⁴, A.M. Rodríguez Vera ^{155b}, S. Roe ³⁶, J.T. Roemer ¹⁵⁸, A.R. Roepe-Gier ¹¹⁹, J. Roggel ¹⁶⁹, O. Røhne ¹²⁴, R.A. Rojas ¹⁶³, B. Roland ⁵⁴, C.P.A. Roland ⁶⁷, J. Roloff ²⁹, A. Romaniouk ³⁷, E. Romano ^{72a,72b}, M. Romano ^{23b}, A.C. Romero Hernandez ¹⁶⁰, N. Rompotis ⁹¹, L. Roos ¹²⁶, S. Rosati ^{74a}, B.J. Rosser ³⁹, E. Rossi ⁴, E. Rossi ^{71a,71b}, L.P. Rossi ^{57b}, L. Rossini ⁴⁸, R. Rosten ¹¹⁸, M. Rotaru ^{27b}, B. Rottler ⁵⁴, D. Rousseau ⁵⁶, D. Rousso ³², G. Rovelli ^{72a,72b}, A. Roy ¹⁶⁰, A. Rozanov ¹⁰¹, Y. Rozen ¹⁴⁹, X. Ruan ^{33g}, A. Rubio Jimenez ¹⁶¹, A.J. Ruby ⁹¹, T.A. Ruggeri ¹, F. Rühr ⁵⁴, A. Ruiz-Martinez ¹⁶¹, A. Rummler ³⁶, Z. Rurikova ⁵⁴, N.A. Rusakovich ³⁸, H.L. Russell ¹⁶³, J.P. Rutherford ⁷, E.M. Rüttinger ¹³⁸, K. Rybacki ⁹⁰, M. Rybar ¹³², E.B. Rye ¹²⁴, A. Ryzhov ³⁷, J.A. Sabater Iglesias ⁵⁶, P. Sabatini ¹⁶¹, L. Sabetta ^{74a,74b}, H.F-W. Sadrozinski ¹³⁵, F. Safai Tehrani ^{74a}, B. Safarzadeh Samani ¹⁴⁵, M. Safdari ¹⁴², S. Saha ¹⁰³, M. Sahinsoy ¹⁰⁹, M. Saimpert ¹³⁴, M. Saito ¹⁵², T. Saito ¹⁵², D. Salamani ³⁶, G. Salamanna ^{76a,76b}, A. Salnikov ¹⁴², J. Salt ¹⁶¹, A. Salvador Salas ¹³, D. Salvatore ^{43b,43a}, F. Salvatore ¹⁴⁵, A. Salzburger ³⁶, D. Sammel ⁵⁴, D. Sampsonidis ¹⁵¹, D. Sampsonidou ^{62d,62c}, J. Sánchez ¹⁶¹, A. Sanchez Pineda ⁴, V. Sanchez Sebastian ¹⁶¹, H. Sandaker ¹²⁴, C.O. Sander ⁴⁸, J.A. Sandesara ¹⁰², M. Sandhoff ¹⁶⁹, C. Sandoval ^{22b}, D.P.C. Sankey ¹³³, A. Sansoni ⁵³, L. Santi ^{74a,74b}, C. Santoni ⁴⁰, H. Santos ^{129a,129b}, S.N. Santpur ^{17a}, A. Santra ¹⁶⁷, K.A. Saoucha ¹³⁸, J.G. Saraiva ^{129a,129d}, J. Sardain ¹⁰¹, O. Sasaki ⁸², K. Sato ¹⁵⁶, C. Sauer ^{63b}, F. Sauerburger ⁵⁴, E. Sauvan ⁴, P. Savard ^{154,ac}, R. Sawada ¹⁵², C. Sawyer ¹³³, L. Sawyer ⁹⁶, I. Sayago Galvan ¹⁶¹, C. Sbarra ^{23b}, A. Sbrizzi ^{23b,23a}, T. Scanlon ⁹⁵, J. Schaarschmidt ¹³⁷, P. Schacht ¹⁰⁹, D. Schaefer ³⁹, U. Schäfer ⁹⁹, A.C. Schaffer ⁶⁶, D. Schaile ¹⁰⁸, R.D. Schamberger ¹⁴⁴, E. Schanet ¹⁰⁸, C. Scharf ¹⁸, V.A. Schegelsky ³⁷, D. Scheirich ¹³², F. Schenck ¹⁸, M. Schernau ¹⁵⁸, C. Scheulen ⁵⁵, C. Schiavi ^{57b,57a}, Z.M. Schillaci ²⁶, E.J. Schioppa ^{69a,69b}, M. Schioppa ^{43b,43a}, B. Schlag ⁹⁹, K.E. Schleicher ⁵⁴, S. Schlenker ³⁶, K. Schmieden ⁹⁹, C. Schmitt ⁹⁹, S. Schmitt ⁴⁸, L. Schoeffel ¹³⁴, A. Schoening ^{63b}, P.G. Scholer ⁵⁴, E. Schopf ¹²⁵, M. Schott ⁹⁹, J. Schovancova ³⁶, S. Schramm ⁵⁶, F. Schroeder ¹⁶⁹, H-C. Schultz-Coulon ^{63a}, M. Schumacher ⁵⁴, B.A. Schumm ¹³⁵, Ph. Schune ¹³⁴,

A. Schwartzman ¹⁴², T.A. Schwarz ¹⁰⁵, Ph. Schwemling ¹³⁴, R. Schwienhorst ¹⁰⁶,
 A. Sciandra ¹³⁵, G. Sciolla ²⁶, F. Scuri ^{73a}, F. Scutti ¹⁰⁴, C.D. Sebastiani ⁹¹, K. Sedlaczek ⁴⁹,
 P. Seema ¹⁸, S.C. Seidel ¹¹¹, A. Seiden ¹³⁵, B.D. Seidlitz ⁴¹, T. Seiss ³⁹, C. Seitz ⁴⁸,
 J.M. Seixas ^{81b}, G. Sekhniaidze ^{71a}, S.J. Sekula ⁴⁴, L. Selem ⁴, N. Semprini-Cesari ^{23b,23a},
 S. Sen ⁵¹, D. Sengupta ⁵⁶, V. Senthilkumar ¹⁶¹, L. Serin ⁶⁶, L. Serkin ^{68a,68b}, M. Sessa ^{76a,76b},
 H. Severini ¹¹⁹, S. Sevova ¹⁴², F. Sforza ^{57b,57a}, A. Sfyrta ⁵⁶, E. Shabalina ⁵⁵, R. Shaheen ¹⁴³,
 J.D. Shahinian ¹²⁷, N.W. Shaikh ^{47a,47b}, D. Shaked Renous ¹⁶⁷, L.Y. Shan ^{14a}, M. Shapiro ^{17a},
 A. Sharma ³⁶, A.S. Sharma ¹⁶², P. Sharma ⁷⁹, S. Sharma ⁴⁸, P.B. Shatalov ³⁷, K. Shaw ¹⁴⁵,
 S.M. Shaw ¹⁰⁰, Q. Shen ^{62c}, P. Sherwood ⁹⁵, L. Shi ⁹⁵, C.O. Shimmin ¹⁷⁰, Y. Shimogama ¹⁶⁶,
 J.D. Shinner ⁹⁴, I.P.J. Shipsey ¹²⁵, S. Shirabe ⁶⁰, M. Shiyakova ³⁸, J. Shlomi ¹⁶⁷,
 M.J. Shochet ³⁹, J. Shojaii ¹⁰⁴, D.R. Shope ¹⁴³, S. Shrestha ¹¹⁸, E.M. Shrif ^{33g}, M.J. Shroff ¹⁶³,
 P. Sicho ¹³⁰, A.M. Sickles ¹⁶⁰, E. Sideras Haddad ^{33g}, O. Sidiropoulou ³⁶, A. Sidoti ^{23b},
 F. Siegert ⁵⁰, Dj. Sijacki ¹⁵, R. Sikora ^{84a}, F. Sili ⁸⁹, J.M. Silva ²⁰, M.V. Silva Oliveira ³⁶,
 S.B. Silverstein ^{47a}, S. Simion ⁶⁶, R. Simoniello ³⁶, E.L. Simpson ⁵⁹, N.D. Simpson ⁹⁷,
 S. Simsek ^{21d}, S. Sindhu ⁵⁵, P. Sinervo ¹⁵⁴, V. Sinetckii ³⁷, S. Singh ¹⁴¹, S. Singh ¹⁵⁴,
 S. Sinha ⁴⁸, S. Sinha ^{33g}, M. Sioli ^{23b,23a}, I. Siral ¹²², S. Yu. Sivoklov ^{37,*}, J. Sjölin ^{47a,47b},
 A. Skaf ⁵⁵, E. Skorda ⁹⁷, P. Skubic ¹¹⁹, M. Slawinska ⁸⁵, V. Smakhtin ¹⁶⁷, B.H. Smart ¹³³,
 J. Smiesko ¹³², S.Yu. Smirnov ³⁷, Y. Smirnov ³⁷, L.N. Smirnova ^{37,a}, O. Smirnova ⁹⁷,
 E.A. Smith ³⁹, H.A. Smith ¹²⁵, J.L. Smith ⁹¹, R. Smith ¹⁴², M. Smizanska ⁹⁰, K. Smolek ¹³¹,
 A. Smykiewicz ⁸⁵, A.A. Snesarev ³⁷, H.L. Snoek ¹¹³, S. Snyder ²⁹, R. Sobie ^{163,v}, A. Soffer ¹⁵⁰,
 C.A. Solans Sanchez ³⁶, E.Yu. Soldatov ³⁷, U. Soldevila ¹⁶¹, A.A. Solodkov ³⁷, S. Solomon ⁵⁴,
 A. Soloshenko ³⁸, K. Solovieva ⁵⁴, O.V. Solovyanov ³⁷, V. Solovyev ³⁷, P. Sommer ³⁶,
 A. Sonay ¹³, W.Y. Song ^{155b}, A. Sopczak ¹³¹, A.L. Sopio ⁹⁵, F. Sopkova ^{28b}, V. Sothilingam ^{63a},
 S. Sottocornola ^{72a,72b}, R. Soualah ^{115c}, Z. Soumami ^{35e}, D. South ⁴⁸, S. Spagnolo ^{69a,69b},
 M. Spalla ¹⁰⁹, F. Spanò ⁹⁴, D. Sperlich ⁵⁴, G. Spigo ³⁶, M. Spina ¹⁴⁵, S. Spinali ⁹⁰,
 D.P. Spiteri ⁵⁹, M. Spousta ¹³², E.J. Staats ³⁴, A. Stabile ^{70a,70b}, R. Stamen ^{63a},
 M. Stamenkovic ¹¹³, A. Stampekis ²⁰, M. Standke ²⁴, E. Stanecka ⁸⁵, B. Stanislaus ^{17a},
 M.M. Stanitzki ⁴⁸, M. Stankaityte ¹²⁵, B. Stapf ⁴⁸, E.A. Starchenko ³⁷, G.H. Stark ¹³⁵,
 J. Stark ¹⁰¹, D.M. Starke ^{155b}, P. Staroba ¹³⁰, P. Starovoitov ^{63a}, S. Stärz ¹⁰³, R. Staszewski ⁸⁵,
 G. Stavropoulos ⁴⁶, J. Steentoft ¹⁵⁹, P. Steinberg ²⁹, A.L. Steinhebel ¹²², B. Stelzer ^{141,155a},
 H.J. Stelzer ¹²⁸, O. Stelzer-Chilton ^{155a}, H. Stenzel ⁵⁸, T.J. Stevenson ¹⁴⁵, G.A. Stewart ³⁶,
 M.C. Stockton ³⁶, G. Stoicea ^{27b}, M. Stolarski ^{129a}, S. Stonjek ¹⁰⁹, A. Straessner ⁵⁰,
 J. Strandberg ¹⁴³, S. Strandberg ^{47a,47b}, M. Strauss ¹¹⁹, T. Strebler ¹⁰¹, P. Strizenc ^{28b},
 R. Ströhmer ¹⁶⁴, D.M. Strom ¹²², L.R. Strom ⁴⁸, R. Stroynowski ⁴⁴, A. Strubig ^{47a,47b},
 S.A. Stucci ²⁹, B. Stugu ¹⁶, J. Stupak ¹¹⁹, N.A. Styles ⁴⁸, D. Su ¹⁴², S. Su ^{62a},
 W. Su ^{62d,137,62c}, X. Su ^{62a,66}, K. Sugizaki ¹⁵², V.V. Sulim ³⁷, M.J. Sullivan ⁹¹,
 D.M.S. Sultan ^{77a,77b}, L. Sultanaliyeva ³⁷, S. Sultansoy ^{3b}, T. Sumida ⁸⁶, S. Sun ¹⁰⁵, S. Sun ¹⁶⁸,
 O. Sunneborn Gudnadottir ¹⁵⁹, M.R. Sutton ¹⁴⁵, M. Svatos ¹³⁰, M. Swiatlowski ^{155a},
 T. Swirski ¹⁶⁴, I. Sykora ^{28a}, M. Sykora ¹³², T. Sykora ¹³², D. Ta ⁹⁹, K. Tackmann ^{48,u},
 A. Taffard ¹⁵⁸, R. Tafirout ^{155a}, J.S. Tafoya Vargas ⁶⁶, R.H.M. Taibah ¹²⁶, R. Takashima ⁸⁷,
 K. Takeda ⁸³, E.P. Takeva ⁵², Y. Takubo ⁸², M. Talby ¹⁰¹, A.A. Talyshv ³⁷, K.C. Tam ^{64b},
 N.M. Tamir ¹⁵⁰, A. Tanaka ¹⁵², J. Tanaka ¹⁵², R. Tanaka ⁶⁶, M. Tanasini ^{57b,57a}, J. Tang ^{62c},
 Z. Tao ¹⁶², S. Tapia Araya ⁸⁰, S. Tapprogge ⁹⁹, A. Tarek Abouelfadl Mohamed ¹⁰⁶, S. Tarem ¹⁴⁹,
 K. Tariq ^{62b}, G. Tarna ^{27b}, G.F. Tartarelli ^{70a}, P. Tas ¹³², M. Tasevsky ¹³⁰, E. Tassi ^{43b,43a},
 A.C. Tate ¹⁶⁰, G. Tateno ¹⁵², Y. Tayalati ^{35e}, G.N. Taylor ¹⁰⁴, W. Taylor ^{155b}, H. Teagle ⁹¹,
 A.S. Tee ¹⁶⁸, R. Teixeira De Lima ¹⁴², P. Teixeira-Dias ⁹⁴, J.J. Teoh ¹⁵⁴, K. Terashi ¹⁵²,
 J. Terron ⁹⁸, S. Terzo ¹³, M. Testa ⁵³, R.J. Teuscher ^{154,v}, N. Themistokleous ⁵²,

T. Theveneaux-Pelzer ¹⁸, O. Thielmann ¹⁶⁹, D.W. Thomas ⁹⁴, J.P. Thomas ²⁰, E.A. Thompson ⁴⁸, P.D. Thompson ²⁰, E. Thomson ¹²⁷, E.J. Thorpe ⁹³, Y. Tian ⁵⁵, V. Tikhomirov ^{37,a}, Yu.A. Tikhonov ³⁷, S. Timoshenko ³⁷, E.X.L. Ting ¹, P. Tipton ¹⁷⁰, S. Tisserant ¹⁰¹, S.H. Tlou ^{33g}, A. Tnourji ⁴⁰, K. Todome ^{23b,23a}, S. Todorova-Nova ¹³², S. Todt ⁵⁰, M. Togawa ⁸², J. Tojo ⁸⁸, S. Tokár ^{28a}, K. Tokushuku ⁸², R. Tombs ³², M. Tomoto ^{82,110}, L. Tompkins ¹⁴², P. Tornambe ¹⁰², E. Torrence ¹²², H. Torres ⁵⁰, E. Torró Pastor ¹⁶¹, M. Toscani ³⁰, C. Tosciri ³⁹, D.R. Tovey ¹³⁸, A. Traeet ¹⁶, I.S. Trandafir ^{27b}, T. Trefzger ¹⁶⁴, A. Tricoli ²⁹, I.M. Trigger ^{155a}, S. Trincaz-Duvoid ¹²⁶, D.A. Trischuk ¹⁶², B. Trocmé ⁶⁰, A. Trofymov ⁶⁶, C. Troncon ^{70a}, L. Truong ^{33c}, M. Trzebinski ⁸⁵, A. Trzupiek ⁸⁵, F. Tsai ¹⁴⁴, M. Tsai ¹⁰⁵, A. Tsiamis ¹⁵¹, P.V. Tsiarehka ³⁷, S. Tsigaridas ^{155a}, A. Tsirigotis ^{151,s}, V. Tsiskaridze ¹⁴⁴, E.G. Tskhadadze ^{148a}, M. Tsopoulou ¹⁵¹, Y. Tsujikawa ⁸⁶, I.I. Tsukerman ³⁷, V. Tsulaia ^{17a}, S. Tsuno ⁸², O. Tsur ¹⁴⁹, D. Tsybychev ¹⁴⁴, Y. Tu ^{64b}, A. Tudorache ^{27b}, V. Tudorache ^{27b}, A.N. Tuna ³⁶, S. Turchikhin ³⁸, I. Turk Cakir ^{3a}, R. Turra ^{70a}, P.M. Tuts ⁴¹, S. Tzamarias ¹⁵¹, P. Tzanis ¹⁰, E. Tzovara ⁹⁹, K. Uchida ¹⁵², F. Ukegawa ¹⁵⁶, P.A. Ulloa Poblete ^{136c}, G. Unal ³⁶, M. Unal ¹¹, A. Undrus ²⁹, G. Unel ¹⁵⁸, K. Uno ¹⁵², J. Urban ^{28b}, P. Urquijo ¹⁰⁴, G. Usai ⁸, R. Ushioda ¹⁵³, M. Usman ¹⁰⁷, Z. Uysal ^{21b}, V. Vacek ¹³¹, B. Vachon ¹⁰³, K.O.H. Vadla ¹²⁴, T. Vafeiadis ³⁶, C. Valderanis ¹⁰⁸, E. Valdes Santurio ^{47a,47b}, M. Valente ^{155a}, S. Valentinetti ^{23b,23a}, A. Valero ¹⁶¹, A. Vallier ¹⁰¹, J.A. Valls Ferrer ¹⁶¹, T.R. Van Daalen ¹³⁷, P. Van Gemmeren ⁶, S. Van Stroud ⁹⁵, I. Van Vulpen ¹¹³, M. Vanadia ^{75a,75b}, W. Vandelli ³⁶, M. Vandenbroucke ¹³⁴, E.R. Vandewall ¹²⁰, D. Vannicola ¹⁵⁰, L. Vannoli ^{57b,57a}, R. Vari ^{74a}, E.W. Varnes ⁷, C. Varni ^{17a}, T. Varol ¹⁴⁷, D. Varouchas ⁶⁶, L. Varriale ¹⁶¹, K.E. Varvell ¹⁴⁶, M.E. Vasile ^{27b}, L. Vaslin ⁴⁰, G.A. Vasquez ¹⁶³, F. Vazeille ⁴⁰, T. Vazquez Schroeder ³⁶, J. Veatch ³¹, V. Vecchio ¹⁰⁰, M.J. Veen ¹¹³, I. Veliscek ¹²⁵, L.M. Veloce ¹⁵⁴, F. Veloso ^{129a,129c}, S. Veneziano ^{74a}, A. Ventura ^{69a,69b}, A. Verbitskiy ¹⁰⁹, M. Verducci ^{73a,73b}, C. Vergis ²⁴, M. Verissimo De Araujo ^{81b}, W. Verkerke ¹¹³, J.C. Vermeulen ¹¹³, C. Vernieri ¹⁴², P.J. Verschuuren ⁹⁴, M. Vessella ¹⁰², M.L. Vesterbacka ¹¹⁶, M.C. Vetterli ^{141,ac}, A. Vgenopoulos ¹⁵¹, N. Viaux Maira ^{136f}, T. Vickey ¹³⁸, O.E. Vickey Boeriu ¹³⁸, G.H.A. Viehhauser ¹²⁵, L. Vigani ^{63b}, M. Villa ^{23b,23a}, M. Villaplana Perez ¹⁶¹, E.M. Villhauer ⁵², E. Vilucchi ⁵³, M.G. Vincter ³⁴, G.S. Virdee ²⁰, A. Vishwakarma ⁵², C. Vittori ^{23b,23a}, I. Vivarelli ¹⁴⁵, V. Vladimirov ¹⁶⁵, E. Voevodina ¹⁰⁹, F. Vogel ¹⁰⁸, P. Vokac ¹³¹, J. Von Ahnen ⁴⁸, E. Von Toerne ²⁴, B. Vormwald ³⁶, V. Vorobel ¹³², K. Vorobev ³⁷, M. Vos ¹⁶¹, J.H. Vosseveld ⁹¹, M. Vozak ¹¹³, L. Vozdecky ⁹³, N. Vranjes ¹⁵, M. Vranjes Milosavljevic ¹⁵, M. Vreeswijk ¹¹³, R. Vuillermet ³⁶, O. Vujanovic ⁹⁹, I. Vukotic ³⁹, S. Wada ¹⁵⁶, C. Wagner ¹⁰², W. Wagner ¹⁶⁹, S. Wahdan ¹⁶⁹, H. Wahlberg ⁸⁹, R. Wakasa ¹⁵⁶, M. Wakida ¹¹⁰, V.M. Walbrecht ¹⁰⁹, J. Walder ¹³³, R. Walker ¹⁰⁸, W. Walkowiak ¹⁴⁰, A.M. Wang ⁶¹, A.Z. Wang ¹⁶⁸, C. Wang ^{62a}, C. Wang ^{62c}, H. Wang ^{17a}, J. Wang ^{64a}, P. Wang ⁴⁴, R.-J. Wang ⁹⁹, R. Wang ⁶¹, R. Wang ⁶, S.M. Wang ¹⁴⁷, S. Wang ^{62b}, T. Wang ^{62a}, W.T. Wang ⁷⁹, W.X. Wang ^{62a}, X. Wang ^{14c}, X. Wang ¹⁶⁰, X. Wang ^{62c}, Y. Wang ^{62d}, Y. Wang ^{14c}, Z. Wang ¹⁰⁵, Z. Wang ^{62d,51,62c}, Z. Wang ¹⁰⁵, A. Warburton ¹⁰³, R.J. Ward ²⁰, N. Warrack ⁵⁹, A.T. Watson ²⁰, M.F. Watson ²⁰, G. Watts ¹³⁷, B.M. Waugh ⁹⁵, A.F. Webb ¹¹, C. Weber ²⁹, M.S. Weber ¹⁹, S.A. Weber ³⁴, S.M. Weber ^{63a}, C. Wei ^{62a}, Y. Wei ¹²⁵, A.R. Weidberg ¹²⁵, J. Weingarten ⁴⁹, M. Weirich ⁹⁹, C. Weiser ⁵⁴, C.J. Wells ⁴⁸, T. Wenaus ²⁹, B. Wendland ⁴⁹, T. Wengler ³⁶, N.S. Wenke ¹⁰⁹, N. Wermes ²⁴, M. Wessels ^{63a}, K. Whalen ¹²², A.M. Wharton ⁹⁰, A.S. White ⁶¹, A. White ⁸, M.J. White ¹, D. Whiteson ¹⁵⁸, L. Wickremasinghe ¹²³, W. Wiedenmann ¹⁶⁸, C. Wiel ⁵⁰, M. Wielers ¹³³, N. Wieseotte ⁹⁹, C. Wiglesworth ⁴², L.A.M. Wiik-Fuchs ⁵⁴, D.J. Wilbern ¹¹⁹, H.G. Wilkens ³⁶, D.M. Williams ⁴¹, H.H. Williams ¹²⁷, S. Williams ³², S. Willocq ¹⁰², P.J. Windischhofer ¹²⁵, F. Winklmeier ¹²², B.T. Winter ⁵⁴, M. Wittgen ¹⁴², M. Wobisch ⁹⁶, A. Wolf ⁹⁹, R. Wölker ¹²⁵, J. Wollrath ¹⁵⁸,

M.W. Wolter ⁸⁵, H. Wolters ^{129a,129c}, V.W.S. Wong ¹⁶², A.F. Wongel ⁴⁸, S.D. Worm ⁴⁸, B.K. Wosiek ⁸⁵, K.W. Woźniak ⁸⁵, K. Wraight ⁵⁹, J. Wu ^{14a,14d}, M. Wu ^{64a}, S.L. Wu ¹⁶⁸, X. Wu ⁵⁶, Y. Wu ^{62a}, Z. Wu ^{134,62a}, J. Wuerzinger ¹²⁵, T.R. Wyatt ¹⁰⁰, B.M. Wynne ⁵², S. Xella ⁴², L. Xia ^{14c}, M. Xia ^{14b}, J. Xiang ^{64c}, X. Xiao ¹⁰⁵, M. Xie ^{62a}, X. Xie ^{62a}, J. Xiong ^{17a}, I. Xioidis ¹⁴⁵, D. Xu ^{14a}, H. Xu ^{62a}, H. Xu ^{62a}, L. Xu ^{62a}, R. Xu ¹²⁷, T. Xu ¹⁰⁵, W. Xu ¹⁰⁵, Y. Xu ^{14b}, Z. Xu ^{62b}, Z. Xu ¹⁴², B. Yabsley ¹⁴⁶, S. Yacoob ^{33a}, N. Yamaguchi ⁸⁸, Y. Yamaguchi ¹⁵³, H. Yamauchi ¹⁵⁶, T. Yamazaki ^{17a}, Y. Yamazaki ⁸³, J. Yan ^{62c}, S. Yan ¹²⁵, Z. Yan ²⁵, H.J. Yang ^{62c,62d}, H.T. Yang ^{17a}, S. Yang ^{62a}, T. Yang ^{64c}, X. Yang ^{62a}, X. Yang ^{14a}, Y. Yang ⁴⁴, Z. Yang ^{62a,105}, W-M. Yao ^{17a}, Y.C. Yap ⁴⁸, H. Ye ^{14c}, J. Ye ⁴⁴, S. Ye ²⁹, X. Ye ^{62a}, I. Yeletsikh ³⁸, M.R. Yexley ⁹⁰, P. Yin ⁴¹, K. Yorita ¹⁶⁶, C.J.S. Young ⁵⁴, C. Young ¹⁴², M. Yuan ¹⁰⁵, R. Yuan ^{62b,j}, L. Yue ⁹⁵, X. Yue ^{63a}, M. Zaazoua ^{35e}, B. Zabinski ⁸⁵, E. Zaid ⁵², T. Zakareishvili ^{148b}, N. Zakharchuk ³⁴, S. Zambito ⁵⁶, J. Zang ¹⁵², D. Zanzi ⁵⁴, O. Zaplatilek ¹³¹, S.V. Zeibner ⁴⁹, C. Zeitnitz ¹⁶⁹, J.C. Zeng ¹⁶⁰, D.T. Zenger Jr ²⁶, O. Zenin ³⁷, T. Ženiš ^{28a}, S. Zenz ⁹³, S. Zerradi ^{35a}, D. Zerwas ⁶⁶, B. Zhang ^{14c}, D.F. Zhang ¹³⁸, G. Zhang ^{14b}, J. Zhang ⁶, K. Zhang ^{14a,14d}, L. Zhang ^{14c}, R. Zhang ¹⁶⁸, S. Zhang ¹⁰⁵, T. Zhang ¹⁵², X. Zhang ^{62c}, X. Zhang ^{62b}, Z. Zhang ⁶⁶, H. Zhao ¹³⁷, P. Zhao ⁵¹, T. Zhao ^{62b}, Y. Zhao ¹³⁵, Z. Zhao ^{62a}, A. Zhemchugov ³⁸, Z. Zheng ¹⁴², D. Zhong ¹⁶⁰, B. Zhou ¹⁰⁵, C. Zhou ¹⁶⁸, H. Zhou ⁷, N. Zhou ^{62c}, Y. Zhou ⁷, C.G. Zhu ^{62b}, C. Zhu ^{14a,14d}, H.L. Zhu ^{62a}, H. Zhu ^{14a}, J. Zhu ¹⁰⁵, Y. Zhu ^{62a}, X. Zhuang ^{14a}, K. Zhukov ³⁷, V. Zhulanov ³⁷, N.I. Zimine ³⁸, J. Zinsser ^{63b}, M. Ziolkowski ¹⁴⁰, L. Živković ¹⁵, A. Zoccoli ^{23b,23a}, K. Zoch ⁵⁶, T.G. Zorbas ¹³⁸, O. Zormpa ⁴⁶, W. Zou ⁴¹, L. Zwalinski ³⁶.

¹Department of Physics, University of Adelaide, Adelaide; Australia.

²Department of Physics, University of Alberta, Edmonton AB; Canada.

³(^a)Department of Physics, Ankara University, Ankara; (^b)Division of Physics, TOBB University of Economics and Technology, Ankara; Türkiye.

⁴LAPP, Univ. Savoie Mont Blanc, CNRS/IN2P3, Annecy; France.

⁵APC, Université Paris Cité, CNRS/IN2P3, Paris; France.

⁶High Energy Physics Division, Argonne National Laboratory, Argonne IL; United States of America.

⁷Department of Physics, University of Arizona, Tucson AZ; United States of America.

⁸Department of Physics, University of Texas at Arlington, Arlington TX; United States of America.

⁹Physics Department, National and Kapodistrian University of Athens, Athens; Greece.

¹⁰Physics Department, National Technical University of Athens, Zografou; Greece.

¹¹Department of Physics, University of Texas at Austin, Austin TX; United States of America.

¹²Institute of Physics, Azerbaijan Academy of Sciences, Baku; Azerbaijan.

¹³Institut de Física d'Altes Energies (IFAE), Barcelona Institute of Science and Technology, Barcelona; Spain.

¹⁴(^a)Institute of High Energy Physics, Chinese Academy of Sciences, Beijing; (^b)Physics Department, Tsinghua University, Beijing; (^c)Department of Physics, Nanjing University, Nanjing; (^d)University of Chinese Academy of Science (UCAS), Beijing; China.

¹⁵Institute of Physics, University of Belgrade, Belgrade; Serbia.

¹⁶Department for Physics and Technology, University of Bergen, Bergen; Norway.

¹⁷(^a)Physics Division, Lawrence Berkeley National Laboratory, Berkeley CA; (^b)University of California, Berkeley CA; United States of America.

¹⁸Institut für Physik, Humboldt Universität zu Berlin, Berlin; Germany.

¹⁹Albert Einstein Center for Fundamental Physics and Laboratory for High Energy Physics, University of Bern, Bern; Switzerland.

- ²⁰School of Physics and Astronomy, University of Birmingham, Birmingham; United Kingdom.
- ²¹(^a)Department of Physics, Bogazici University, Istanbul;(^b)Department of Physics Engineering, Gaziantep University, Gaziantep;(^c)Department of Physics, Istanbul University, Istanbul;(^d)Istinye University, Sariyer, Istanbul; Türkiye.
- ²²(^a)Facultad de Ciencias y Centro de Investigaciones, Universidad Antonio Nariño, Bogotá;(^b)Departamento de Física, Universidad Nacional de Colombia, Bogotá; Colombia.
- ²³(^a)Dipartimento di Fisica e Astronomia A. Righi, Università di Bologna, Bologna;(^b)INFN Sezione di Bologna; Italy.
- ²⁴Physikalisches Institut, Universität Bonn, Bonn; Germany.
- ²⁵Department of Physics, Boston University, Boston MA; United States of America.
- ²⁶Department of Physics, Brandeis University, Waltham MA; United States of America.
- ²⁷(^a)Transilvania University of Brasov, Brasov;(^b)Horia Hulubei National Institute of Physics and Nuclear Engineering, Bucharest;(^c)Department of Physics, Alexandru Ioan Cuza University of Iasi, Iasi;(^d)National Institute for Research and Development of Isotopic and Molecular Technologies, Physics Department, Cluj-Napoca;(^e)University Politehnica Bucharest, Bucharest;(^f)West University in Timisoara, Timisoara; Romania.
- ²⁸(^a)Faculty of Mathematics, Physics and Informatics, Comenius University, Bratislava;(^b)Department of Subnuclear Physics, Institute of Experimental Physics of the Slovak Academy of Sciences, Kosice; Slovak Republic.
- ²⁹Physics Department, Brookhaven National Laboratory, Upton NY; United States of America.
- ³⁰Universidad de Buenos Aires, Facultad de Ciencias Exactas y Naturales, Departamento de Física, y CONICET, Instituto de Física de Buenos Aires (IFIBA), Buenos Aires; Argentina.
- ³¹California State University, CA; United States of America.
- ³²Cavendish Laboratory, University of Cambridge, Cambridge; United Kingdom.
- ³³(^a)Department of Physics, University of Cape Town, Cape Town;(^b)iThemba Labs, Western Cape;(^c)Department of Mechanical Engineering Science, University of Johannesburg, Johannesburg;(^d)National Institute of Physics, University of the Philippines Diliman (Philippines);(^e)University of South Africa, Department of Physics, Pretoria;(^f)University of Zululand, KwaDlangezwa;(^g)School of Physics, University of the Witwatersrand, Johannesburg; South Africa.
- ³⁴Department of Physics, Carleton University, Ottawa ON; Canada.
- ³⁵(^a)Faculté des Sciences Ain Chock, Réseau Universitaire de Physique des Hautes Energies - Université Hassan II, Casablanca;(^b)Faculté des Sciences, Université Ibn-Tofail, Kénitra;(^c)Faculté des Sciences Semlalia, Université Cadi Ayyad, LPHEA-Marrakech;(^d)LPMR, Faculté des Sciences, Université Mohamed Premier, Oujda;(^e)Faculté des sciences, Université Mohammed V, Rabat;(^f)Institute of Applied Physics, Mohammed VI Polytechnic University, Ben Guerir; Morocco.
- ³⁶CERN, Geneva; Switzerland.
- ³⁷Affiliated with an institute covered by a cooperation agreement with CERN.
- ³⁸Affiliated with an international laboratory covered by a cooperation agreement with CERN.
- ³⁹Enrico Fermi Institute, University of Chicago, Chicago IL; United States of America.
- ⁴⁰LPC, Université Clermont Auvergne, CNRS/IN2P3, Clermont-Ferrand; France.
- ⁴¹Nevis Laboratory, Columbia University, Irvington NY; United States of America.
- ⁴²Niels Bohr Institute, University of Copenhagen, Copenhagen; Denmark.
- ⁴³(^a)Dipartimento di Fisica, Università della Calabria, Rende;(^b)INFN Gruppo Collegato di Cosenza, Laboratori Nazionali di Frascati; Italy.
- ⁴⁴Physics Department, Southern Methodist University, Dallas TX; United States of America.
- ⁴⁵Physics Department, University of Texas at Dallas, Richardson TX; United States of America.
- ⁴⁶National Centre for Scientific Research "Demokritos", Agia Paraskevi; Greece.

- 47^(a) Department of Physics, Stockholm University;^(b) Oskar Klein Centre, Stockholm; Sweden.
- 48 Deutsches Elektronen-Synchrotron DESY, Hamburg and Zeuthen; Germany.
- 49 Fakultät Physik, Technische Universität Dortmund, Dortmund; Germany.
- 50 Institut für Kern- und Teilchenphysik, Technische Universität Dresden, Dresden; Germany.
- 51 Department of Physics, Duke University, Durham NC; United States of America.
- 52 SUPA - School of Physics and Astronomy, University of Edinburgh, Edinburgh; United Kingdom.
- 53 INFN e Laboratori Nazionali di Frascati, Frascati; Italy.
- 54 Physikalisches Institut, Albert-Ludwigs-Universität Freiburg, Freiburg; Germany.
- 55 II. Physikalisches Institut, Georg-August-Universität Göttingen, Göttingen; Germany.
- 56 Département de Physique Nucléaire et Corpusculaire, Université de Genève, Genève; Switzerland.
- 57^(a) Dipartimento di Fisica, Università di Genova, Genova;^(b) INFN Sezione di Genova; Italy.
- 58 II. Physikalisches Institut, Justus-Liebig-Universität Giessen, Giessen; Germany.
- 59 SUPA - School of Physics and Astronomy, University of Glasgow, Glasgow; United Kingdom.
- 60 LPSC, Université Grenoble Alpes, CNRS/IN2P3, Grenoble INP, Grenoble; France.
- 61 Laboratory for Particle Physics and Cosmology, Harvard University, Cambridge MA; United States of America.
- 62^(a) Department of Modern Physics and State Key Laboratory of Particle Detection and Electronics, University of Science and Technology of China, Hefei;^(b) Institute of Frontier and Interdisciplinary Science and Key Laboratory of Particle Physics and Particle Irradiation (MOE), Shandong University, Qingdao;^(c) School of Physics and Astronomy, Shanghai Jiao Tong University, Key Laboratory for Particle Astrophysics and Cosmology (MOE), SKLPPC, Shanghai;^(d) Tsung-Dao Lee Institute, Shanghai; China.
- 63^(a) Kirchoff-Institut für Physik, Ruprecht-Karls-Universität Heidelberg, Heidelberg;^(b) Physikalisches Institut, Ruprecht-Karls-Universität Heidelberg, Heidelberg; Germany.
- 64^(a) Department of Physics, Chinese University of Hong Kong, Shatin, N.T., Hong Kong;^(b) Department of Physics, University of Hong Kong, Hong Kong;^(c) Department of Physics and Institute for Advanced Study, Hong Kong University of Science and Technology, Clear Water Bay, Kowloon, Hong Kong; China.
- 65 Department of Physics, National Tsing Hua University, Hsinchu; Taiwan.
- 66 IJCLab, Université Paris-Saclay, CNRS/IN2P3, 91405, Orsay; France.
- 67 Department of Physics, Indiana University, Bloomington IN; United States of America.
- 68^(a) INFN Gruppo Collegato di Udine, Sezione di Trieste, Udine;^(b) ICTP, Trieste;^(c) Dipartimento Politecnico di Ingegneria e Architettura, Università di Udine, Udine; Italy.
- 69^(a) INFN Sezione di Lecce;^(b) Dipartimento di Matematica e Fisica, Università del Salento, Lecce; Italy.
- 70^(a) INFN Sezione di Milano;^(b) Dipartimento di Fisica, Università di Milano, Milano; Italy.
- 71^(a) INFN Sezione di Napoli;^(b) Dipartimento di Fisica, Università di Napoli, Napoli; Italy.
- 72^(a) INFN Sezione di Pavia;^(b) Dipartimento di Fisica, Università di Pavia, Pavia; Italy.
- 73^(a) INFN Sezione di Pisa;^(b) Dipartimento di Fisica E. Fermi, Università di Pisa, Pisa; Italy.
- 74^(a) INFN Sezione di Roma;^(b) Dipartimento di Fisica, Sapienza Università di Roma, Roma; Italy.
- 75^(a) INFN Sezione di Roma Tor Vergata;^(b) Dipartimento di Fisica, Università di Roma Tor Vergata, Roma; Italy.
- 76^(a) INFN Sezione di Roma Tre;^(b) Dipartimento di Matematica e Fisica, Università Roma Tre, Roma; Italy.
- 77^(a) INFN-TIFPA;^(b) Università degli Studi di Trento, Trento; Italy.
- 78 Universität Innsbruck, Department of Astro and Particle Physics, Innsbruck; Austria.
- 79 University of Iowa, Iowa City IA; United States of America.
- 80 Department of Physics and Astronomy, Iowa State University, Ames IA; United States of America.
- 81^(a) Departamento de Engenharia Elétrica, Universidade Federal de Juiz de Fora (UFJF), Juiz de Fora;^(b) Universidade Federal do Rio De Janeiro COPPE/EE/IF, Rio de Janeiro;^(c) Instituto de Física,

- Universidade de São Paulo, São Paulo;^(d)Rio de Janeiro State University, Rio de Janeiro; Brazil.
- ⁸²KEK, High Energy Accelerator Research Organization, Tsukuba; Japan.
- ⁸³Graduate School of Science, Kobe University, Kobe; Japan.
- ⁸⁴(^a)AGH University of Science and Technology, Faculty of Physics and Applied Computer Science, Krakow;^(b)Marian Smoluchowski Institute of Physics, Jagiellonian University, Krakow; Poland.
- ⁸⁵Institute of Nuclear Physics Polish Academy of Sciences, Krakow; Poland.
- ⁸⁶Faculty of Science, Kyoto University, Kyoto; Japan.
- ⁸⁷Kyoto University of Education, Kyoto; Japan.
- ⁸⁸Research Center for Advanced Particle Physics and Department of Physics, Kyushu University, Fukuoka ; Japan.
- ⁸⁹Instituto de Física La Plata, Universidad Nacional de La Plata and CONICET, La Plata; Argentina.
- ⁹⁰Physics Department, Lancaster University, Lancaster; United Kingdom.
- ⁹¹Oliver Lodge Laboratory, University of Liverpool, Liverpool; United Kingdom.
- ⁹²Department of Experimental Particle Physics, Jožef Stefan Institute and Department of Physics, University of Ljubljana, Ljubljana; Slovenia.
- ⁹³School of Physics and Astronomy, Queen Mary University of London, London; United Kingdom.
- ⁹⁴Department of Physics, Royal Holloway University of London, Egham; United Kingdom.
- ⁹⁵Department of Physics and Astronomy, University College London, London; United Kingdom.
- ⁹⁶Louisiana Tech University, Ruston LA; United States of America.
- ⁹⁷Fysiska institutionen, Lunds universitet, Lund; Sweden.
- ⁹⁸Departamento de Física Teórica C-15 and CIAFF, Universidad Autónoma de Madrid, Madrid; Spain.
- ⁹⁹Institut für Physik, Universität Mainz, Mainz; Germany.
- ¹⁰⁰School of Physics and Astronomy, University of Manchester, Manchester; United Kingdom.
- ¹⁰¹CPPM, Aix-Marseille Université, CNRS/IN2P3, Marseille; France.
- ¹⁰²Department of Physics, University of Massachusetts, Amherst MA; United States of America.
- ¹⁰³Department of Physics, McGill University, Montreal QC; Canada.
- ¹⁰⁴School of Physics, University of Melbourne, Victoria; Australia.
- ¹⁰⁵Department of Physics, University of Michigan, Ann Arbor MI; United States of America.
- ¹⁰⁶Department of Physics and Astronomy, Michigan State University, East Lansing MI; United States of America.
- ¹⁰⁷Group of Particle Physics, University of Montreal, Montreal QC; Canada.
- ¹⁰⁸Fakultät für Physik, Ludwig-Maximilians-Universität München, München; Germany.
- ¹⁰⁹Max-Planck-Institut für Physik (Werner-Heisenberg-Institut), München; Germany.
- ¹¹⁰Graduate School of Science and Kobayashi-Maskawa Institute, Nagoya University, Nagoya; Japan.
- ¹¹¹Department of Physics and Astronomy, University of New Mexico, Albuquerque NM; United States of America.
- ¹¹²Institute for Mathematics, Astrophysics and Particle Physics, Radboud University/Nikhef, Nijmegen; Netherlands.
- ¹¹³Nikhef National Institute for Subatomic Physics and University of Amsterdam, Amsterdam; Netherlands.
- ¹¹⁴Department of Physics, Northern Illinois University, DeKalb IL; United States of America.
- ¹¹⁵(^a)New York University Abu Dhabi, Abu Dhabi;^(b)United Arab Emirates University, Al Ain;^(c)University of Sharjah, Sharjah; United Arab Emirates.
- ¹¹⁶Department of Physics, New York University, New York NY; United States of America.
- ¹¹⁷Ochanomizu University, Otsuka, Bunkyo-ku, Tokyo; Japan.
- ¹¹⁸Ohio State University, Columbus OH; United States of America.
- ¹¹⁹Homer L. Dodge Department of Physics and Astronomy, University of Oklahoma, Norman OK; United

States of America.

¹²⁰Department of Physics, Oklahoma State University, Stillwater OK; United States of America.

¹²¹Palacký University, Joint Laboratory of Optics, Olomouc; Czech Republic.

¹²²Institute for Fundamental Science, University of Oregon, Eugene, OR; United States of America.

¹²³Graduate School of Science, Osaka University, Osaka; Japan.

¹²⁴Department of Physics, University of Oslo, Oslo; Norway.

¹²⁵Department of Physics, Oxford University, Oxford; United Kingdom.

¹²⁶LPNHE, Sorbonne Université, Université Paris Cité, CNRS/IN2P3, Paris; France.

¹²⁷Department of Physics, University of Pennsylvania, Philadelphia PA; United States of America.

¹²⁸Department of Physics and Astronomy, University of Pittsburgh, Pittsburgh PA; United States of America.

¹²⁹^(a)Laboratório de Instrumentação e Física Experimental de Partículas - LIP, Lisboa;^(b)Departamento de Física, Faculdade de Ciências, Universidade de Lisboa, Lisboa;^(c)Departamento de Física, Universidade de Coimbra, Coimbra;^(d)Centro de Física Nuclear da Universidade de Lisboa, Lisboa;^(e)Departamento de Física, Universidade do Minho, Braga;^(f)Departamento de Física Teórica y del Cosmos, Universidad de Granada, Granada (Spain);^(g)Departamento de Física, Instituto Superior Técnico, Universidade de Lisboa, Lisboa; Portugal.

¹³⁰Institute of Physics of the Czech Academy of Sciences, Prague; Czech Republic.

¹³¹Czech Technical University in Prague, Prague; Czech Republic.

¹³²Charles University, Faculty of Mathematics and Physics, Prague; Czech Republic.

¹³³Particle Physics Department, Rutherford Appleton Laboratory, Didcot; United Kingdom.

¹³⁴IRFU, CEA, Université Paris-Saclay, Gif-sur-Yvette; France.

¹³⁵Santa Cruz Institute for Particle Physics, University of California Santa Cruz, Santa Cruz CA; United States of America.

¹³⁶^(a)Departamento de Física, Pontificia Universidad Católica de Chile, Santiago;^(b)Millennium Institute for Subatomic physics at high energy frontier (SAPHIR), Santiago;^(c)Instituto de Investigación Multidisciplinario en Ciencia y Tecnología, y Departamento de Física, Universidad de La Serena;^(d)Universidad Andres Bello, Department of Physics, Santiago;^(e)Instituto de Alta Investigación, Universidad de Tarapacá, Arica;^(f)Departamento de Física, Universidad Técnica Federico Santa María, Valparaíso; Chile.

¹³⁷Department of Physics, University of Washington, Seattle WA; United States of America.

¹³⁸Department of Physics and Astronomy, University of Sheffield, Sheffield; United Kingdom.

¹³⁹Department of Physics, Shinshu University, Nagano; Japan.

¹⁴⁰Department Physik, Universität Siegen, Siegen; Germany.

¹⁴¹Department of Physics, Simon Fraser University, Burnaby BC; Canada.

¹⁴²SLAC National Accelerator Laboratory, Stanford CA; United States of America.

¹⁴³Department of Physics, Royal Institute of Technology, Stockholm; Sweden.

¹⁴⁴Departments of Physics and Astronomy, Stony Brook University, Stony Brook NY; United States of America.

¹⁴⁵Department of Physics and Astronomy, University of Sussex, Brighton; United Kingdom.

¹⁴⁶School of Physics, University of Sydney, Sydney; Australia.

¹⁴⁷Institute of Physics, Academia Sinica, Taipei; Taiwan.

¹⁴⁸^(a)E. Andronikashvili Institute of Physics, Iv. Javakhishvili Tbilisi State University, Tbilisi;^(b)High Energy Physics Institute, Tbilisi State University, Tbilisi;^(c)University of Georgia, Tbilisi; Georgia.

¹⁴⁹Department of Physics, Technion, Israel Institute of Technology, Haifa; Israel.

¹⁵⁰Raymond and Beverly Sackler School of Physics and Astronomy, Tel Aviv University, Tel Aviv; Israel.

¹⁵¹Department of Physics, Aristotle University of Thessaloniki, Thessaloniki; Greece.

- ¹⁵²International Center for Elementary Particle Physics and Department of Physics, University of Tokyo, Tokyo; Japan.
- ¹⁵³Department of Physics, Tokyo Institute of Technology, Tokyo; Japan.
- ¹⁵⁴Department of Physics, University of Toronto, Toronto ON; Canada.
- ¹⁵⁵(^a) TRIUMF, Vancouver BC; (^b) Department of Physics and Astronomy, York University, Toronto ON; Canada.
- ¹⁵⁶Division of Physics and Tomonaga Center for the History of the Universe, Faculty of Pure and Applied Sciences, University of Tsukuba, Tsukuba; Japan.
- ¹⁵⁷Department of Physics and Astronomy, Tufts University, Medford MA; United States of America.
- ¹⁵⁸Department of Physics and Astronomy, University of California Irvine, Irvine CA; United States of America.
- ¹⁵⁹Department of Physics and Astronomy, University of Uppsala, Uppsala; Sweden.
- ¹⁶⁰Department of Physics, University of Illinois, Urbana IL; United States of America.
- ¹⁶¹Instituto de Física Corpuscular (IFIC), Centro Mixto Universidad de Valencia - CSIC, Valencia; Spain.
- ¹⁶²Department of Physics, University of British Columbia, Vancouver BC; Canada.
- ¹⁶³Department of Physics and Astronomy, University of Victoria, Victoria BC; Canada.
- ¹⁶⁴Fakultät für Physik und Astronomie, Julius-Maximilians-Universität Würzburg, Würzburg; Germany.
- ¹⁶⁵Department of Physics, University of Warwick, Coventry; United Kingdom.
- ¹⁶⁶Waseda University, Tokyo; Japan.
- ¹⁶⁷Department of Particle Physics and Astrophysics, Weizmann Institute of Science, Rehovot; Israel.
- ¹⁶⁸Department of Physics, University of Wisconsin, Madison WI; United States of America.
- ¹⁶⁹Fakultät für Mathematik und Naturwissenschaften, Fachgruppe Physik, Bergische Universität Wuppertal, Wuppertal; Germany.
- ¹⁷⁰Department of Physics, Yale University, New Haven CT; United States of America.
- ^a Also Affiliated with an institute covered by a cooperation agreement with CERN.
- ^b Also at Borough of Manhattan Community College, City University of New York, New York NY; United States of America.
- ^c Also at Bruno Kessler Foundation, Trento; Italy.
- ^d Also at Center for High Energy Physics, Peking University; China.
- ^e Also at Centro Studi e Ricerche Enrico Fermi; Italy.
- ^f Also at CERN, Geneva; Switzerland.
- ^g Also at Département de Physique Nucléaire et Corpusculaire, Université de Genève, Genève; Switzerland.
- ^h Also at Departament de Física de la Universitat Autònoma de Barcelona, Barcelona; Spain.
- ⁱ Also at Department of Financial and Management Engineering, University of the Aegean, Chios; Greece.
- ^j Also at Department of Physics and Astronomy, Michigan State University, East Lansing MI; United States of America.
- ^k Also at Department of Physics and Astronomy, University of Louisville, Louisville, KY; United States of America.
- ^l Also at Department of Physics, Ben Gurion University of the Negev, Beer Sheva; Israel.
- ^m Also at Department of Physics, California State University, East Bay; United States of America.
- ⁿ Also at Department of Physics, California State University, Sacramento; United States of America.
- ^o Also at Department of Physics, King's College London, London; United Kingdom.
- ^p Also at Department of Physics, University of Fribourg, Fribourg; Switzerland.
- ^q Also at Department of Physics, University of Thessaly; Greece.
- ^r Also at Department of Physics, Westmont College, Santa Barbara; United States of America.
- ^s Also at Hellenic Open University, Patras; Greece.

- ^t Also at Institutio Catalana de Recerca i Estudis Avancats, ICREA, Barcelona; Spain.
- ^u Also at Institut für Experimentalphysik, Universität Hamburg, Hamburg; Germany.
- ^v Also at Institute of Particle Physics (IPP); Canada.
- ^w Also at Institute of Physics, Azerbaijan Academy of Sciences, Baku; Azerbaijan.
- ^x Also at Institute of Theoretical Physics, Ilia State University, Tbilisi; Georgia.
- ^y Also at Lawrence Livermore National Laboratory, Livermore; United States of America.
- ^z Also at Physics Department, An-Najah National University, Nablus; Palestine.
- ^{aa} Also at The City College of New York, New York NY; United States of America.
- ^{ab} Also at The Collaborative Innovation Center of Quantum Matter (CICQM), Beijing; China.
- ^{ac} Also at TRIUMF, Vancouver BC; Canada.
- ^{ad} Also at Università di Napoli Parthenope, Napoli; Italy.
- ^{ae} Also at University of Chinese Academy of Sciences (UCAS), Beijing; China.
- ^{af} Also at University of Colorado Boulder, Department of Physics, Colorado; United States of America.
- ^{ag} Also at Yeditepe University, Physics Department, Istanbul; Türkiye.
- * Deceased